

Cobalt promoted ruthenium catalysts for the hydrogenation of sugar, furfural and furfuryl alcohol

By

Kadam Jyoti Ramesh

10CC18J26010

A thesis submitted to the
Academy of Scientific & Innovative Research
for the award of the degree of
DOCTOR OF PHILOSOPHY
in
SCIENCE

Under the supervision of

Dr. Paresh Laxmikant Dhepe



CSIR-National Chemical Laboratory, Pune



Academy of Scientific and Innovative Research

AcSIR Headquarters, CSIR-HRDC campus

Sector 19, Kamla Nehru Nagar,

Ghaziabad, U.P. – 201 002, India

November, 2023

Certificate

This is to certify that the work incorporated in this Ph.D. thesis entitled, "*Cobalt promoted ruthenium catalysts for the hydrogenation of sugar, furfural and furfuryl alcohol*" submitted by **Ms. Kadam Jyoti Ramesh** to the Academy of Scientific and Innovative Research (AcSIR), in partial fulfilment of the requirements for the award of the Degree of **Doctor of Philosophy in Science**, embodies original research work carried-out by the student. We, further certify that this work has not been submitted to any other University or Institution in part or full for the award of any degree or diploma. Research material(s) obtained from other source(s) and used in this research work has/have been duly acknowledged in the thesis. Image(s), illustration(s), figure(s), table(s) etc., used in the thesis from other source(s), have also been duly cited and acknowledged.



Research Student

Ms. Kadam Jyoti Ramesh

Date: 09/11/2023



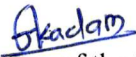
Research Supervisor

Dr. Paresh L. Dhepe


Date: 09/11/2023

STATEMENTS OF ACADEMIC INTEGRITY

I, Kadam Jyoti Ramesh, a Ph.D. student of the Academy of Scientific and Innovative Research (AcSIR) with Registration No. 10CC18J26010 hereby undertake that the thesis entitled “Cobalt promoted ruthenium catalysts for the hydrogenation of sugar, furfural and furfuryl alcohol” has been prepared by me and that the document reports original work carried out by me and is free of any plagiarism in compliance with the UGC Regulations on “Promotion of Academic Integrity and Prevention of Plagiarism in Higher Educational Institutions (2018)” and the CSIR Guidelines for “Ethics in Research and in Governance (2020)”.


Signature of the Student
Date: 09/11/2023
Place: Pune

It is hereby certified that the work done by the student, under my/~~our~~ supervision, is plagiarism-free in accordance with the UGC Regulations on “Promotion of Academic Integrity and Prevention of Plagiarism in Higher Educational Institutions (2018)” and the CSIR Guidelines for “Ethics in Research and in Governance (2020)”.


Signature of the Supervisor
Name: Dr. Paresh L. Dhepe
Date: 09/11/2023
Place: Pune

This thesis is dedicated to

My parents...

Acknowledgement

Acknowledgement

*First of all, I want to thank my research supervisor, **Dr. Paresh Laxmikant Dhepe** his continuous guidance and support during my doctoral study. I would like to thank him for giving me the opportunity to join his research group. I am grateful towards him for his immense contribution of time and ideas to make my Ph.D. work productive and stimulating. His enthusiasm for research was inspiring and motivational for me during tough time in my research life. I consider extremely fortunate to have an advisor who not only educated me in chemistry but also taught me discipline and shown unique ways to achieve my goals. His valuable guidance and suggestions for being good researcher as well as responsible person in social life are truly encouraging. Without his guidance and persistent help this dissertation would not have been possible. I would like to pay my sincere thanks to him for all the support and care that I received from him throughout entire period.*

*I want to convey my sincere regards to my Doctoral Advisory Committee members, **Dr. S. B. Mhaske, Dr. Kavita Joshi and Dr. C. P. Vinod** for their constructive comments, valuable suggestions and encouragement during my Ph. D. journey.*

*My sincere thanks to **Dr. Ashish Lele** (Director, CSIR-NCL), **Prof. A. K. Nangia** (Former Director, CSIR-NCL), **Dr. D. Srinivas** (Former Head, Catalysis and Inorganic Chemistry Division), **Dr. C. S. Gopinath** (Former Head, Catalysis and Inorganic Chemistry Division) and **Dr. S. B. Umbarkar** (Head, Catalysis and Inorganic Chemistry Division) for giving me the opportunity and providing all necessary infrastructure and facilities to carry out my research work. I convey my sincere gratitude for all former and present scientists of Catalysis and Inorganic Chemistry Division for their help whenever I need. I would like to acknowledge all the supporting staffs, technical staffs of Catalysis and Inorganic Chemistry Division for their valuable help and co-operation.*

*I would like to thank all my colleagues and lab mates (former and present) for their helpful hand and cheerful attitude as I have spent most of my time with them and learnt many things from them. It is pleasure to thank all my former and present lab mates **Dr. Manisha, Dr. Nilesh,***

Acknowledgement

Dr. Shilpa, Dr. Dheerendra, Dr. Neha, Dr. Sunita, Priya, Lavanya, Tufeil, Kruti, Deepak, Deepali, Waseem, Akshay, Rushikesh, Dhairyashil, Sameer, Jayprakash, Sandip, Vipul, Ankit, Rohit, Yayati, Shiv, Neetu, Kalyani, Akhilendra, Manuraj, Titto, Surabhi, Sheetal, Sheethal, Shinju, Sivanesh for the lively and cooperative environment in lab during my whole journey. I am thankful to all students of catalysis division for their help and support.

I would like to extend my special thanks to my friends **Tufeil Khan, Ashwini Nakate and Vaishali Kadam** for their encouragement and support during my Ph.D. life.

I am grateful to my teachers from school and colleges for their encouragement in nurturing my mind towards higher education. I would like to thank **Dr. Balasaheb R. Arbad** to inspire me for pursuing Ph.D.

I gratefully acknowledge University Grant Commission (UGC), New Delhi for providing me a research fellowship and Academy of Scientific & Innovative Research (AcSIR) for registering me for the Ph. D. degree.

Last but not least, I am very much grateful to thank my parents, sisters and brother for immense love, support, patience, trust and encouragement.

.....**Jyoti**

Contents

List of schemes	i
List of figures	ii
List of tables	vii
List of abbreviations	viii
Synopsis of the thesis	xi

Chapter 1. General introduction and literature survey

1.1. Introduction to biomass	3
1.2. Concept of biorefinary	3
1.3. Classification of biomass	4
1.3.1. Chemical composition and structure of lignocellulosic biomass	5
1.3.2. Sources and advantages of lignocellulosic biomass	8
1.4. Biomass conversion	9
1.4.1. Conversion of cellulose to platform chemicals	9
1.4.2. Conversion of hemicellulose to platform chemicals	10
1.4.3. Conversion of furfural to platform chemicals	11
1.5. Applications of sorbitol, xylitol and cyclopentanone	12
1.5.1. Applications of sorbitol and xylitol	12
1.5.2. Applications of cyclopentanone	13
1.6. Global market of sorbitol, xylitol and cyclopentanone	13
1.7. Literature survey	14
1.7.1. Literature survey for the hydrogenation of sugars to sugar alcohols	14
1.7.2. Literature survey for the conversion of furfural (FAL) to cyclopentanone (CPO)	17

Contents

1.8. Catalysts	21
1.8.1. Supported metal catalysts	21
1.8.2. Preparation methods of supported metal catalysts	22
1.8.3. Monometallic and bimetallic catalysts	23
1.9. Aim and objectives of the thesis	24
1.10. Hypothesis of the work	25
1.11. Outline of the thesis	26
1.12. References	27

Chapter 2. Catalyst synthesis and characterization

2.1. Introduction	37
2.2. Catalyst synthesis	37
2.2.1. Materials	37
2.2.2. Catalyst synthesis procedure	38
2.3. Catalyst characterization	40
2.3.1. Catalyst characterization techniques	40
2.3.2. Results and discussion	41
2.3.2.1. X-ray diffraction (XRD) analysis	41
2.3.2.2. X-ray photoelectron spectroscopy (XPS) analysis	45
2.3.2.3. N ₂ sorption analysis	48
2.3.2.4. Transmission electron microscopy (TEM) analysis	50
2.3.2.5. Inductively coupled Plasma-Optical emission spectroscopic (ICP-OES) analysis	55
2.4. Conclusion	56

2.5. References	58
------------------------	----

Chapter 3. Hydrogenation of sugars to sugar alcohols

Chapter 3A. Hydrogenation of glucose to sorbitol

3A.1. Introduction	62
3A.2. Experimental	64
3A.2.1. Materials	64
3A.2.2. Catalyst synthesis	64
3A.2.3. Reaction set-up and analysis of reaction mixtures	64
3A.2.4. Calculations	65
3A.3. Results and discussion	65
3A.3.1. Effect of different supports	66
3A.3.2. Effect of Ru metal loading	69
3A.3.3. Effect of Co metal loading	70
3A.3.4. Effect of different reaction parameters	74
3A.3.5. Hydrogenation of different C6 sugars	80
3A.3.6. Recycle study	81
3A.3.7. Spent catalyst characterization	88
3A.3.8. Reaction in flow mode reactor	83
3A.3.9. Purification of sorbitol	85
3A.4. Conclusion	87
3A.5. References	89

Chapter 3B. Hydrogenation of xylose to xylitol

3B.1. Introduction	93
3B.2. Experimental	94
3B.2.1. Materials	94
3B.2.2. Catalyst synthesis	94
3B.2.3. Reaction set-up and analysis of reaction mixtures	94
3B.3. Results and discussion	95
3B.3.1. Effect of monometallic and bimetallic catalyst	96
3B.3.2. Effect of different reaction parameters	97
3B.3.3. Hydrogenation of different C5 sugars	100
3B.3.4. Recycle study	101
3B.3.5. Reaction in flow mode reactor	102
3B.3.6. Purification of xylitol	103
3B.4. Conclusion	105
3B.5. References	106

Chapter 4. Hydrogenative ring rearrangement of furfural (FAL) to cyclopentanone (CPO)

4.1. Introduction	110
4.2. Experimental	112
4.2.1. Materials	112
4.2.2. Catalyst synthesis	112

Contents

4.2.3. Reaction set-up and analysis of reaction mixtures	112
4.2.4. Calculations	113
4.3. Results and discussion	113
4.3.1. Effect of different catalysts	113
4.3.2. Effect of monometallic and bimetallic catalysts	115
4.3.3. Effect of varying Co loading	117
4.3.4. Effect of different reaction parameters	118
4.3.5. Effect of acetic acid treated (2)Ru(1.5)Co/Al-B catalyst	123
4.3.6. Recycle study	124
4.4. Conversion of FAL to CPO using commercial (5)Ru/Al catalyst	125
4.4.1 Effect of reaction parameters for the conversion of FAL to CPO over commercial (5)Ru/Al catalyst	125
4.5. Reactions with crude FAL	128
4.5.1. Synthesis of FAL from hydrolysed hemicellulose (Industry sample)	128
4.5.2. Conversion of crude FAL to CPO	131
4.6. Conclusion	133
4.7. References	134

Chapter 5. Hydrogenation of furfuryl alcohol (FOL) to cyclopentanone (CPO)

5.1. Introduction	138
5.2. Experimental	140

Contents

5.2.1. Materials	140
5.2.2. Catalyst synthesis	140
5.2.3. Reaction set-up and analysis of reaction mixtures	140
5.2.4. Calculations	141
5.3. Results and discussion	141
5.3.1. Effect of different reaction parameters	142
5.3.2. Stability of products	148
5.3.3. Reaction pathway for the conversion of FAL to CPO	150
5.4. Conversion of FOL to CPO using commercial (5)Ru/Al catalyst	151
5.5. Conclusion	152
5.6. References	154

Chapter 6. Summary and conclusions

Summary and conclusion	157
-------------------------------	-----

Abstract for indexing	163
List of publications	164
List of posters	165
List of conference attended	168
Copy of SCI publications	167
Erratum	169

List of schemes

Chapter 1.

Scheme 1.1.	Conversion of cellulose to chemicals	10
Scheme 1.2.	Conversion of hemicellulose to chemicals	11
Scheme 1.3.	Conversion of furfural (FAL) to chemicals	12

Chapter 3A.

Scheme 3A.1.	Hydrogenation of glucose to sorbitol	63
Scheme 3A.2.	Glucose to fructose isomerization	73

Chapter 3B.

Scheme 3B.1.	Hydrogenation of xylose to xylitol	94
---------------------	------------------------------------	----

Chapter 4.

Scheme 4.1	Conversion of furfural (FAL) to cyclopentanone (CPO)	111
-------------------	--	-----

Chapter 5.

Scheme 5.1	Conversion of furfuryl alcohol (FOL) to cyclopentanone (CPO)	139
-------------------	--	-----

List of figures

Chapter 1.

Figure 1.1.	Biomass as a carbon neutral feedstock	4
Figure 1.2.	Classification of biomass	5
Figure 1.3.	Structure of cellulose	6
Figure 1.4.	Structure of hemicellulose (xylan)	7
Figure 1.5.	Structure of lignin monomers	7
Figure 1.6.	Sources of biomass	8

Chapter 2.

Figure 2.1.	Wet impregnation method of catalyst synthesis	38
Figure 2.2.	Reduction program of catalyst	39
Figure 2.3.	XRD pattern Al-Basic supported (1.5)Ru and (3)Co loaded monometallic and bimetallic catalysts	41
Figure 2.4.	XRD pattern Al-Basic supported (2)Ru and (1.5)Co loaded monometallic and bimetallic catalysts	42
Figure 2.5.	XRD pattern of Al-Acidic, Al-Basic and Al-Neutral supported bimetallic catalysts.	43
Figure 2.6.	XRD pattern Al-Basic supported Ru monometallic catalysts	44
Figure 2.7.	XRD pattern Al-Basic supported Ru and Co loaded bimetallic catalysts.	44
Figure 2.8.	XPS spectra of Al-Basic supported monometallic Co catalysts at Co 2p core level	45
Figure 2.9.	XPS spectra of Al-Basic supported monometallic Co catalysts	

List of figures

	at Co 2p core level	46
Figure 2.10.	XPS spectra of Al-Basic supported monometallic Ru catalysts at Ru 3p core level	47
Figure 2.11.	XPS spectra of Al-Basic supported bimetallic Ru catalysts at Ru 3p core level	48
Figure 2.12.	TEM images and particle size distributuion of monometallic Ru ad Co catalysts	51
Figure 2.13.	TEM images and particle size distributuion of bimetallic Ru and Co catalysts	53
Figure 2.14.	TEM images ad particle size distributuion of bimetallic catalysts with differet Co loading	54
Figure 2.15.	HRTEM images of bimetallic (2)Ru(1.5)Co/Al-Basic catalyst	55
Figure 2.16.	Elemental mappig images of (1.5)Ru(3)Co/Al-Basic catalyst	55
 Chapter 3A.		
Figure 3A.1.	Effect of different supports on glucose hydrogenation	66
Figure 3A.2.	UV-Vis analysis of a water solution of glucose	68
Figure 3A.3.	Effect of Ru loading on glucose hydrogenation	69
Figure 3A.4.	Effect of Co loading on glucose hydrogenation	72
Figure 3A.5.	Glucose-Cobalt interactions	72
Figure 3A.6.	Effect of temperature on glucose hydrogenation over (1.5)Ru(3)Co/Al-Basic catalyst	75

List of figures

Figure 3A.7.	Effect of H ₂ pressure on glucose hydrogenation over (1.5)Ru(3)Co/Al-Basic catalyst	76
Figure 3A.8.	Effect of time on glucose hydrogenation over (1.5)Ru(3)Co/Al-Basic catalyst	77
Figure 3A.9.	Effect of S/C ratio on glucose hydrogenation over (1.5)Ru(3)Co/Al-Basic catalyst	78
Figure 3A.10.	Effect of glucose concentration on glucose hydrogenation over (1.5)Ru(3)Co/Al-Basic catalyst	79
Figure 3A.11.	Hydrogenation of different C6 sugars over (1.5)Ru(3)Co/Al-Basic catalyst	80
Figure 3A.12.	Recycle study of (1.5)Ru(3)Co/Al-Basic catalyst	
Figure 3A.13.	TEM image and particle size distribution of (1.5)Ru(3)Co/Al-Basic (a) fresh and (b) spent catalyst	83
Figure 3A.14.	Continuous flow mode reaction for glucose hydrogenation over (1.5)Ru(3)Co/Al-Basic catalyst	85
Figure 3A.15.	¹ H NMR profile of purified sorbitol	86
Figure 3A.16.	HRMS profile of purified sorbitol	87
Chapter 3B.		
Figure 3B.1.	Effect of monometallic and bimetallic catalyst on xylose hydrogenation	96
Figure 3B.2.	Effect of temperature on xylose hydrogenation over (1.5)Ru(3)Co/Al-Basic catalyst	97

List of figures

Figure 3B.3.	Effect of H ₂ pressure on xylose hydrogenation over (1.5)Ru(3)Co/Al-Basic catalyst	98
Figure 3B.4.	Effect of xylose concentration on xylose hydrogenation over (1.5)Ru(3)Co/Al-Basic catalyst	99
Figure 3B.5.	Hydrogenation of different C5 sugars over (1.5)Ru(3)Co/Al-Basic catalyst	100
Figure 3B.6.	Recycle study of (1.5)Ru(3)Co/Al-Basic catalyst	101
Figure 3B.7.	Continuous flow mode reaction for xylose hydrogenation over (1.5)Ru(3)Co/Al-Basic catalyst	103
Figure 3B.8.	¹ H NMR profile of purified xylitol	104
Figure 3B.9.	HRMS profile of purified xylitol	104
 Chapter 4.		
Figure 4.1.	Effect of different catalyst for the conversion of FAL to CPO	115
Figure 4.2.	Effect of mono and bimetallic catalyst for the conversion of FAL to CPO	117
Figure 4.3.	Effect of varying Co loading for the conversion of FAL to CPO	118
Figure 4.4.	Effect of H ₂ pressure for the conversion of FAL to CPO	120
Figure 4.5.	Effect of temperature for the conversion of FAL to CPO	121
Figure 4.6.	Effect of time for the conversion of FAL to CPO	123

List of figures

Figure 4.7.	Recycle study of (2)Ru(1.5)Co/Al-Basic catalyst for the conversion of FAL to CPO	124
Figure 4.8.	Effect of temperature for the conversion of FAL to CPO using commercial catalyst	126
Figure 4.9.	Effect of time for the conversion of FAL to CPO using commercial catalyst	127
Figure 4.10.	Effect of H ₂ pressure for the conversion of FAL to CPO using commercial catalyst	128
Figure 4.11.	HPLC profile of hydrolysed hemicellulose (Industry sample)	129
Figure 4.12.	Effect of time for the conversion of hydrolysed hemicellulose to FAL in 300mL reactor	130
Figure 4.13.	Effect of time for the conversion of hydrolysed hemicellulose to FAL in 1L reactor	131
Figure 4.14.	Effect of time for the conversion of crude FAL to CPO	132
Chapter 5.		
Figure 5.1.	Effect of H ₂ pressure for the conversion of FOL to CPO	143
Figure 5.2.	Effect of temperature for the conversion of FOL to CPO	145
Figure 5.3.	Effect of time for the conversion of FOL to CPO	146
Figure 5.4.	Effect of S/Ru ratio for the conversion of FAL to CPO	147
Figure 5.5.	Reaction pathway for the conversion of FAL to CPO	150
Figure 5.6.	Effect of time for the conversion of FAL to CPO	152

List of tables

Chapter 1.

Table 1.1.	Literature survey for the hydrogenation of glucose to sorbitol	15
Table 1.2.	Literature survey for the hydrogenation of xylose to xylitol	17
Table 1.3.	Literature survey for the conversion of FAL to CPO	20

Chapter 2.

Table 2.1.	List of synthesized monometallic and bimetallic catalysts	39
Table 2.2.	Structural properties of the catalysts	49
Table 2.3.	Summary of results obtained from ICP-OES analysis	56

Chapter 4.

Table 4.1.	Quantification of hydrolysed hemicellulose (Industry samples)	129
------------	---	-----

Chapter 5.

Table 5.1.	Thermal stability study	149
------------	-------------------------	-----

List of abbreviations

AC	Activated Carbon
AFPS	amine functionalized nanoporous polymer
Al	γ -Alumina
APR	Aqueous-phase reforming
BET	Braunauer-Emmett-Teller
C	Carbon
CAGR	Compound Annual Growth Rate
CCD	carbonized cassava dregs
CB	Carbon Black
CEO	2-cyclopentenone
CNT	Carbon Nanotube
CPO	Cyclopentanone
CPL	Cyclopentanol
3D	Three dimensional
DHA	Dihydroxyacetone
DHMF	2,5-dihydroxymethylfuran
DMTHF	2,5-dimethyl tetrahydrofuran
FAL	Furfural
FDCA	2, 5-furan dicarboxylic acid
FID	Flame Ionization Detector
FOL	Furfuryl Alcohol
GC	Gas Chromatography
GVL	γ -valerolactone
HZSM	Zeolite Socony Mobil (H-form)


List of abbreviations

HMF	5-hydroxymethylfurfural
HPLC	High Performance Liquid Chromatography
HRMS	High-resolution Mass Spectrometry
HRTEM	High-resolution Transmission Electron Microscopy
HT	Hydrotalcite
ICP-OES	Inductively Coupled Plasma-Optical Emission Spectroscopy
JCPDS	Joint Committee on Powder Diffraction Standards
MCM	Mobil Composition of Matter
2-MF	2-methylfuran
MOF	Metal-organic Framework
2-MTHF	2-methyltetrahydrofuran
5-MF	5-methylfurfural
NMR	Nuclear Magnetic Resonance
1,2-PDO	Pantane-1,2-diol
1,4-PDO	Pantane-1,4-diol
1,5-PDO	Pantane-1,5-diol
2,4-PDO	Pantane-2,4-diol
RID	Refractive index detector
RPM	Rotation per Minute
SA	Silica-Alumina
SAPO	Silicoaluminophosphate
SBA	Santa Barbara Amorphous
Si	Silica
THF	Tetrahydrofuran
THFA	Tetrahydrofurfuryl alcohol
TEM	Transmission Electron Microscopy

List of abbreviations

TOF	Turn Over Frequency
UV-Vis	Ultra violet- Visible
XPS	X-Ray Photoelectron Spectroscopy
XRD	X-Ray Diffraction

Synopsis of the thesis

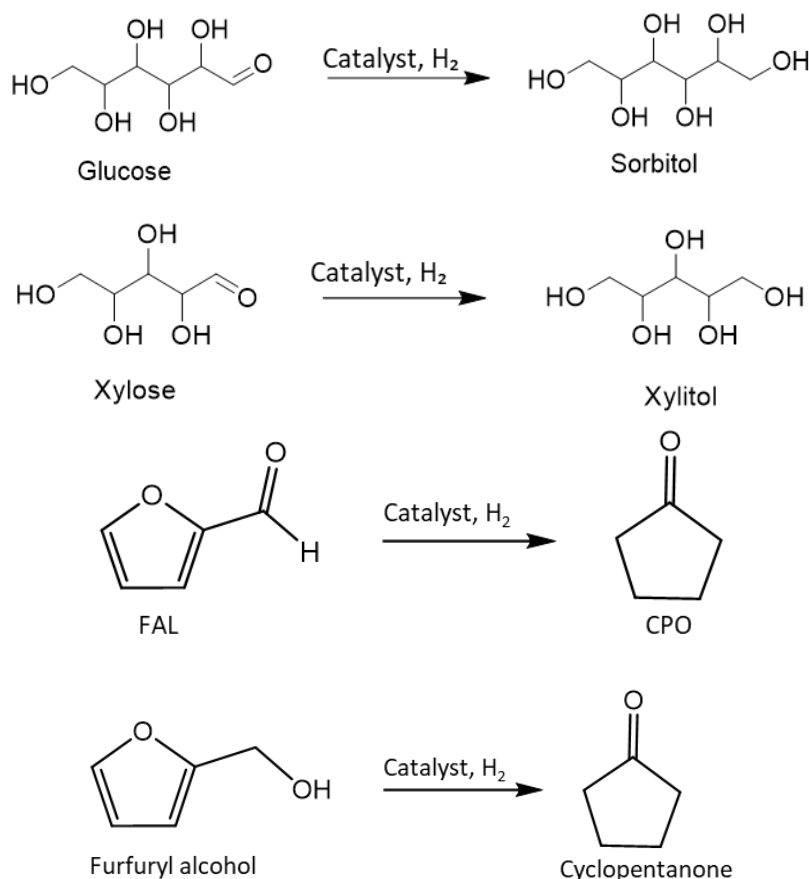
	Synopsis of the Thesis to be submitted to the Academy of Scientific and Innovative Research for Award of the Degree of Doctor of Philosophy in Chemical Sciences
Name of the Candidate	Kadam Jyoti R.
Degree Enrollment No. & Date	10CC18J26010 & January 2018
Laboratory	National Chemical Laboratory, Pune.
Title of the Thesis	Cobalt promoted ruthenium catalysts for the hydrogenation of sugar, furfural and furfuryl alcohol.
Research Supervisor	Dr. Paresh L. Dhepe

1. Introduction:

Biomass is a biological material which is obtained from living or recently dead things like wood, grass, crops etc. and it can be processed into fuels, chemicals and energy. Chemically biomass is carbon based material mainly consists of C, H, O with small amount of N, S and some minerals like Na, K, Mg etc.^[1] Lignocellulosic biomass is most abundant natural and renewable resource for the production of fuels and chemicals. Lignocellulosic biomass is composed of cellulose, hemicellulose and lignin. Cellulose is homo-polysaccharide in which glucose units are linked together via β -(1, 4) glycosidic linkage and its abundance is 35-50%.^[2] Hemicellulose is hetero-polysaccharide made up of C5 and C6 sugars. These sugars are arranged randomly and hence hemicellulose is amorphous in nature and its abundance is 20-30%.^[3] Lignin is 3D, amorphous, hetero polymer consists of coniferyl, sinapyl and coumaryl alcohols which are linked together via C-C and C-O-C linkage and its abundance is 10-25%.^[4] Cellulose on hydrolysis in presence of acid produces glucose and glucose on hydrogenation in presence of H₂ it gives Sorbitol. Similarly, hemicellulose on acid hydrolysis produces xylose which on hydrogenation it gives xylitol. Sorbitol and Xylitol have wide applications in food and pharmaceutical industries. Both are used as a low-calorie sweetener, refreshing agent and for the synthesis of Vitamin C.^[5] Sorbitol is a world's most consumed polyol, it holds biggest market among sugar alcohols i.e. 1.85 million tons in 2015 and is expected to register 2.4 million ton by 2023.^[6]

Xylose on dehydration produces furfural (FAL). Further furfural can be converted into furfuryl alcohol (FOL) and cyclopentanone (CPO). CPO have wide applications in various industries. It is used for the synthesis of fungicides, pharmaceuticals, rubber chemicals, flavour and fragrance chemicals.^[7] It is also used for the preparation of polyamides,^[8] jet fuels and polyolefin.^[8] CPO holds market 107.6 million in 2021 and it is expected to reach USD 101.7 million by the end of 2025 at a growing CAGR of 1.4%.^[9]

Scheme:



2. Statement of the problem:

In literature people have reported noble metal (Pt, Pd, Ru etc.) based catalysts with 3-5 wt% metal loading exhibits high activity but used of noble metal with high metal loading increases the catalyst cost. Non noble metal based catalyst are also reported but these catalysts are less active towards the reactions and hence they require harsh reaction conditions like high

temperature and high H₂ pressure. So considering these applications there is a need to develop an efficient cost effective catalyst system which can be operate at lower temperature and lower H₂ pressure.

3. Methodology:

Many non-noble as well as non noble metal supported catalysts are reported. It is reported that non noble metal based catalysts are less active towards hydrogenation and hence require harsh reaction conditions. Noble metals are well known for hydrogenation but because of their less abundance and high price limits the commercialization. It is well known that among the noble metals,

Ruthenium is reported as highly active metal for the hydrogenation reactions. Previously in literature, different bimetallic catalysts such as Pt,Sn/Al, Pt,Co/C were synthesized and reported that addition of second metal (Sn, Co), which acts as a promoter, will increase the catalytic activity. So considering these reported things, I have synthesised bimetallic catalyst with the combination of Ru metal (with lower loading) and Co metal supported on basic alumina ((1.5)Ru(3)Co/Al-B). Catalyst synthesis was done by wet impregnation method and characterization of catalysts was done by TEM, XRD, XPS, N₂ physisorption methods. Synthesized catalyst was applied for the hydrogenation of sugar, furfural and furfuryl alcohol.

Objectives:

- Optimization of reaction parameters to achieve maximum yield and selectivity
- Study the stability and recyclability of the catalyst system developed
- Carry out the reactions at higher substrate concentrations (10 wt%, 15 wt%, 20 wt% etc.), to make system industrially feasible

4. Results and their interpretation:

Catalyst synthesis and characterization: Catalyst synthesis was done by wet impregnation method and characterization of catalysts was done by TEM, XRD, XPS, N₂ physisorption methods.

TEM analysis: TEM analysis was done to know the particle size and dispersion of metal particles on support. TEM image (Figure 1) of all the monometallic ((1.5)Ru/Al-Basic,

Ru(2)/Al-Basic, (1.5)Co/Al-Basic and (3)Co/Al-Basic) and bimetallic ((1.5)R(3)Co/Al-B and (2)R(1.5)Co/Al-B) catalysts show highly dispersed metal particles on support. Compare to monometallic catalyst (2-4 nm), in bimetallic catalyst decrease in particle size (1.6 nm) was observed. Elemental mapping of bimetallic (1.5)R(3)Co/Al-B catalyst was also done and elemental mapping confirms presence of Co and Ru metals with homogeneous dispersion on support.

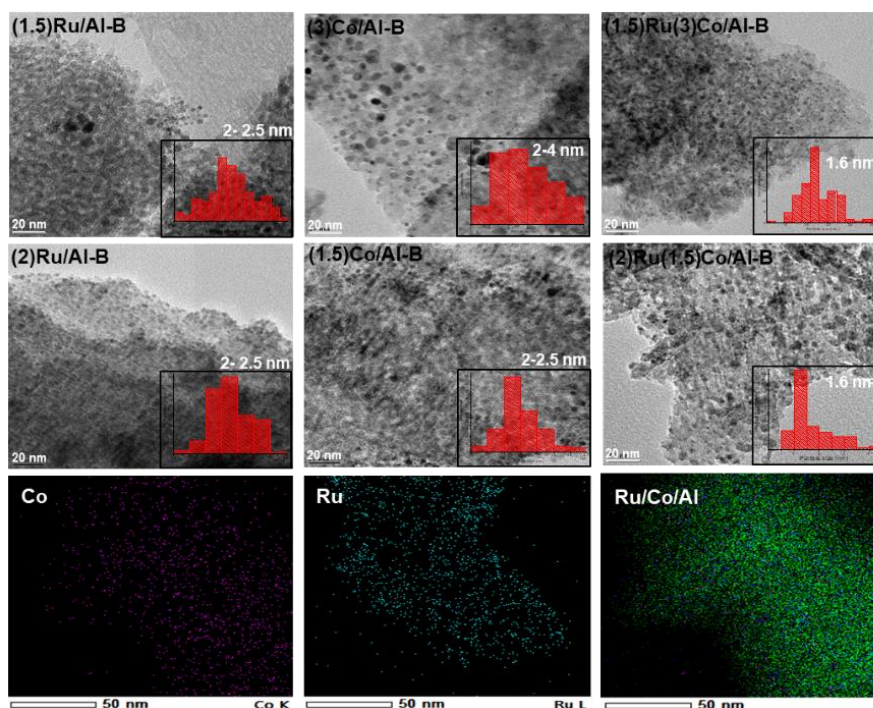


Figure 1. TEM images of monometallic and bimetallic catalysts

XRD analysis: XRD analysis of the monometallic and bimetallic catalyst was done to know the crystalline planes of Ru and Co present in the catalysts. XRD patterns of Ru(1.5)Co(3)/Al-B (Figure 2) shows peaks at around 2θ of 19° , 37.6° , 39.4° , 42.5° , 45.8° , 67° and 85° (JCPDS 00-010-0425) are correspond to the Al_2O_3 support. No Peaks are observed for Ru and Co metal in XRD pattern. This might be due to the lower metal loading or higher dispersion of metal particles on support.

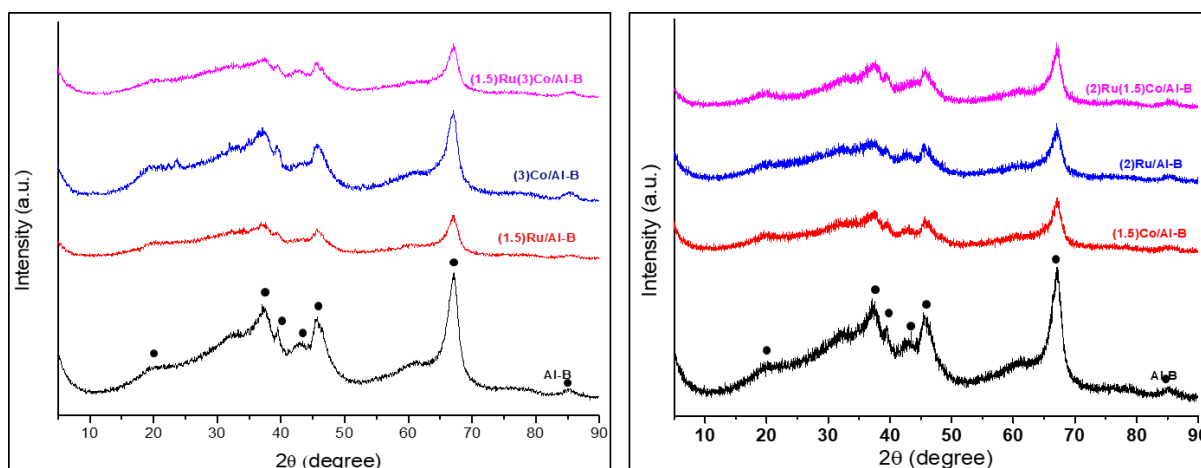


Figure 2. XRD pattern of Ru(1.5)Co(3)/Al-B catalyst

XPS analysis: XPS analysis of mono and bimetallic catalysts were done to find the oxidation states of metals present in the catalyst. In XPS spectrum (Figure 3) of (3)Co/Al catalyst, peaks are observed at B.E. 780.72eV and 796.37eV are corresponds to the Co present in (II) and (III) oxidation state and in monometallic (1.5)Ru/Al catalyst, peaks are observed at B. E. 460.55eV, 463.42eV, 482.3eV and 485.03eV shows Ru is present in (0) and (IV)oxidation state. Same eaks for Co and R were observed in bimetallic catalyst (1.5)Ru, (3)Co/Al also, It meand in bimetallic catalysts also Co is resent in (II) and (III) oxidation state and Ru is resent in (IV) and (0) oxidation state.

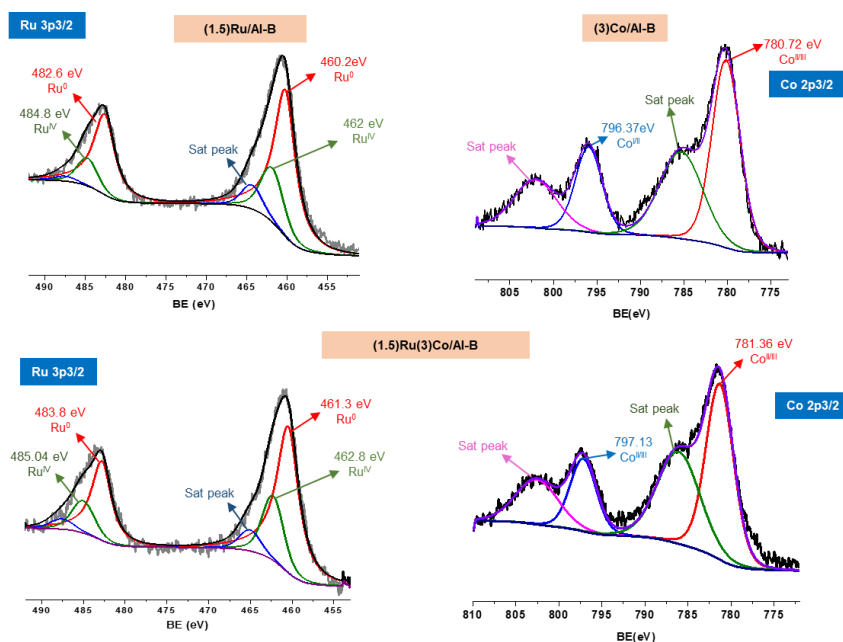


Figure 3. XPS analysis of monometallic and bimetallic catalyst

Hydrogenation of glucose to sorbitol: To check the activity of catalyst for the conversion of glucose to sorbitol, reactions were done in batch mode reactor in water as a solvent at temperature range from 100°C to 140°C and pressure 10 to 15 bar (H₂) pressure. Analysis of reaction mixture was done by HPLC. In HPLC, along with the peak of sorbitol small amount of mannitol (2-3%) was observed.

Reactions were done using monometallic Ru(1.5)/Al-B as well as bimetallic Ru(1.5)Co(3)/Al-B catalyst. Monometallic Ru(1.5)/Al-B catalyst gives 82% conversion of glucose with 68% yield of sorbitol while bimetallic catalyst Ru(1.5)Co(3)/Al-B gives 100% conversion with 91% yield of sorbitol. Bimetallic catalyst shows good activity than monometallic catalyst.

Hydrogenation of xylose to xylitol: To check the activity of catalyst for the conversion of xylose to xylitol, reactions were done in batch mode reactor in water as a solvent at temperature range from 100°C to 120°C and 5 to 15 bar (H₂) pressure. It was observed that by increase in temperature and pressure, increase in conversion and yield was observed. Highest yield of sorbitol (93%) with complete glucose conversion (100%) was observed at 130°C temperature, 15 bar H₂ pressure and 3 h reaction time. Analysis of reaction mixture was done by HPLC. In HPLC, along with the peak of xylitol small amount of Arabinose (2%) and Arabitol (4%) was observed.

Reactions were done using monometallic Ru(1.5)/Al-B as well as bimetallic Ru(1.5)Co(3)/Al-B catalyst. Monometallic Ru(1.5)/Al-B catalyst gives 89% conversion of xylose with 72% yield of xylitol at 120°C temperature, 15 bar H₂ pressure and 3 h reaction time while using same reaction condition bimetallic catalyst Ru(1.5)Co(3)/Al-B gives 100% conversion with 93% yield of xylitol. Bimetallic catalyst shows good activity than monometallic catalyst.

Hydrogenation furfural to cyclopentanone: To check the activity of catalysts for the conversion of FAL to CPO, reactions were done at different temperature ranging from 160 to 200°C and pressure ranging from 10 to 16 bar H₂. And it is observed that Ru(2)Co(1.5)/Al-B catalyst shows best activity in toluene/water solvent at 160°C temperature, 13 bar H₂ pressure and 6h is the reaction time. Ru(2)Co(1.5)/Al-B catalyst shows 100% FAL conversion with 74% CPO and 2% cyclopentanol (CPL) yield. Analysis of reaction mixture was done using GC and HPLC.

Hydrogenation furfuryl alcohol (FOL) to cyclopentanone: Activity of Ru(2)Co(1.5)/Al-B catalyst was checked for the conversion of FOL to CPO, reactions were done at 170°C to 200°C temperature, 10 to 15 bar H₂ pressure for different reaction time. And it is observed that catalyst Ru(2)Co(1.5)/Al-B shows best activity for the conversion of FOL to CPO at reaction condition 190°C, 13 bar H₂ pressure and 80 min reaction time. (2)Ru,(1.5)Co/Al-basic catalyst shows 100% FOL conversion with 74% CPO, 4-5% THFA, 2% cyclopentanol (CPL) yield. Analysis of reaction mixture was done by HPLC. In HPLC small amount of diols was also observed.

Conclusions:

- Synthesis of a bimetallic catalyst RuCo/Al-B demonstrate better activity for the hydrogenation of sugars, furfural and furfuryl alcohol
- Effect of basicity of the support has been elucidated in activation of carbonyl groups
- Promotional effect of Coⁿ⁺ in the catalyst in activation C-O bond in carbonyl group has been verified in the hydrogenation sugars (both C5 & C6)
- Catalyst developed is having high recyclability and stability under the optimized reaction conditions
- Milder reaction conditions make the process energy efficient
- Use of reduced amount of noble metal
- The studied systems can be commercially viable and scale up of the process is feasible.

References:

1. <http://www.biomassenergycentre.org.uk>
2. M. Berchel, J. Haddad, S. p. S. Le Corre, J.P. Haelters and P.A. JaffrÃs, *Tetrahedron Letters*, 2015, **56**, 2345-2348.
3. A. Demirbas, *Energy conversion and Management*, 2000, **41**, 633-646.
4. E. Sjöström, *Wood Chemistry. Fundamentals and Applications*, 2nd edition, Academic Press, San Diego, CA, USA, 1993.
5. J. Zhang, J. B. Li, S. B. Wu and Y. Liu, *Industrial and Engineering Chemistry Research*, 2013, **52**, 11799.

- Catalyst developed is having high recyclability and stability under the optimized reaction conditions
- Milder reaction conditions makes the process energy efficient
- Use of reduced amount of noble metal
- The studied systems can be commercially viable and scale up of the process is feasible.

References:

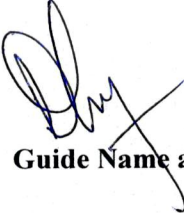
1. <http://www.biomassenergycentre.org.uk>
2. M. Berchel, J. Haddad, S. p. S. Le Corre, J.P. Haelters and P.A. JaffrÃs, *Tetrahedron Letters*, **2015**, *56*, 2345-2348.
3. A. Demirbas, *Energy conversion and Management*, **2000**, *41*, 633-646.
4. E. Sjöström, *Wood Chemistry. Fundamentals and Applications*, 2nd edition, Academic Press, San Diego, CA, USA, **1993**.
5. J. Zhang, J. B. Li, S. B. Wu and Y. Liu, *Ind. Eng. Chem. Res.*, **2013**, *52*, 11799.
6. <http://industry-experts.com/verticals/food-and-beverage/xylitol-a-global-market-overview>, **2017**.
7. Y. Wang et al., *Chemical Engineering Journal*, **2016**, *299*, 104–111.
8. M. Hronec et al., *Applied Catalysis A: General*, **2012**, *437–438*, 104–111.
9. <https://www.decisiondatabases.com/ip/17276-cyclopentanone-market-analysis-report>

Publications:

1. J. R. Kadam, T. S. Khan and P. L. Dhepe, Designing an industrially viable bimetallic catalyst for the polyol synthesis, *New Journal of Chemistry*, **2023**, *47*, 7548-7555.


Student Name and signature

Name- Kadam Jyoti R.


Guide Name and Signature

Name- P. L. Dhepe

Chapter 1.

Introduction and literature survey

1.1. Introduction to biomass:

Many of the chemicals we use everyday life are manufactured from raw materials (coal, natural gases and crude oil etc.) which are derived from non-renewable fossil feedstock's. However, the main issues with these resources are their lack of renewability and sustainability and limited availability. Another major issue with these resources is an environmental issue. Use of fossil feedstock's generates carbon oxides (CO and CO₂), nitrogen oxides (NO₂ and N₂O) and sulfur oxides (SO₂ and SO₃), which causes global warming, acid rain etc. Biomass is a renewable, sustainable and environmentally friendly resource for the synthesis of products with added value.¹ After fossil feedstock's (coal and oil) the only world's third largest source of energy is biomass.² Biomass is a biological material which is obtained from living or recently dead things like wood, grass, crops etc. and it can be processed into fuels, chemicals and energy. Chemically biomass is a material mainly made up of carbon (C), hydrogen (H), oxygen (O) with small amount of nitrogen (N), sulphur (S) and some minerals like Na, K, Mg etc.³ Biomass which is non-edible to human being is commonly known as lignocellulosic biomass and is consist of cellulose, hemicellulose and lignin.⁴ The transformation of lignocellulosic biomass to value-added products such as fuels and chemicals is currently attracting the interest of researchers as it is a renewable, widely accessible, environmentally friendly, and sustainable bio resource.

1.2. Concept of biorefinary:

A biorefinary concepts was defined by the US department of energy in 1990's.⁵ It is an industry facility that converts biomass feedstock's such as lignocellulosic biomass to fuels, energy and chemicals with added value in sustainable manner. Petro-refineries, often known as oil refineries, are a process that uses fossil feedstock's to generate fuels and chemicals. Due to the rapidly diminishing supply of fossil feedstock's, Biomass feedstock's gaining more importance on a global scale through biorefinary concept. Biomass feedstock's are easily available and renewable, emitted less number of hazardous products and greenhouse gases and lowers the environment pollution. C, H and O are the main constituents of the chemicals which are produced from biomass. When these chemicals are used, they emit CO₂. Plants absorbs that

emitted CO₂ through the process of photosynthesis and convert it into carbohydrates, making the process carbon neutral (Figure 1.1). Consequently, the idea of biorefinery is a step towards the developing the sustainable system of the formation of energy, fuels and chemicals. Therefore, with a goal to reduce the issues related to fossil feedstock's, it is essential that we use biomass in addition to fossil feedstock's

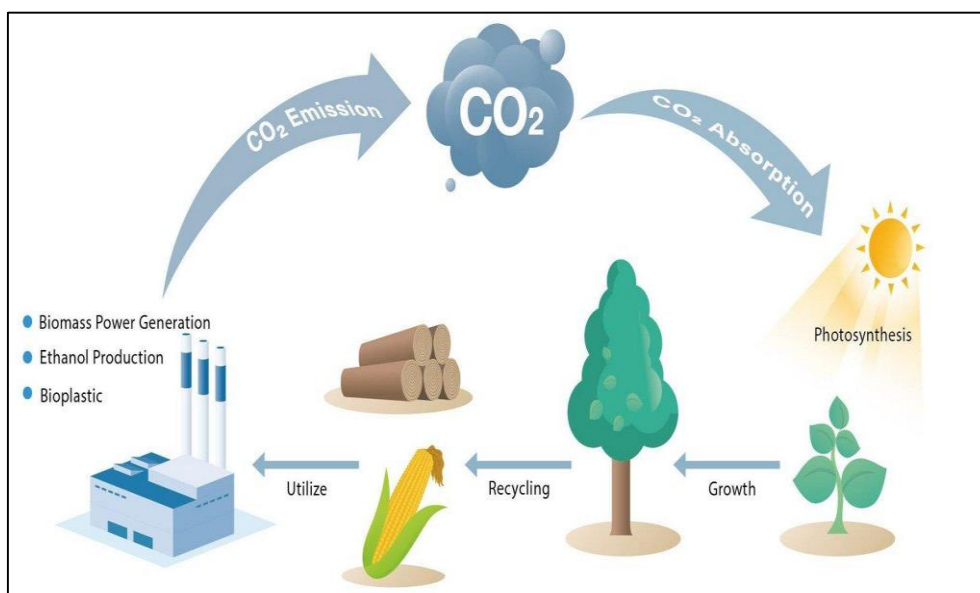


Figure 1.1. Biomass as a carbon neutral feedstock.

1.3. Classification of biomass:

Depending on their sources, biomass is primarily divided into two categories: animal derived biomass and plant derived biomass. Chitin, algae, cow dung etc. are the examples of animal derived biomass and crops, wood, garbage etc. are the examples of plant derived biomass. Again, plant derived biomass is divided into edible and non-edible biomass. Starch and oils such as mustard oil, coconut oil, corn oil, etc. are examples of edible plant biomass that humans use in their daily lives. And non-edible type of biomass is often referred as

lignocellulosic biomass and over the past decade, lignocellulosic biomass has drawn a lot of attention. Figure 1.2 represents the classification of biomass.

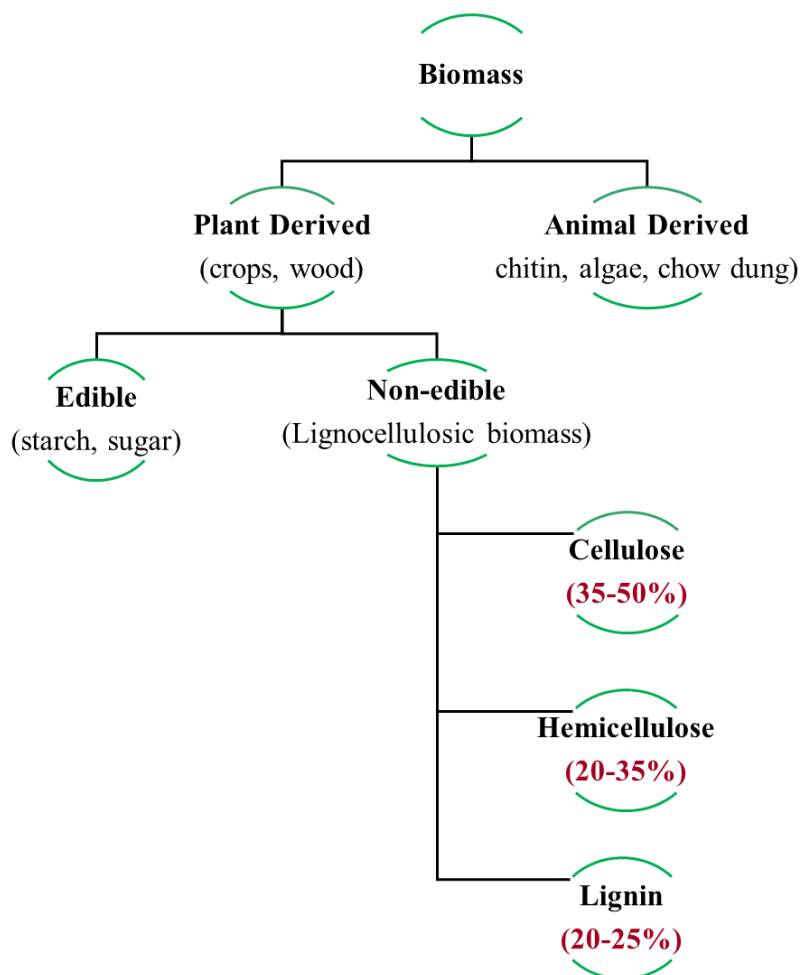


Figure 1.2. Classification of biomass

1.3.1. Chemical composition and structure of lignocellulosic biomass:

Lignocellulosic biomass is a structure made up of cellulose, hemicellulose and lignin. The components of these lignocelluloses can be separated into individual compound by physical, chemical or biological treatment.

Cellulose is an organic substance classified as polysaccharides which is obtained in the primary cell wall of green plant. It is a most abundant polymer on earth. Cellulose is natural

linear homo-polysaccharide in which glucose units are connected together by β -(1 \rightarrow 4) glycosidic linkage (Figure 1.3) and its abundance is 35-50%.⁶ The cellulose molecule naturally has a strong crystalline structure because of its inter and intra molecular hydrogen interactions.^{7,8}

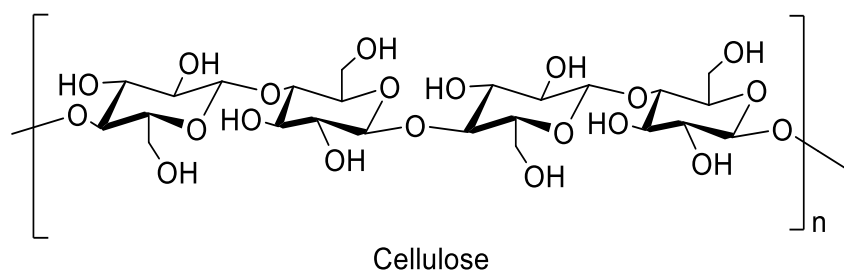


Figure 1.3. Structure of cellulose.

Hemicellulose is a wide category of polysaccharide which is present in both primary and secondary cell walls of plants. After cellulose, hemicellulose is a second most abundant component of lignocellulosic biomass. Unlike cellulose, hemicellulose is a branched heteropolysaccharide composed of different C₅ and C₆ sugars (xylose, mannose, arabinose, glucose etc.), depending upon the plant in which they occur. As shown in Figure 1.4, in hemicellulose various sugar units are connected together by β -(1 \rightarrow 4), β -(1 \rightarrow 3), α -(1 \rightarrow 2) glycosidic linkages.⁹ Hemicellulose has an abundance of 20–30% and is amorphous in nature due to the random arrangement of sugar units.¹⁰

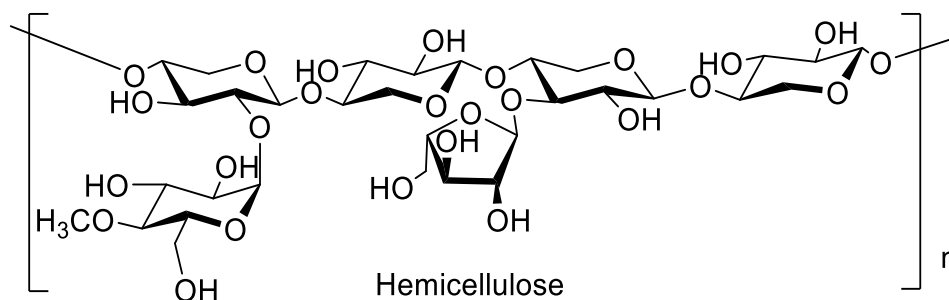


Figure 1.4. Structure of hemicellulose (xylan).

Lignin is 3D, amorphous, hetero-polymer of cross-linked aromatic compounds. It is made up of three structural units i.e. sinapyl alcohol, coniferyl alcohol and coumaryl alcohols (Figure 1.5) that are bound together by C-C and C-O-C linkage. Natural abundance of lignin in lignocellulosic is 10-30%.^{11,12} Hardwood is made up of 20-25% of lignin and softwood contains about 30% of lignin.¹³ After cellulose and hemicellulose, lignin is the third most abundant element of lignocellulosic biomass. Because of the rigid structure of lignin, it increases the rigidity of plants cell wall.

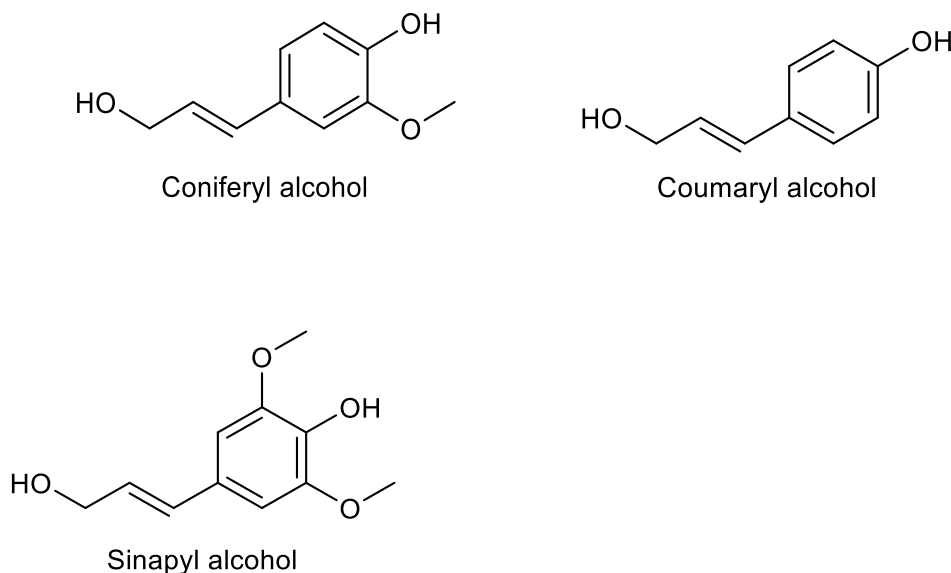


Figure 1.5. Structure of lignin monomers

1.3.2. Sources and advantages of lignocellulosic biomass:

As show in Figure 1.6, the most widely available sources of lignocellulosic biomass are:

- **Agriculture crop wastes:** rice husk, wheat straw, corn cob etc.
- **Forest products:** wood, logging residues, trees, shrubs, etc.
- **Aquatic biomass:** algae, water weed, etc.



Figure 1.6. Sources of biomass

Advantages of lignocellulosic biomass:

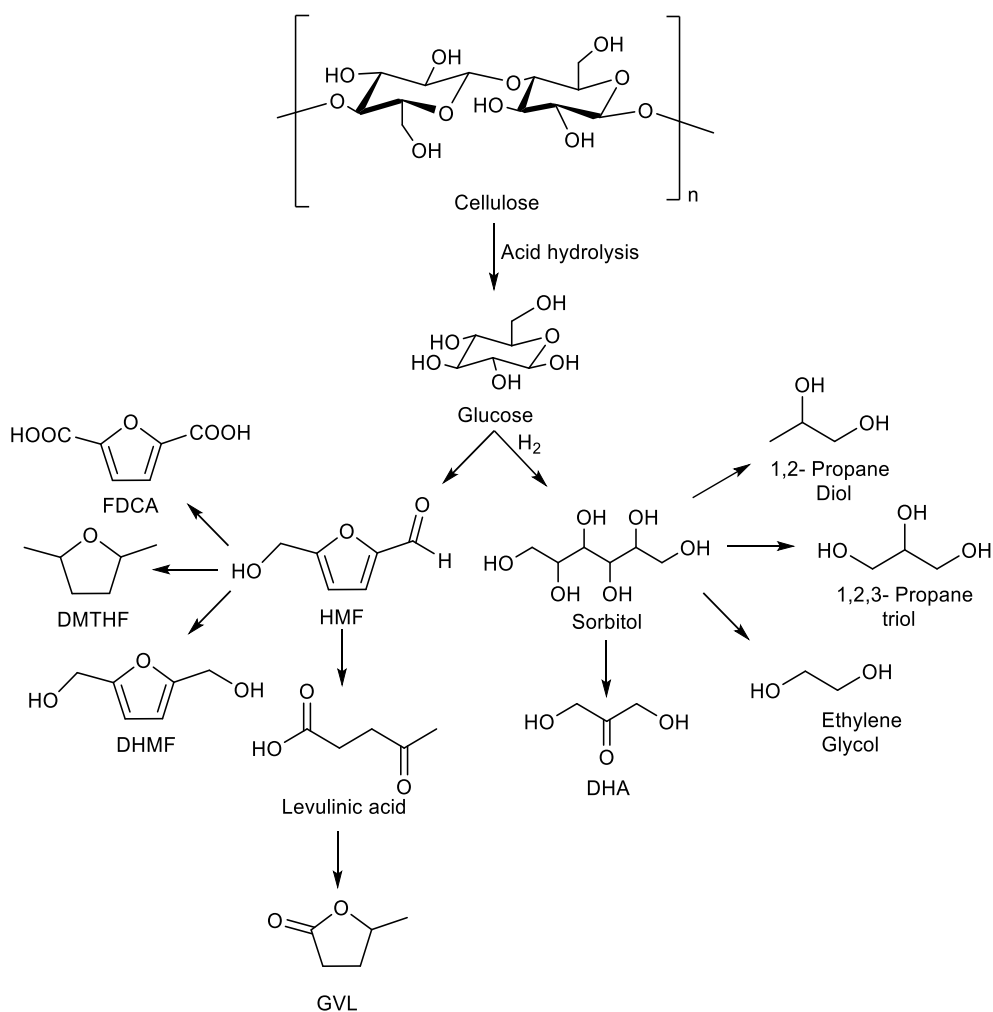
Since lignocellulosic biomass is a sustainable and renewable resource, it has several advantages. Currently it is receiving a lot of attention in many industries. The key advantages of lignocellulosic biomass are listed below:

- Renewable – Easily generated within short time.
- Non- edible to humans
- Most widely and easily available
- Cost effective- Readily available at low cost.
- Biodegradable
- Carbon neutral- Plants take CO₂ and turn it into carbohydrates during the photosynthesis process, making the process environmentally friendly.

1.4. Biomass conversion:

1.4.1. Conversion of cellulose to platform chemicals:

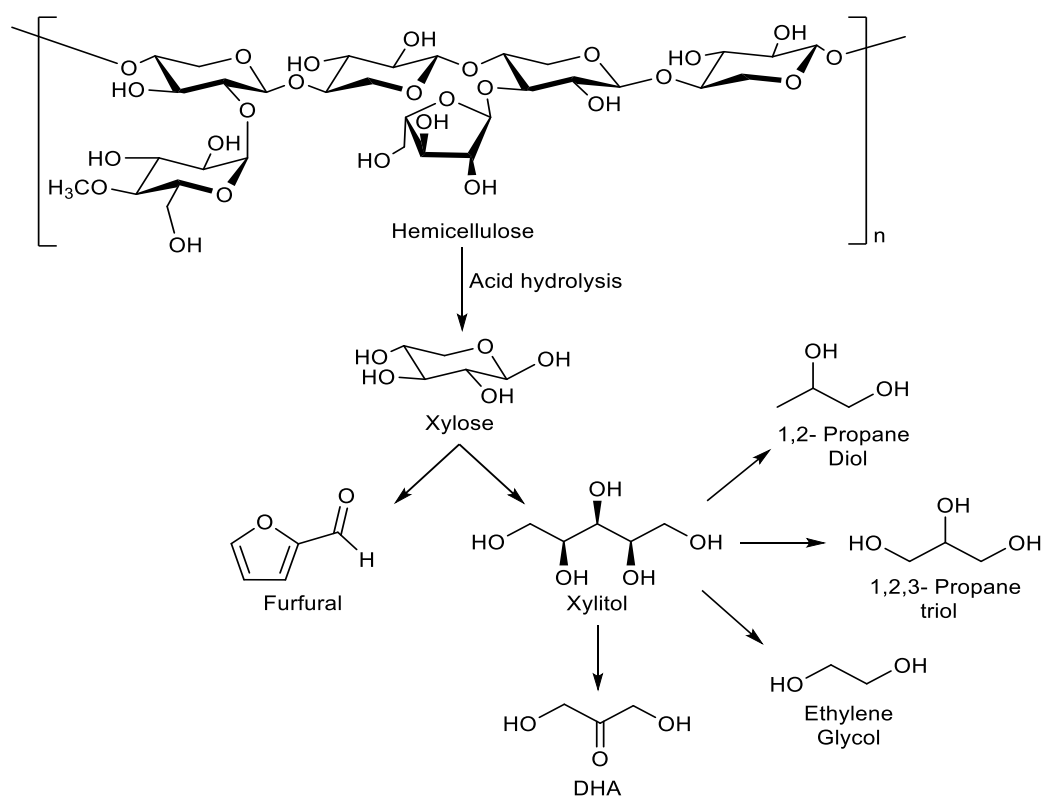
As shown in Scheme 1.1, cellulose which is made up from glucose units, which on hydrolysis in presence of acids it produces glucose.¹⁴⁻¹⁷ Glucose undergoes several reactions produces different chemicals. Glucose undergoes dehydration reaction produces 5-hydroxymethylfurfural (HMF).^{18,19} HMF can further be converted to levulinic acid, 2,5-furandicarboxylic acid (FDCA), 2,5-dimethyl tetrahydrofuran (DMTHF), 2,5-dihydroxymethylfuran (DHMF) γ -valerolactone (GVL) etc. Glucose upon hydrogenation produces sorbitol. Sorbitol can further catalytic hydrogenolysis forms glycols.²⁰⁻²²



Scheme 1.1. Conversion of cellulose to chemicals

1.4.2. Conversion of hemicellulose to platform chemicals:

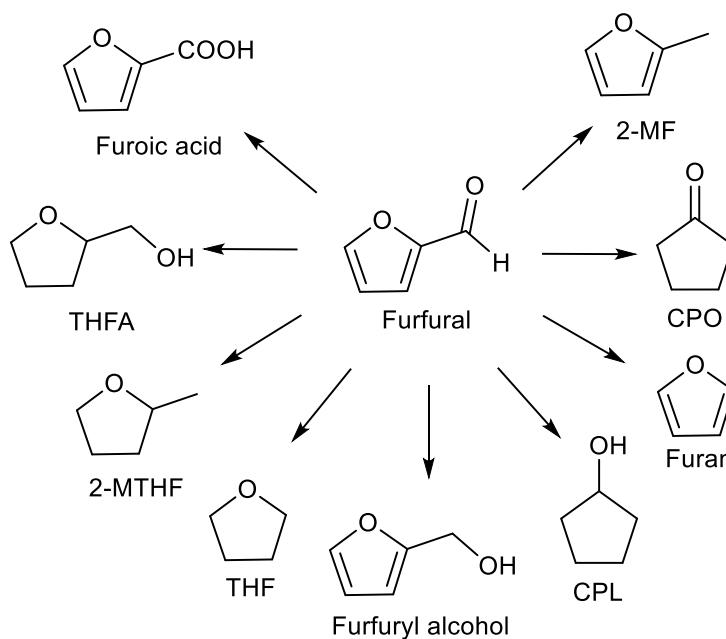
Hemicellulose (xylan) is made up of xylose units, which on acid hydrolysis produces xylose (Scheme 1.2).^{23,24} Xylose undergoes acid dehydration reactions produces furfural.^{25,26} Xylose on hydrogenation it gives xylitol. Xylose can be further converted into glycols, dihydroxyacetone (DHA) etc.



Scheme 1.2. Conversion of hemicellulose to chemicals

1.4.3. Conversion of furfural to platform chemicals:

One of the most important compounds produced from lignocellulosic biomass is furfural. As discussed, in section 1.4.2 (Scheme 1.2), furfural can be synthesized by acid-catalysed dehydration of xylose. As shown in Scheme 1.3, furfural can further be transformed into number of useful chemicals with additional value, such as furfuryl alcohol, cyclopentanone (CPO), cyclopentanol (CPL), tetrahydrofurfuryl alcohol (THFA), furan, tetrahydrofuran (THF), 2-methylfuran (2-MF), 2-methyltetrahydrofuran (2-MTHF), furoic acid etc.²⁷⁻³⁰



Scheme 1.3. Conversion of furfural (FAL) to chemicals

As mentioned above, biomass can be transformed into a variety of chemicals. Among them sugar alcohols (sorbitol and xylitol) and cyclopentanone (CPO) possesses wide range of applications in different industries, including food, cosmetics, pharmaceuticals etc. Additionally, U. S. department of energy (DOE), listed sorbitol and xylitol in the top 12 value added chemicals from biomass. Owing its significance and numerous applications, sorbitol, xylitol and cyclopentanone (CPO) hold a substantial marketplace.

1.5. Applications of sorbitol, xylitol and cyclopentanone:

1.5.1. Applications of sorbitol and xylitol:

Sorbitol is a most commonly and commercially available polyol used as a sweetener which is obtained from hydrogenation of glucose. Sorbitol is utilized extensively in the pharmaceutical, cosmetics and food sectors as low-calorie sweetener, texturizing and anti-crystalizing agent.³¹ It also acts as starting material for the production of, L-ascorbic acid as well as lactic acid.^{32,33} Sorbitol is also used in food and cosmetics. It is also used as an

additive in paper and leather industries. Isosorbide which is an important chemical in synthesis polymer and medicine, can be synthesized from sorbitol.^{34,35} Sorbitol is also used as a plasticizer.³⁶ It is possible to produce polyols, hydrogen and light alkanes (primarily methane) by aqueous-phase reforming (APR) of biomass-derived oxygenates, including glucose, sorbitol, and glycerol.³⁷ Xylitol obtained from xylose can be used as artificial low calorie sweetener in food and pharmaceuticals.³⁸ Due to the antibacterial properties of xylitol, it is also used in the prevention of dental and other infections.³⁹

1.5.2. Applications of cyclopentanone:

Cyclopentanone is used for the synthesis of fungicides, pharmaceuticals, rubber chemicals, flavour and fragrance chemicals.^{40,41} Cyclopentanone is used as a raw material for the synthesis of precursors of diesel and jet fuels having C15 and C17 molecules.⁴² It can be used for the preparation of polyamides and polyolefin stabilizers.^{43,44}

1.6. Global market of sorbitol, xylitol and cyclopentanone:

- The global market of sorbitol was valued USD 1.47 billion in 2022 and it is estimated to reach USD 2.48 billion in 2029 with a growing CAGR of 6.2%.⁴⁵
- The market of mannitol was estimated to be worth USD 0.398 billion in 2020 and is anticipated to reach USD 0.516 billion by 2026, expanding at a CAGR of 4.14%.⁴⁶
- The global xylitol market was reported USD 0.901 billion in 2020 and it is expected to grow at a CAGR of 2.59 from 2021 to 2028 and it is expected to report USD 1.1 billion in 2028.⁴⁷
- The market size of FAL was globally estimated at USD 0.556 billion in 2022 and it is projected to grow at a CAGR of 7.0% from 2023 to 2030.⁴⁸
- The size of global market for furfuryl alcohol was evaluated USD 0.472 billion in 2020 and it is anticipated to increase at a CAGR of 7.2% from 2021 to 2028.⁴⁹
- In 2021, the global market for cyclopentanone was estimated USD 0.127 billion and it is anticipated to grow to 0.175 billion in 2031 with a projected CAGR of 3.3%.⁵⁰

1.7. Literature survey:

1.7.1. Literature survey for the hydrogenation of sugars to sugar alcohols:

It is widely accepted that conversion of sugars to sugar alcohols can be carried out via enzymatic, microbiological, or chemical processes.⁵¹⁻⁵⁵ Of all three, the biological method results in lower sugar conversions and lower sugar alcohol yields and also necessitates longer reaction durations. Therefore, it is appearing that the chemical approach of producing sugar alcohols is more effective than the biological method and hence it is used in industry. commercially sorbitol and xylitol are produced using the RANEY® nickel catalyst because of its low cost and earth abundant nature. However, hydrogenation over the RANEY® nickel catalyst takes place under very high H₂ pressures such as 40–150 bar.⁵⁶⁻⁶² Despite it is commercially used, major drawback of RANEY® nickel catalyst is, it easily turned inactive due to the metal leaching, metal sintering or carbon deposition on active sites.⁶³ Additionally, the sugar alcohol and leached metal combine to form a complex, which adds extra step to the product purification process.

Ni/SiO₂ catalyst is reported for the conversion of glucose to sorbitol shows no significant nickel leaching but catalyst is less active and shows lower sorbitol yield 42%.⁶⁴ In addition to nickel, scientists have reported range of various noble metals based catalysts, such as Ru, Pt, Pd etc. to achieve better conversion and yield for the sugars to sugar alcohols reactions.^{65,66} Among them Ru based catalysts exhibits greater activity when compared to other metal based catalysts.⁶⁷ Numerous studies have been conducted on Ru based catalysts. Ru catalyst supported on NiO-TiO₂ with a Ru loading of 1% ((1)Ru/NiO-TiO₂) is also known to have a high yield of sorbitol (93%) at 120°C, 55 bar H₂ pressure.⁶⁸ Ru nanoparticles with different Ru loading supported amine functionalized nanoporous polymer catalyst (Ru/AFPS) reported and showed complete glucose conversion and highest sorbitol yield of 98% with (5)Ru/AFPS catalyst at 100°C and 55 bar H₂ pressure.⁶⁹ The impact of carbonized cassava dregs (CCD) supported on Ru catalysts have been investigated and reported 99% conversion and 98% sorbitol yield.⁷⁰

Table1.1. Literature survey for the hydrogenation of glucose to sorbitol

Sr. No.	Catalyst	Temp (°C)	H ₂ pressure (bar)	xylose conversion (%)	xylitol yield (%)	Ref.
1.	((1)Ru/NiO-TiO ₂)	120	55	100	93	68
2.	(5)Ru/AFPS	100	55	100	98	69
3.	Ru/CCD	120	30	99	98	70
4.	(8.33)Fe(8.33)Ni/CB	140	30	44	25	77
5.	(13)Ni(2)Ru@PCS	140	30	99	99	78
6.	Ni-Co-HZSM-5	120	30	100	98	79
7.	(5)Cu/ SiO ₂	130	30	45	35	80
8.	(5)Ni/Al ₂ O ₃	130	30	60	50	80

Numerous researchers have also conducted in-depth studies on the effects of different supports (NiO, SiO₂, TiO₂, AC, KLTL zeolite, etc.) to convert xylose into xylitol. Ru nanoparticle supported on a zeolite Y ((1)Ru/HYZ-80) were reported 62% xylose conversion with 61% xylitol yield at 120°C under 55 bar H₂ pressure.⁷¹ Pt/Al catalyst was reported 99% xylose conversion and 78% xylitol yield at 60°C and 16 bar H₂ pressure in presence of HT.⁷² 99% xylitol yield was reported with 100% xylose conversion using Ru@Dowex-H catalyst at 120°C under 30 bar H₂ pressure.⁷³ Complete xylose conversion and 98% xylitol production were reported using (5)Co/SiO₂ catalyst at 140°C and 50 bar H₂ pressure. The stability study of (5)Co/SiO₂ catalyst was investigated and reported that the catalyst is displaying significant deactivation.⁷⁴ Ru/TiO₂ catalyst reported 98% xylitol yield with complete conversion at 120°C under 20 bar H₂ pressure.⁷⁵ Besides this, various Ru-based catalysts with different supports

such as Al₂O₃, ZrO₂, Al₂O₃-ZrO₂, phosphated zirconia (Z-P) and phosphated zirconia alumina (ZP-A) etc. are reported for the hydrogenation of glucose and xylose.⁷⁶

Noble metal-based catalysts exhibit good activity, but due to the high price of precious metals, it is now an increasingly common area of study to replace these (at least partially) with non-noble metals. It has been observed that a number of non-noble metal-based catalysts including (8.33)Fe(8.33)Ni/CB (140°C, 30 bar H₂, conv: 44%, yield: 25%),⁷⁷ (13)Ni(2)Ru@PCS (140°C, 30 bar H₂, conv: 99%, yield: 99%),⁷⁸ Ni-Co-HZSM-5 (120°C, 30 bar H₂, conv: 100%, yield: 98%),⁷⁹ (5)Cu/ SiO₂ (130°C, 30 bar H₂, conv: 45%, yield: 35%), and (5)Ni/Al₂O₃ (130°C, 30 bar H₂, conv: 60%, yield: 50%),⁸⁰ have been reported to convert glucose to sorbitol. But the issues with these catalysts include active metal sintering, leaching, and recycling, and they exhibit reduced selectivity for sorbitol production as compared to noble metal-based catalysts.

Different monometallic as well as bimetallic catalysts with the combination of noble as well as non-noble metals were reported to convert glucose to sorbitol and xylose to xylitol under different reaction conditions. According to reports, noble metals like Pt, Ru etc. exhibits high activity. However, these metals are used with high metal loading (3-5 wt%) which drive up the catalyst's cost. Non-noble metal (Ni, Fe etc.) based catalyst were also employed, however because of their low activity, these catalysts require high temperature and pressure. Commercially, sugar alcohols are produced from sugar using Raney nickel catalyst but this catalyst operates at harsh reaction conditions (80°C – 120°C and 100 - 150 bar H₂ pressure). Also, Ni forms a complex with sugar alcohols that causes leaching, reduces catalyst recyclability and increases the cost of product separation. Considering these limitations of literature survey, it has to be done to develop a recyclable, cost effective catalytic system that can operate at lower temperature and H₂ pressure

Table 1.2. Literature survey for the hydrogenation of xylose to xylitol

Sr. No.	Catalyst	Temp (°C)	H ₂ pressure (bar)	xylose conversion (%)	xylitol yield (%)	Ref.
1.	(1)Ru/HYZ-80	120	55	62	61	71
2.	(3.5)Pt/Al+HT	60	16	99	78	72
3.	(0.2)Ru@Dowex-H	120	30	100	99	73
4.	(5)Co/SiO ₂	140	50	100	98	74
5.	Ru/TiO ₂	120	20	100	98	75

1.7.2. Literature survey for the conversion of furfural (FAL) to cyclopentanone (CPO)

Cyclopentanone (CPO) produced from furfural (FAL) hydrogenation has various applications in different industries, as mentioned in section 1.5.2. Different chemical processes were used for the conversion of FAL to CPO. Initially CPO was synthesised from cyclopentene under dioxygen atmosphere.⁸¹ Moreover, CPO was also been produced by the catalytic cyclization of 1,6-hexaediol and adipic acid.^{82,83} All of these processes use costly fossil feedstock based starting material. These methods are not economically and environmentally sustainable since they use a lot of energy and create waste that is difficult to dispose of. A novel method for producing cyclopentanone from the bio based chemical furfural has been developed to overcome these problems.

The hydrogenation of FAL to CPO is being explored using commercial catalysts made up of noble metals Ru, Pt, and Pd supported over activated carbon. It was found that Ru/C and Pd/C catalysts, Pt/C catalysts selectively forms CPO and CPL at 160°C under 80 bar H₂ pressure.^{84,85} NiCu-50/SBA-15 catalyst was also studied to convert FAL to CPO and reported 62% CPO yield with 99% FAL conversion at 160°C and 40 bar H₂ pressure.⁸⁶ 60% CPO yield

and 100% FAL conversion were accomplished using the CuZnAl-500-0.5 catalyst in 6 h at 150°C under 40 bar H₂ pressure. However, the deactivation of catalyst due to metal leaching and coke deposition was reported in recycle study.⁸⁷ HNO₃ pre-treated CNT supported (30)Ni/CNT catalyst reported up to 83% CPO yield in water medium under 140°C and 50 bar H₂ pressure and 10 h reaction time. Here, a high H₂ pressure was employed and catalyst recyclability was also not shown.⁸⁸ 96% CPO yield was reported using Cu-Ni-Al hydrotalcite based catalyst under 40 bar H₂ and 140°C temperature.⁸⁹ At 160°C and 20 bar H₂ pressure, the Cu-Co catalyst was reported to produce a 62% of CPO.⁹⁰ Complete FAL conversion with 96% CPO yield was achieved using acidic MOF assisted Ru/MIL-101 catalysts when used at 160°C and 40 bar H₂ pressure.⁹¹ Raney Nickel catalyst was also examined to convert FAL to CPO using methanol as hydrogen donor under N₂ atmosphere and achieved 98% FAL conversion and 40% CPO yield at 180°C within 4 h reaction time.⁹² CuNi@C was additionally applied for FAL to CPO reactions at 160°C under 50 bar H₂ pressure; these reactions resulted in 99% conversion of FAL with 97% CPO yield and it can be recycled four times with good stability and activity.⁹³ Pd-Cu supported on carbon catalyst ((5)Pd(10)Cu/C) has been discovered to be very active and selective catalysts for the conversion of FAL to CPO. Under 30 bar H₂ pressure and 160°C temperature, this catalyst showed 98% FAL conversion and 92% CPO yield, however the recycle study was not reported.⁹⁴ The (6)Ru/CNT catalyst in aqueous media successfully produces 91% CPO at 160°C and 10 bar H₂ pressure. But even though a catalyst contains large amount of metal loading, it is not recyclable.⁹⁵ The promoter effect for the hydrogenation of FAL to CPO was examined by adding of metals Ni, Zn, Mo, and Co metal to the Cu/CNT catalyst. The best CPO yield (85%) is shown by the Cu/CNT catalyst ((17)Cu(3)Zn/CNT) at 140°C under 40 bar H₂ pressure.⁹⁶ At 150°C and 30 bar pressure, a (5)Pt/NC-BS-500 catalyst was examined that produced 76% CPO yield in water medium and catalyst was stable and readily recyclable.⁹⁷ Carbon nanotube (CNT) supported Pd and Ru metal based monometallic as well as bimetallic catalysts were also examined and found that in contrast with monometallic, bimetallic catalysts were more active. Under 80 bar H₂ pressure and 200°C, achieved 77% CPO yield with complete FAL conversion.⁹⁸ TiO₂ supported Ni based bimetallic (NiCo/TiO₂ and NiFe/TiO₂ with Ni/Co or Ni/Fe molar ratio of 3) catalysts are being examined for FAL to CPO conversion. Very low CPO (27%) yield was obtained under

30 bar H₂ and 110°C, very little CPO (27%) yield was reported with these catalysts.⁹⁹ The performance of several silica supported Pd catalysts has been studied, and it was shown that the fumed silica supported (4)Pd/f-SiO₂ catalyst performed the best, 100% FAL conversion and 87% CPO formation at 160°C under 35 bar H₂ pressure.¹⁰⁰ 91% CPO yield with 100% FAL conversion was reported using Cu/ZrO₂ catalyst at 150°C and 15 bar H₂ pressure.¹⁰¹ Bimetallic (3)Pt(3)Co/C catalysts operating at 180°C and 10 bar H₂ pressure have also been reported to convert FAL to CPO, with a reported 75% CPO yield using a biphasic solvent system.¹⁰² Further using Fe-MIL supported Pd nanoparticle catalyst (Pd/Fe-MIL-100), 85% CPO yield with 100% FAL conversion was reported with easy recyclability of catalysts up to five runs.¹⁰³ Pd/Cu-MOF catalyst was reported 99% conversion of FAL with 91% yield of CPO within 24 h reaction time at 40 bar H₂ pressure and 150°C.¹⁰⁴ The conversion of FAL to CPO was studied using the NiFe/SBA-15 catalyst, and it was discovered that adding Fe to Ni catalysts inhibits the furan ring hydrogenation and THFA formation and increases the CPO yield. The NiFe/SBA-15 catalyst possesses the good catalytic efficiency, 90% CPO yield at 160°C and 35 bar H₂ pressure.¹⁰⁵ Using Pd/UiO-66-NO₂ catalyst exhibits excellent performance and reported 94% CPO yield at 120°C and 30 bar H₂ pressure.¹⁰⁶ Ni-P-Al₂O₃ catalysts modified with phosphorus exhibited 97% FAL conversion and 72% CPO yield at 190°C and 30 bar H₂ pressure.¹⁰⁷ It was also reported that, over Ni/TiO₂ catalyst the conversion of FAL to CPO has been done at 160°C under 30 bar H₂ pressure and achieved complete FAL conversion with 83% CPO yield within 3 h reaction time.¹⁰⁸ 87% CPO yield and 100% FAL conversion at 130°C and 15 bar H₂ pressure was reported over Ni@NP-C catalyst pyrolyzed at 400°C.¹⁰⁹ Nitrogen doped Co catalyst (Co@NC) at 200°C and 30 bar H₂ pressure exhibits complete FAL conversion with 86% CPO yield but because of the agglomeration of Co particles under reaction condition the catalyst is not recyclable.¹¹⁰

Table 1.3. Literature survey for the conversion of FAL to CPO

Sr. No.	Catalyst	Temp (°C)	H₂ pressure (bar)	FAL conversion (%)	CPO yield (%)	Ref.
1.	NiCu-50/SBA-15	160	40	99	60	86
2.	CuZnAl-500-0.5	150	40	100	60	87
3.	(30)Ni/CNT	140	50	96	83	88
4.	Cu-Ni-Al-HT	140	40	100	96	89
5.	Cu-Co	160	20	100	62	90
6.	Ru/MIL-101	160	40	100	96	91
7.	CuNi@C	160	50	99	97	93
8.	(5)Pd(10)Cu/C	160	30	98	92	94
9.	(6)Ru/CNT	160	10	99	91	95
10.	(17)Cu(3)Zn/CNT	140	40	95	85	96
11.	(5)Pt/NC-BS-500	150	30	100	76	97
12.	(4)Pd/f-SiO ₂	160	35	100	87	100
13.	Cu/ZrO ₂	150	15	100	91	101
14.	(3)Pt(3)Co/C	180	10	100	75	102
15.	Pd/Cu-MOF	150	40	99	91	104
16.	NiFe/SBA-15	160	35	99	90	105
17.	Pd/UiO-66-NO ₂	120	30	99	94	106
18.	Ni-P-Al ₂ O ₃	190	30	97	72	107

19.	Ni/TiO ₂	160	30	100	83	108
20.	Ni@NP-C	130	15	100	87	109
21.	Co@NC	200	30	100	86	110

1.8. Catalysts:

Catalysts are the substances that lowers the activation energy of the reaction and speed up the process without being consumed. And the process involves altering the rate of reaction by the addition of catalyst is called catalysis. Catalysts are divided into two primary groups including heterogeneous and homogeneous catalysts. Heterogeneous catalysts are those that are present in different phase than the reaction mixture such as supported metal catalysts, zeolites, metal oxides etc. whereas homogeneous catalysts are present in the same phase such as soluble metal salts, acids and bases etc. There are various drawbacks of homogeneous catalysts such as the difficulty in recovering the catalyst from the reaction medium, limited thermal stability, contamination of catalyst with the product etc. On the other hand, heterogeneous catalysts are easily recoverable and generable, have good thermal stability and are simple to separate. When compared to homogeneous catalysts, heterogeneous catalysts have several advantages. Therefore, nowadays, lot of people are working on heterogeneous catalysts. Since in my thesis, I have used heterogeneous supported metal catalysts for the hydrogenation of sugars, furfural and furfuryl alcohol, I will provide brief introduction to supported metal catalysts.

1.8.1. Supported metal catalysts:

A supported metal catalysts are frequently employed in industry for a variety of processes.¹¹¹ The catalysts in which metal particles are anchored on appropriate supports are known as supported metal catalysts. Metal and support play a role in supported metal catalysts. High surface area provided by support aids in the dispersion and stabilization of metal particles. The general catalytic characteristics of supported metal catalysts are influenced by three fundamental factors.

- i) **Nature of the support:** Role of support in supported metal catalysts is to disperse and stabilize the metal particles. The dispersion of metal particle is directly proportional to the surface area of support. Higher the surface area of support, higher will be the dispersion of metal particles and higher will be the surface area of catalysts. There are three different types of supports that can be used for the synthesis of supported metal catalysts: acidic, basic, and neutral.

- ii) **Nature of the metal:** Nature of metal is a one of the key factors that affects the catalytic properties of supported metal catalysts. Not every metal can be active for all the reactions. The key factor that influences the activity and selectivity of catalysts for a particular reaction is electronic properties of metal. Transition metals, commonly noble metals are used in catalysts synthesis, because of their incompletely filled d orbital and capability to display different oxidation states.

- iii) **Metal-support interactions:** The reactivity, stability and selectivity of the catalyst are significantly influenced by the metal-support interaction. Various interactions can be present in support and metal and the nature of these interactions can be depends upon the synthesis method of catalysts (calcination temperature, pH of the solution etc.) as well as the nature of metal and the nature of support used. In the supported metal catalysts, metal and support are bound together through some chemical interactions. These interactions can result in change on electronic structure of metal particles present in catalyst. Dispersion of metal particles on support is also deepens upon the interactions between the support and the metal. As the interactions between metal and supports becomes stronger, the dispersion of metal particles will be higher and the agglomeration will be less. Metal support interactions can also impact on the size and stability of metal particles

1.8.2. Preparation methods of supported metal catalysts:

The impregnation method and precipitation method, these two methods are often employed to synthesise supported metal catalyst.¹¹²

Impregnation method: A popular method to synthesize supported metal catalysts is impregnation method. Impregnation method involves the implantation of metal particles on a solid support. This process is well renowned for its adaptability and capacity to regulate the loading of metal on the support. In the impregnation method, a certain quantity of the metal precursor solution will be added to the support solution and agitated for a predetermined period of time. Following the removal of extra solvent, calcination or reduction will take place. There are two types of Impregnation methods i) Wet impregnation in which the extra metal precursor solution will be absorbed into the support solution and ii) Incipient wetness impregnation, often referred as dry impregnation method, involves the use of metal precursor volume equivalent to the support's pore volume.

Precipitation method: Precipitation method is one of the widely used method for the synthesis of single or mixed catalysts.¹¹³ The synthesis procedure of this method includes the following steps: The first step is the dissolution process in which precursor salt of active substances dissolved in suitable solvent to form uniform solution. Step two is a precipitation step in which pH of the solution is adjusted to cause the precipitation of those salts. This process is known as a hydrothermal process because the salts may hydrolyze into hydroxide forms or oxides during this precipitation. In third step the solid mass is then collected and dried. And fourth step involves the calcination step. The calcination process is used to transform the active ingredient's salt or hydroxide forms into oxides by reacting with air at the proper temperature.

1.8.3. Monometallic and bimetallic catalysts:

The two varieties of supported metal catalysts that are frequently used in different chemical processes are monometallic and bimetallic. Monometallic catalysts are those that consist of only one metal along with support while bimetallic catalysts are consist of two different metals along with support and these metals can be present as alloys or clusters. The primary driver of catalytic activity for monometallic catalysts is the single metal species while the activity of bimetallic catalysts might be depending upon both the metal. The additional metal in bimetallic catalysts may work as a promoter. Promoter is a component added into the

catalyst with a goal to enhance the efficacy of catalyst.¹¹⁴ The mutual interaction between promoter and active metal species is the main cause responsible for the increase in activity of bimetallic catalysts. Bimetallic catalysts frequently exhibit enhanced catalytic activity and stability when compared to monometallic catalysts. As mentioned in above section 1.8.1, the properties of both monometallic and bimetallic catalysts rely on the type of support and metal, and metal-support and metal-metal interactions. The choice of monometallic or bimetallic catalysts is depends on the particular need of a given reaction.

1.9. Aim and objectives of the thesis:

The literature review and significance of sugar alcohols and cyclopentanone are discussed in section 1.6 and section 1.7. Considering the constraints of a literature review and importance of products, the primary goal of my thesis work is to develop a commercially viable, cost-effective catalytic system to convert sugars, furfural and furfuryl alcohol. The following are my objectives that I have set for my work:

- Synthesis of a suitable catalyst system for the hydrogenation (study different noble & non-noble metal combinations on different supports).

Although noble metal based catalysts with high metal loading are known to have good catalytic activity towards hydrogenation of sugars, furfural and furfuryl alcohol but using those in a catalytic system increases the cost of the system. It is possible to reduce the cost of the catalytic system and make the system acceptable for commercial use by using non-noble metals as a promoter in a combination with noble metals that have a lower metal loading. Also in supported metal catalysts, Support also plays a crucial role. The activity of supported metal catalysts depends on the support, metal and metal support interactions. In order to examine the effects of metal, promoters and supports, different monometallic and bimetallic catalysts with the combination of noble and non-noble metals supported on different supports will be synthesized.

- Optimization of reaction parameters to achieve maximum yield and selectivity.

In order to design an efficient catalytic method and to obtain maximum conversion and yield of desired products, effect of various reaction parameters including pressure, temperature, S/C ratio, time etc. will be studied

- Study the stability and recyclability of the catalyst system developed.

Recyclability is one of the most essential factors from an industrial standpoint, to develop cost effective catalytic system. There are many catalysts have been reported that exhibits excellent activity towards the hydrogenation of sugars, furfural and furfuryl alcohol; Nevertheless, the recyclability remains a concern. Thus, it is essential to development a catalyst system which will be recyclable and cost effective.

- Carry out the reactions at higher substrate concentrations (10 wt%, 15 wt%, 20 wt% etc.).

To make the catalytic system industrially practicable, reactions with higher substrate concentrations will be recommended.

1.10. Hypothesis of the work:

- The combined effect of hydrogen dissociation capability of a noble metal and the C=O bond polarizing effect of a non-noble metal could enhance the hydrogenation of sugars and furfural.

Ru metal is widely known for its ability to activate H₂ molecule during hydrogenation reactions. Co, a non-noble metal can act as Lewis acid and helps to polarize C=O bond of the carbonyl group in sugars and furfural. Interactions of Co⁺ with carbonyl oxygen will increase the electrophilicity of carbonyl carbon and promote the hydride attack on the carbonyl carbon and can help to enhance the hydrogenation of sugars and furfural. Therefore, it is anticipated that bimetallic RuCo/Support catalyst with both metallic and Lewis acidic sites will perform better for the conversion of sugars and furfural.

1.11. Outline of the thesis:

There are a total of six chapters in this thesis. In chapter 1, a thorough introduction to biomass and its classification is discussed. Additional information on lignocellulosic biomass, including its sources, benefits and composition is also included. This chapter also includes the thorough literature survey on the conversion of sugars into sugar alcohols, FAL to CPO and FOL to CPO. The global market and importance of sugar alcohols and cyclopentanone is also covered in this chapter. Supported metal catalysts and their synthesis methods are also discussed in this chapter.

In chapter two, detailed discussions on catalyst synthesis methods and their characterization techniques are covered.

In chapter three the detail experimental procedure for converting of sugars to sugar alcohols is covered. This chapter divided into two sections. section A contains comprehensive experimental procedures, discussions and conclusions regarding the transformation of glucose to sorbitol and part B consist of experimental methods, results and discussions to transform of xylose into xylitol. Additionally, the effect of different C5 and C6 sugars is also discussed. Discussions on higher substrate concentration reactions and a catalyst recycling and spent catalyst characterization also included in both section A and section B of the chapter. Isolation and purification of xylitol and sorbitol is also discussed.

The conversion of FAL to CPO via hydrogenative ring rearrangement is covered in chapter four. This chapter includes the impact of various monometallic and bimetallic catalysts supported on varied supports. Study of different parameters of the reaction including time, pressure and temperature etc. and catalyst recycle study is also carried out.

Chapter five discusses the catalytic activity to convert of FOL to CPO with effect of different reactions parameters (temperature, pressure, time, S/C ratio etc.). The detailed mechanistic study for the conversion of FOL to CPO is also discussed in this chapter.

Chapter six comprises the summery and novelty of the thesis work.

1.12. References:

1. M. J. Ahmed, B. H. Hameed, *Journal of the Taiwan Institute of Chemical Engineers*, 2019, **96**, 341-352.
2. D. W. Bapat, S. V. Kulkarni, and V. P. Bhandarkar, United States: N. p., 1997. Web.
3. <http://www.biomassenergycentre.org.uk>.
4. F. H. Isikgor and C. R. Becer, *Polymer Chemistry*, 2015, **6**, 4497–4559.
5. S. Takkellapati, T. Li, and M. A. Gonzalez, *Clean Technologies and Environmental Policy*, 2018, **20**, 1615–1630.
6. M. Berchel, J. Haddad, S. p. S. Le Corre, J.P. Haelters and P.A. Jaffrès, *Tetrahedron Letters*, 2015, **56**, 2345-2348.
7. M. Hall, P. Bansal, J. H. Lee, M. J. Realff and A. S. Bommarius, *FEBS Journal*, 2010, **277**, 1571-1582.
8. Chun-Hui Zhou, Xi Xia, Chun-Xiang Lin, Dong-Shen Tonga and Jorge Beltramini, *Chemical Society Reviews*, 2011, **40**, 5588–5617.
9. W. Farhat, R. A. Venditti, M. Hubbe, M. Taha, F. Becquart, and A. Ayoub, *ChemSusChem*, 2017, **10**, 305 –323.
10. A. Demirbas, *Energy conversion and Management*, 2000, **41**, 633-646.
11. G. de Gonzalo, D. I. Colpa, M. H. M. Habib and M. W. Fraaije, *Journal of Biotechnology*, 2016, **236**, 110-119.
12. Deepa A. K., Dhepe P. L., *ACS Catalysis*, 2015, **5**, 365-379.
13. F. G. Calvo-Flores and J. A. Dobado, *ChemSusChem*, 2010, **3**, 1227 – 1235
14. Yao-Bing Huang and Yao Fu, *Green Chemistry*, 2013, **15**, 1095–1111.
15. L. Hua, L. Linc, Z. Wua, S. Zhoua, S. Liu, *Applied Catalysis B: Environmental*, 2015, **174–175**, 225–243.

16. Tao Wu, N. Li, X. Pan, Sheng-Li Chen, *Cellulose*, 2020, **27**, 9201–9215.
17. A. Galadima, A. Masudi, O. Muraza, *Microporous and Mesoporous Materials*, 2022, **336**, 111846.
18. Q. Hou, M. Zhen, W. Li, L. Liu, J. Liu, S. Zhang, Y. Nie, C. Bai, X. Bai, M. Ju, *Applied Catalysis B: Environmental*, 2019, **253**, 1–1.
19. M. Zunita, D. M. Yuan, A. S. Laksono, *Chemical Engineering Journal Advances*, 2022, **11**, 100307.
20. P. L. Dhepe, A. Fukuoka, *Catalysis Surveys from Asia*, 2007, **11**, 186–191.
21. L. Zhaoa, J.H. Zhou, Z.J. Sui, X.G. Zhou, *Chemical Engineering Science*, 2010, **65**, 30-35.
22. Y. Jia and H. Liu, *Catalysis Science & Technologies*, 2016, **6**, 7042–7052.
23. P. L. Dhepe and R. Sahu, *Green Chemistry*, 2010, **12**, 2153–2156,
24. B. M. Matsagar and P. L. Dhepe, *New Journal of Chemistry*, 2017, **41**, 6137—6144.
25. V. Choudhary, S. I. Sandler, and D. G. Vlachos, *ACS Catalysis*, 2012, **2**, 2022–2028,
26. C. Wu, W. Yuan, Y. Huang, Y. Xia, H. Yang, H. Wang, X. Liu, *Catalysis Letter*, 2017, **147**, 953–963.
27. Á. O’Driscoll, J.J. Leahya, T. Curtin, *Catalysis Today*, 2017, **279**, 194–201.
28. J. Parikh, S. Srivastava, and Girijsinh C. Jadeja, *Industrial & Engineering Chemistry Research*, 2019, **58**, 16138–16152.
29. Z. Wang, Z. Fu, W. Lin, S. Li and W. Song, *Korean Journal of Chemical Engineering*, 2019, **36**, 1235-1242.
30. B. Li, L. Li, Ha. Sun, and C. Zhao, *ACS Sustainable Chemistry & Engineering*, 2018, **6**, 12096–12103.

31. A. W. Newman, I. M. Vitez, R. L. Mueller, C. C. Kiesnowski, W. P. Findlay, C. Rodriguez, M. Davidovich, G. McGeorge, *Analytical profiles of drug substances and excipients*, 1999, **26**, 459-502.
32. P. Gallezot, P. J. Cerino, B. Blanc, G. Fleche and P. Fuertes, *Journal of Catalysis*, 1994, **146**, 93-102.
33. Ramírez-López, C. A., Ochoa-Gómez, J. R., Gil-Río, S., Gómez-Jiménez-Aberasturi, O., Torrecilla-Soriaa, J., *Journal of Chemical Technology & Biotechnology*, 2011, **86**, 867.
34. J. Xia, D. Yu, Y. Hu, B. Zou, P. Sun, H. Li, H. Huang, *Catalysis Communications*, 2011, **12**, 544–547.
35. N. A. Khana, D. K. Mishra, I. Ahmeda, J. W. Yoonb, Jin-Soo Hwang, S. H. Jung, *Applied Catalysis A: General*, 2013, **452**, 34–38.
36. H. Tian, D. Liu, Y. Yao, S. Ma, X. Zhang, and A. Xiang, *Journal of Food Science*, 2017, **82**, 12.
37. G. W. Huber, R. D. Cortright, and J. A. Dumesic, *Angewandte Chemie*, 2004, **116**, 1575–1577.
38. M. Yadav, D. K. Mishra and J.-S. Hwang, *Applied Catalysis A*, 2012, **425**, 110–116,
39. A. Kogje and A. Ghosalkar, *3 Biotech*, 2016, **6**, 1–10
40. J. Scognamiglio, L. Jones, C.S. Letizia, A.M. Api, *Food and Chemical Toxicology*, 2012, **50**, 608-612.
41. Y. Wang, S. Sang, W. Zhu, L. Gao, G. Xiao, *Chemical Engineering Journal*, 2016, **299**, 104–111.
42. M.Hronec, K. Fulajtárova, T. Liptaj, M. Štolcová, N. Prónayová, T. Soták, *Biomass and Bioenergy*, 2014, **63**, 291-299.

43. Takeshige Takahashi, Kazuhiko Ueno and Takami Kai, *Microporous Materials*, 1993, **1**, 323-327.
44. J. Rychlý, L. Rychla, A. Fiedlerova , S. Chmela, M. Hronec, *Polymer Degradation and Stability*, 2014, **108**, 41-47.
45. <https://exactitudeconsultancy.com/reports/4182/sorbitol-market/>
46. <https://www.globalmarketestimates.com/market-report/global-mannitol-market>
47. <https://www.grandviewresearch.com/industry-analysis/xylitol-market>
48. <https://www.grandviewresearch.com/industry-analysis/furfural-market>
49. <https://www.grandviewresearch.com/industry-analysis/furfuryl-alcohol-market>
50. <https://www.businessresearchinsights.com/market-reports/cyclopentanone-market-100113>.
51. P. Nigam and D. Singh, *Process Biochemistry*, 1995, **30**, 117- 124.
52. T.- B. Kim, Y.- J. Lee, P. Kim, C. S. Kim and D.- K. Oh, *Biotechnology Letters*, 2004, **26**, 623- 627.
53. S.- G. Kwon, S.- W. Park and D.- K. Oh, *Journal of Bioscience and Bioengineering*, 2006, **101**, 13- 18.
54. S.- M. Bae, Y.- C. Park, T.- H. Lee, D.- H. Kweon, J.- H. Choi, S.- K. Kim, Y.- W. Ryu and J.- H. Seo, *Enzyme Microbial Technology*, 2004, **35**, 545- 549.
55. M. M. Silveira · R. Jonas, *Applied Microbiology and Biotechnology*, 2002, **59**, 400–408.
56. M. Herskowitz, *Chemical Engineering Science*, 1985, **40**, 1309-1311.
57. B. Hoffer, E. Crezee, F. Devred, P. Mooijman, W. Sloof, P. Kooyman, A. Van Langeveld, F. Kapteijn and J. Moulijn, *Applied Catalysis A*, 2003, **253**, 437–452.
58. D. Shi, R. Wojcieszak, S. Paul and E. Marceau, *Catalysts*, 2019, **9**, 451.

59. J. Wisniak, M. Hershkowitz and S. Stein, *Product Research and Development*, 1974, **13**, 232–236.
60. T.-t Gao, Y.-g Sun, Y.-b Zhu, F. Lin, Y.-d Zhong, Y.-y Li, W.-x Ji and Y.-l Ma, *New Journal of Chemistry*, 2022, **46**, 16058–16067.
61. A. Fehér, C. Fehér, M. Rozbach, G. Rácz, M. Fekete, L. Hegedűs, Z. Barta, *Chemical Engineering & Technology*, 2018, **41**, No. 3, 496–503.
62. H. Du, X. Ma, M. Jiang, P. Yan, Y. Zhao, Z.C. Zhang, *Catalysis Today*, 2021, **365**, 265–273.
63. D. Shi, R. Wojcieszak, S. Paul and E. Marceau, *Catalysts*, 2019, **9**, 451.
64. S. Schimpf, C. Louis, P. Claus, *Applied Catalysis A: General*, 2007, **318**, 45–53.
65. J. Wisniak, M. Hershkowitz and S. Stein, *Product Research and Development*, 1974, **13**, 232–236.
66. M. Makkee, A. P. Kieboom and H. van Bekkum, *Carbohydrate Research*, 1985, **138**, 225–236.
67. B. J. Arena, *Applied Catalysis A*, 1992, **87**, 219–229.
68. D. K. Mishra, J. –M. Lee, J. –S. Chang, J. –S. Hwang, *Catalysis Today*, 2012, **185**, 104–108.
69. A. A. Dabbawala, D. K. Mishra, J. –S. Hwang, *Catalysis Today*, 2016, **265**, 163–173.
70. Z. Li, Y. Liu, S. Wu, *Bioresources*, 2018, **13**, 1278-1288.
71. D. K. Mishra, A. A. Dabbawala and J.-S. Hwang, *Journal of Molecular Catalysis A: Chemical*, 2013, **376**, 63–70.
72. A Tathod, T. Kane, E.S. Sanil, P. L. Dhepe, *Journal of Molecular Catalysis A: Chemical*, 2014, **388–389**, 90–99.
73. P. Barbaro, F. Liguori and C. Moreno-Marrodan, *Green Chemistry*, 2016, **18**, 2935–2940.

74. M. Audemar, W. Ramdani, T. Junhui, A. Raluca Ifrim, A. Ungureanu, F. Jérôme, S. Royer and K. de Oliveira Vigier, *ChemCatChem*, 2020, **12**, 1973–1978.
75. C. Hernandez-Mejia, E. S. Gnanakumar, A. Olivos-Suarez, J. Gascon, H. F. Greer, W. Zhou, G. Rothenberg and N. Raveendran Shiju, *Catalysis Science & Technology*, 2016, **6**, 577–582.
76. J. J. Musci, M. Montaña, E. Rodríguez-Castellón, Ileana D. Lick, Mónica L. Casella, *Molecular Catalysis*, 2020, **495**, 111150.
77. Y. Fu, L. Ding, M. L. Singleton, H. Idrissi and S. Hermans, *Applied Catalysis B*, 2021, **288**, 119997.
78. R. Xi, Y. Tang, R. L. Smith, X. Liu, L. Liu and X. Qi, *Green Energy Environment*, 2022, DOI: 10.1016/j.gee.2022.04.003.
79. B. Zada, L. Yan and Y. Fu, *Science China Chemistry*, 2018, **61**, 1167–1174.
80. L. Silvester, F. Ramos, J. Thuriot-Roukos, S. Heyte, M. Araque, S. Paul and R. Wojcieszak, *Catalysis Today*, 2019, **338**, 72–80.
81. A. Kishi, T. Higashino, S. Sakaguchi and Y. Ishii, *Tetrahedron Letters*, 2000, **41**, 99–102.
82. T. Akashi, S. Sato, R. Takahashi, T. Sodesawa, K. Inui, *Catalysis Communications*, 2003, **4**, 411–416.
83. M. Renz, *European Journal of Organic Chemistry*, 2005, **2005**, 979–988.
84. M. Hronec, K. Fulajtarová, *Catalysis Communications*, 2012, **24**, 100–104.
85. M. Hronec, K. Fulajtarová, T. Liptaj, *Applied Catalysis A: General*, 2012, **437–438**, 104–111.
86. Y. Yang, Z. Du, Y. Huang, F. Lu, F. Wang, J. Gao and J. Xu, *Green Chemistry*, 2013, **15**, 1932–1940.

87. J. Guo, G. Xu, Z. Han, Y. Zhang, Y. Fu, and Q. Guo, *ACS Sustainable Chemistry & Engineering*, 2014, **2**, 2259–2266.
88. M. Zhou, H. Zhu, L. Niu, G. Xiao, R. Xiao, *Catalysis Letter*, 2014, **144**, 235–241.
89. H. Zhu, M. Zhou, Z. Zeng, G. Xiao, and R. Xiao, *Korean Journal of Chemical Engineering*, 2014, **31**, 593–597.
90. Xing-Long Li, J. Deng, J. Shi, T. Pan, Chu-Guo Yu, Hua-Jian Xu and Y. Fu, *Green Chemistry*, 2015, **17**, 1038–1046.
91. R. Fang, H. Liu, R. Luque and Y. Li, *Green Chemistry*, 2015, **17**, 4183–4188.
92. Y. Xu, S. Qiu, J. Long, C. Wang, J. Chang, J. Tan, Q. Liu, L. Ma, T. Wang and Q. Zhang, *RSC Advances*, 2015, **5**, 91190–91195.
93. Y. Wang, S. Sang, W. Zhu, L. Gao, G. Xiao, *Chemical Engineering Journal*, 2016, **299**, 104–111.
94. M. Hronec, K. Fulajtárová, I. Vávra, T. Soták, E. Dobrocka, M. Micusík, *Applied Catalysis B: Environmental*, 2016, **181**, 210–219.
95. Y. Liu, Z. Chen, X. Wang, Y. Liang, X. Yang, and Z. Wang, *ACS Sustainable Chemistry & Engineering*, 2017, **5**, 744–751.
96. M. Zhou, J. Li, K. Wang, H. Xia, J. Xu, J. Jiang, *Fuel*, 2017, **202**, 1–11.
97. X. Liu, B. Zhang, B. Fei, X. Chen, J. Zhang and X. Mu, *Faraday Discussions*, 2017, **202**, 79–98.
98. R. M. Mironenko, O. B. Belskaya, A. V. Lavrenov, and V. A. Likholobov, *Kinetics and Catalysis*, 2018, **59**, 347–354.
99. Y. Li, X. Guo, D. Liu, X. Mu, X. Chen and Y. Shi, *Catalysts*, 2018, **8**, 193.
100. N. S. Date, S. E. Kondawar, R. C. Chikate, and C. V. Rode, *ACS Omega*, 2018, **3**, 9860–9871.
101. Y. Zhang, G. Fan, L. Yang, F. Li, *Applied Catalysis A: General*, 2018, **561**, 117–126.

102. M. Dohade and P. L. Dhepe, *Catalysis Science & Technology*, 2018, **8**, 5259–5269.
103. X. Lia, Q. Deng, L. Zhang, J. Wang, R. Wang, Z. Zeng, S. Deng, *Applied Catalysis A: General*, 2019, **575**, 152–158.
104. Q. Deng, X. Wen, P. Zhang, *Catalysis Communications*, 2019, **126**, 5-9.
105. P. Jia, X. Lan, X. Li, and T. Wang, *ACS Sustainable Chemistry & Engineering*, 2019, **7**, 15221–15229.
106. Y. Wang, C. Liu, X. Zhang, *Catalysis Letters*, 2020, **150**, 2158–2166.
107. G. Gao, Y. Shao, Y. Gao, T. Wei, G. Gao, S. Zhang, Y. Wang, Q. Chen and X. Hu, *Catalysis Science and Technology*, 2021, **11**, 575–593.
108. H. Tian, G. Gao, Q. Xu, Z. Gao, S. Zhang, G. Hu, L. Xu, X. Hu, *Molecular Catalysis*, 2021, **510**, 111697.
109. Z. Hu, A. Xie, C. Chen, Z. Zou, Y. Shen, Z. Fu, Y. Zhang, H. Zhang, H. Zhao, G. Wang, *Fuel*, 2022, **319**, 123815.
110. H. Li, J. Liu, C. Cai, H. Wang, Y. Huang, C. Wang, L. Ma, *Fuel*, 2023, **332**, 126057.
111. M. Sankar, Q. He, R. V. Engel, M. A. Sainna, A. J. Logsdail, A. Roldan, D. J. Willock, N. Agarwal, C. J. Kiely, and G. J. Hutchings, *Chemical Reviews*, 2020, **120**, 3890–3938.
112. H. HuaJie, S. DongPing & W. Xin, *Chinese Science Bulletin*, 2012, **57**, 3071- 3079.
113. N. M. Deraz, *Journal of Industrial and Environmental Chemistry*, 2018, **1**, 19-21.
114. H. Wang, Y. Yanga, J. Xu, H. Wang, M. Ding, Y. Li, *Journal of Molecular Catalysis A: Chemical*, 2010, **326**, 29–40

Chapter 2.

Catalyst synthesis and characterization

2.1. Introduction:

In order to hydrogenate sugars, furfural and furfuryl alcohol, an efficient catalyst must be developed. As discussed in chapter 1, it is widely known that supported metal catalysts can catalyse the hydrolytic hydrogenation of sugars and furans.¹⁻⁶ Wet impregnation method is one of the simplest, most effective and commonly used method for synthesizing supported metal catalysts. In light of the significance of these catalysts, numerous supported metal catalyst has been designed and evaluate for the hydrogenation of sugars, furfural and furfuryl alcohol. The use of different metals and supports as well as different metal-metal and metal-support interactions could affect the catalysts activity. Additionally, the impact of promoter metal was also investigated. To connect the catalytic activity to the physicochemical parameters of the synthesised catalysts, the catalysts were characterized by different characterization methods.

In current chapter, Ru and Co based various monometallic and bimetallic catalysts with varying metal loading and different supports were synthesized. This chapter covered the specific synthesis process used to synthesise monometallic and bimetallic catalysts. The details regarding metal precursors and materials utilised for the manufacturing of catalyst are also included in this chapter. The detailed regarding different characterization techniques like XRD, XPS, TEM, N₂ sorption and ICP-OES are also mentioned.

2.2. Catalyst synthesis:

2.2.1. Materials: Catalysts have been synthesized using Ru and Co metals loaded on various supports like γ -Al₂O₃ (Al) (acidic, basic and neutral), SiO₂ (Si), SiO₂-Al₂O₃ (Si-Al), ZrO₂ etc. Sigma-Aldrich Chemicals, USA provided the ruthenium chloride trihydrate (RuCl₃.3H₂O), sorbitol (99%) and γ -Al₂O₃ (Al) (acidic, basic and neutral) supports. Activated carbon (C) support, Cobalt nitrate hexahydrate (Co(NO₃)₂.3H₂O), sodium hydroxide (NaOH) (98%) and Sodium carbonate anhydrous GR (Na₂CO₃) (99.5%) bought from Loba Chemie, India. SAPO was prepared as per the procedure described in literature.⁷

2.2.2. Procedure for catalyst synthesis:

Preparation of monometallic and bimetallic catalysts were done using the wet impregnation co-impregnation method respectively using commercial γ - Al_2O_3 (Al-Acidic, Al-Basic and Al-Neutral), SiO_2 (Si), SiO_2 - Al_2O_3 (Si-Al), ZrO_2 , Activated carbon (C), SAPO as the supports. As illustrated in Figure 2.1, for the preparation of catalysts, first a support was evacuated in vacuum oven for 6 h at 150°C under vacuum (-500 mbar). In a typical procedure, a known quantity of water and activated support were stirred at 35°C for half an hour. After half an hour, an aqueous solution of metal precursor with known concentration was added dropwise to the water suspended support. For the synthesis of Ru catalysts, aqueous solution of $\text{RuCl}_3 \cdot 3\text{H}_2\text{O}$ precursor ($\text{Ru}, 12 \text{ mg mL}^{-1}$) was used and the precursor solution was added in accordance with the appropriate weight percent loading of the metal. Then the slurry was allowed to be stirred at room temperature for 16 h. After removing water using a rotary evaporator at 60°C it was then kept for drying at 60°C for 12 h in a laboratory oven and then dried at 150°C for 4 h in vacuum oven (-500 mbar). The obtained powder was subsequently reduced for two hours at 400°C under the flow of H_2 ($\text{H}_2, 16 \text{ mL min}^{-1}$) (Figure 2.2).

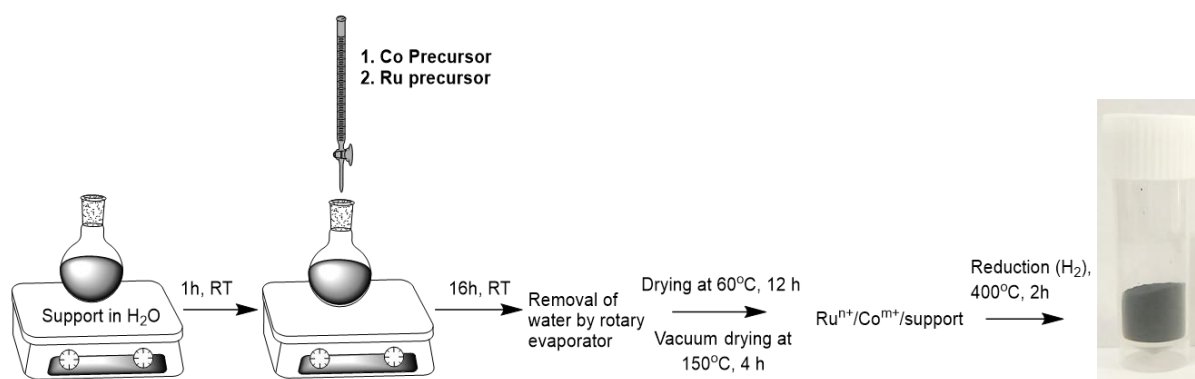


Figure 2.1. Wet impregnation method of catalyst synthesis

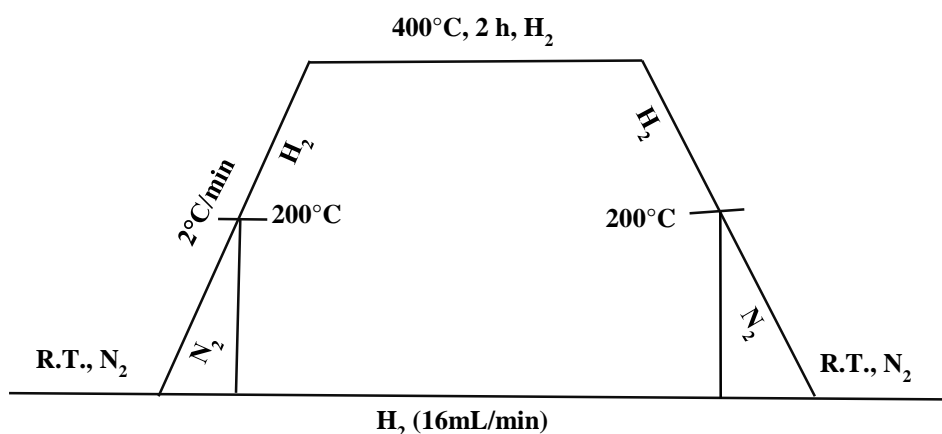


Figure 2.2. Reduction program of catalyst

Bimetallic catalysts were also synthesized using the above procedure. To synthesize bimetallic catalysts, first, the cobalt metal precursor ($\text{Co}(\text{NO}_3)_2 \cdot 3\text{H}_2\text{O}$) (Co , 12 mg mL^{-1}) was added to the suspended support followed by the addition of the ruthenium precursor ($\text{RuCl}_3 \cdot 3\text{H}_2\text{O}$) (Ru , 12 mg mL^{-1}). When 1.5 wt% Ru and 3 wt% Co were impregnated on a basic alumina support then the catalyst was represented as (1.5)Ru(3)Co/Al-Basic. Similarly, other catalysts were named. Using the same process, by altering the ruthenium and cobalt loadings and using different supports (Al, AC, Si, Si-Al, ZrO_2 , SAPO etc.), a series of catalysts were synthesized. All the synthesized monometallic and bimetallic catalysts are listed in Table 2.1.

Table 2.1. List of monometallic and bimetallic catalysts synthesized.

Sr. No.	Catalyst
1.	(0.5)Ru/Al-Basic
2.	(1)Ru/Al-Basic
3.	(1.5)Ru/Al-Basic
4.	(2)Ru/Al-Basic
5.	(3)Ru/Al-Basic

6.	(3)Ru/Al-Acidic
7.	(3)Ru/Al-Neutral
8.	(3)Ru/Si
9.	(3)Ru/Si-Al
10.	(3)Ru/C
11.	(1.5)Co/Al-Basic
12.	(3)Co/Al-Basic
13.	(1.5)Ru(1.5)Co/Al-Basic
14.	(1.5)Ru(3)Co/Al-Basic
15.	(1.5)Ru(4.5)Co/Al-Basic
16.	(1.5)Ru(4.5)Co/ZrO ₂
17.	(1.5)Ru(4.5)Co/SAPO
18.	(2)Ru(1.5)Co/Al-Basic
19.	(2)Ru(3)Co/Al-Basic
20.	(2)Ru(0.5)Co/Al-Basic

2.3. Catalyst characterization:

2.3.1. Catalyst characterization techniques:

Several physico-chemical techniques were used to characterize the catalysts. The powdered X-ray diffraction (XRD) equipment from Philips was used to record X-ray diffraction peaks using Cu K α radiation. The FET Techni TF-30 Transmission Electron Microscopy (TEM) machine was used to assess the size of the metal particles present in a catalyst. Using the Inductively Coupled Plasma-Optical Emission Spectroscopy (ICP-OES; SPECTRO ARCOS Germany, FHS12 instrument) technique, the catalyst's metal content has been determined. By using X-ray Photoelectron Spectroscopy (XPS; VG Micro Tech ESCA3000 instrument) technique, the oxidation states of the metals were determined. The

Autosorb iQ Quantachrome equipment, manufactured in USA, was used to measure the catalyst's surface area.

2.3.2. Results and discussion:

2.3.2.1. X-ray diffraction (XRD) analysis:

XRD analysis of all the support and synthesized monometallic and bimetallic catalysts was done. Using XRD method, the morphology of all the supports and synthesized catalysts was examined. The XRD pattern of basic alumina (Al-Basic) is shown in Figure 2.3. shows the diffraction peaks at 2θ of 19° , 37.6° , 39.4° , 42.5° , 45.8° , 67° and 85° (JCPDS 00-010-0425). Besides this (Figure 2.3), no diffraction peaks for Ru and Co were seen in monometallic (1.5)Ru/Al-Basic, (3)Co/Al-Basic and bimetallic (1.5)Ru(3)Co/Al-Basic catalysts. Similarly, no diffraction peaks for Ru and Co were seen in monometallic (2)Ru/Al-Basic, (1.5)Co/Al-Basic and bimetallic (2)Ru(1.5)Co/Al-Basic catalysts (Figure 2.4.).

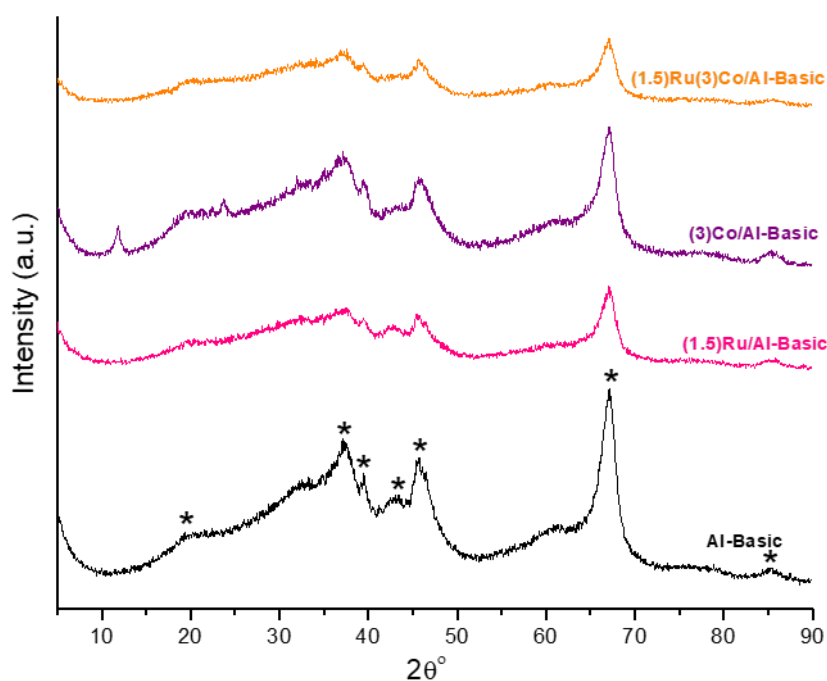


Figure 2.3. XRD pattern Al-Basic supported (1.5)Ru and (3)Co loaded monometallic and bimetallic catalysts.

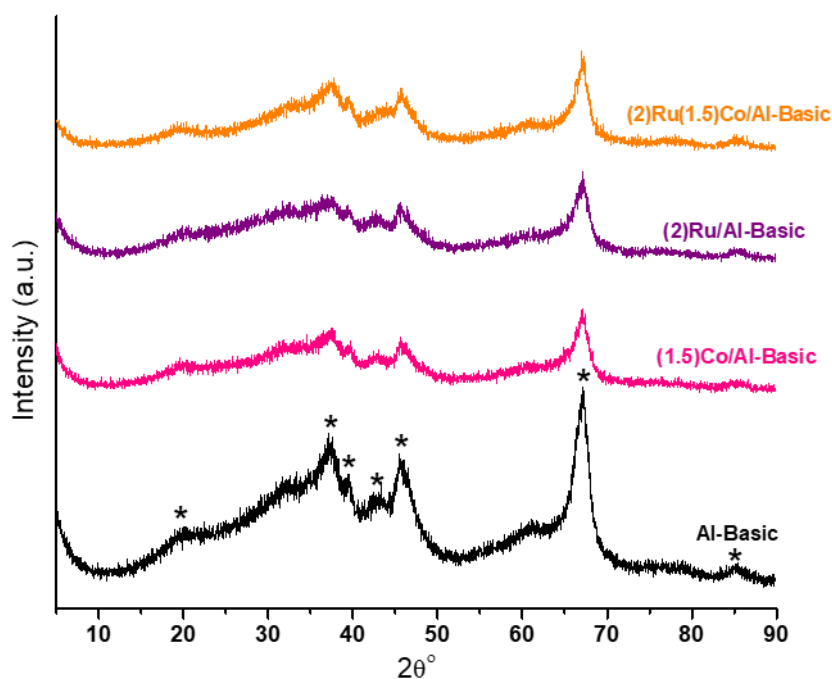


Figure 2.4. XRD pattern Al-Basic supported (2)Ru and (1.5)Co loaded monometallic and bimetallic catalysts.

The XRD pattern of acidic, basic and neutral alumina supported bimetallic (1.5)Ru(3)Co/Al-Basic, (1.5)Ru(3)Co/Al-Acidic, (1.5)Ru(3)Co/Al-Neutral is shown in Figure 2.5. These catalysts were also not showing any diffraction peaks for Ru and Co metal. This suggests that both Ru and Co are highly dispersed on the supports and also very low metal loading is another factor for the absence of the diffraction peaks for Ru and Co.

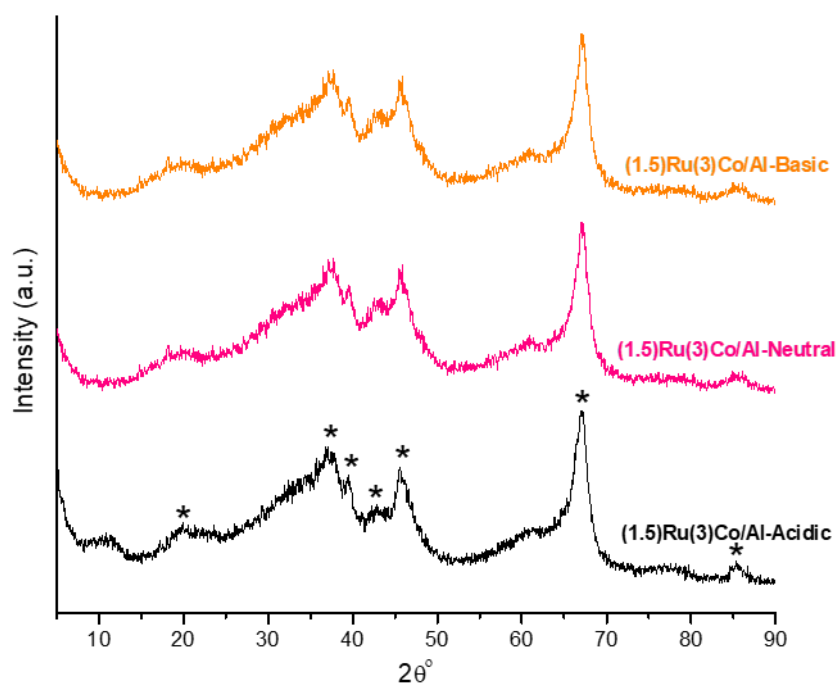


Figure 2.5. XRD pattern of Al-Acidic, Al-Basic and Al-Neutral supported bimetallic catalysts.

Additionally, XRD analysis was performed for monometallic Ru catalysts with varying Ru loading (Figure 2.6.) including (1)Ru/Al-Basic, (2)Ru/Al-Basic, (3)Ru/Al-Basic catalysts. As shown in Figure 2.7, XRD diffraction pattern of bimetallic catalysts with varying Co loading was also recorded. In both monometallic and bimetallic catalysts with varying Ru and Co loading also no Ru and Co diffraction peaks were observed, not even at 3wt% Ru as well as Co loading. Additionally, from TEM analysis it was confirmed that very small metal particle that are highly dispersed all over support. This may have been the reason for absence of diffraction peaks for both metals in XRD analysis.

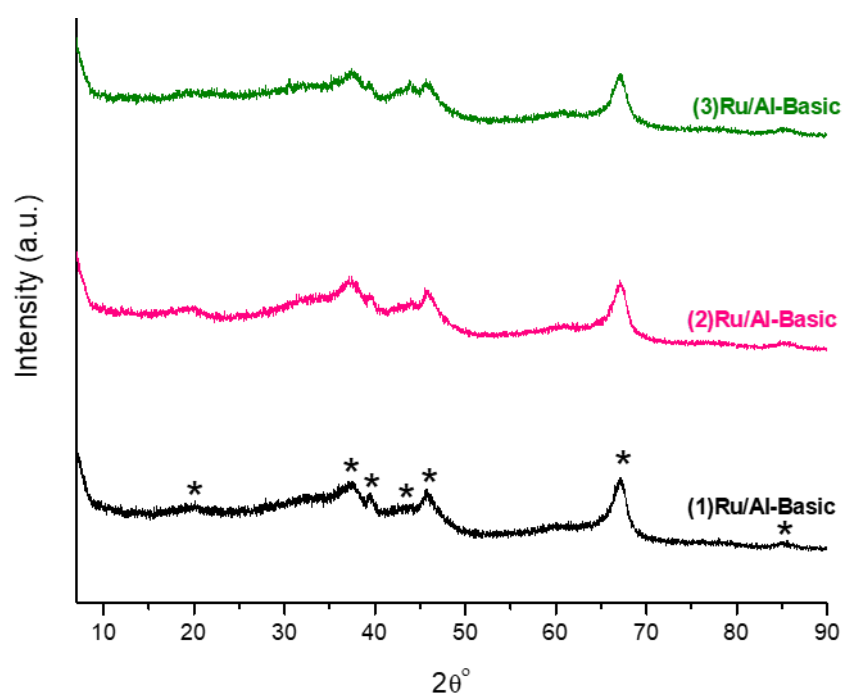


Figure 2.6. XRD pattern Al-Basic supported Ru monometallic catalysts.

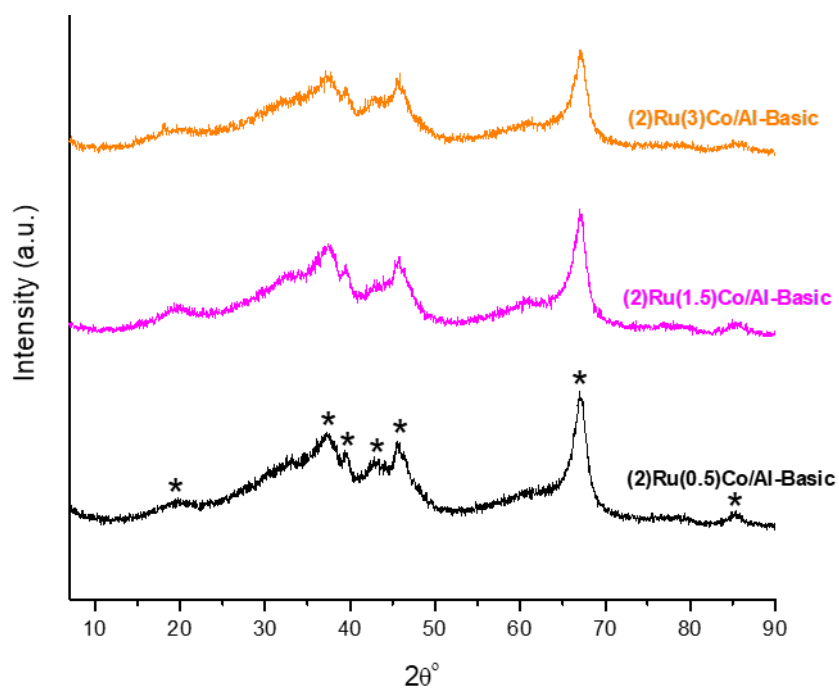


Figure 2.7. XRD pattern Al-Basic supported Ru and Co loaded bimetallic catalysts.

2.3.2.2. X-ray photoelectron spectroscopy (XPS) analysis:

To understand the oxidation states of Ru and Co, XPS analysis of all the synthesized monometallic as well as bimetallic catalysts was performed. As illustrated in Figure 2.8, the monometallic (1.5)Co/Al-Basic and (1.5)Co/Al-Basic catalysts exhibits the Co 2p spectrum with peaks located near binding energies, 780-781 eV as well as 796-797 eV. These peaks are associated with the Co 2p_{3/2} and 2p_{1/2} core level which are related to the Co (II) and (III) oxidation state. Two satellite peaks located around binding energies, 788.4 eV and 804.8 eV show the contribution from the CoO species.⁸ Additionally, the XPS spectrum of bimetallic catalysts shown in Figure 2.9. shows peaks at B. E. 781-783 eV and 797-799 eV, which are also corresponding to the Co (II) and (III) oxidation state. In both monometallic and bimetallic catalysts, Co present in (II) and (III) oxidation state and these oxidation states represented the formation of CoO and Co₃O₄ species. A small increase in binding energise of Co were observed in (2)Ru(1.5)Co/Al-Basic catalyst. This could be attributed to the higher loading of electronegative Ru metal. Ru has high electronegative potential (2.3) than Co (1.88), and because of the difference in electronegativity, Ru pulls electrons from Co and make Co more electro deficient and hence more energy will be required to eject electros from its core shell compared to monometallic catalysts. This could be the reason of Co appears at higher B. E. in (2)Ru(1.5)Co/Al-Basic catalyst than other bimetallic catalysts.

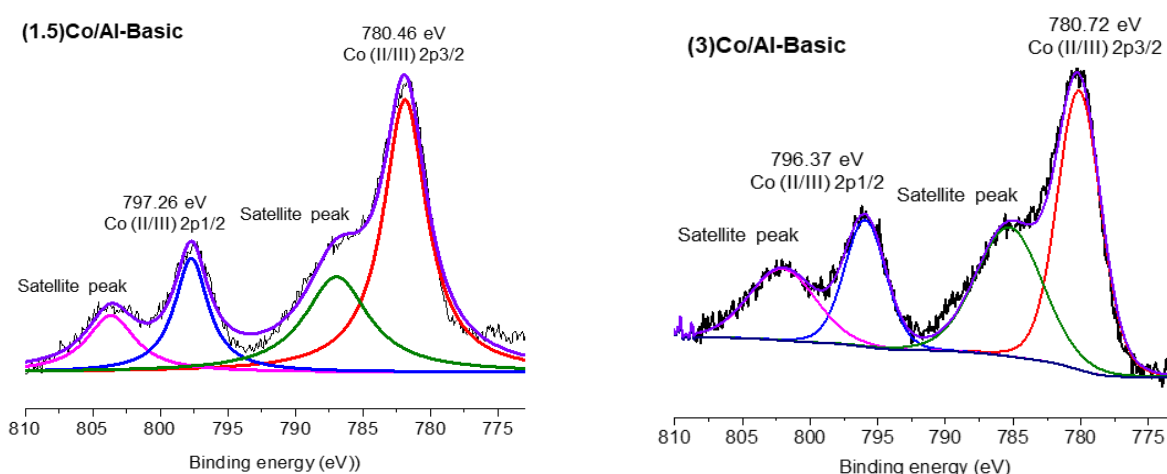


Figure 2.8. XPS spectra of Al-Basic supported monometallic Co catalysts at Co 2p core level

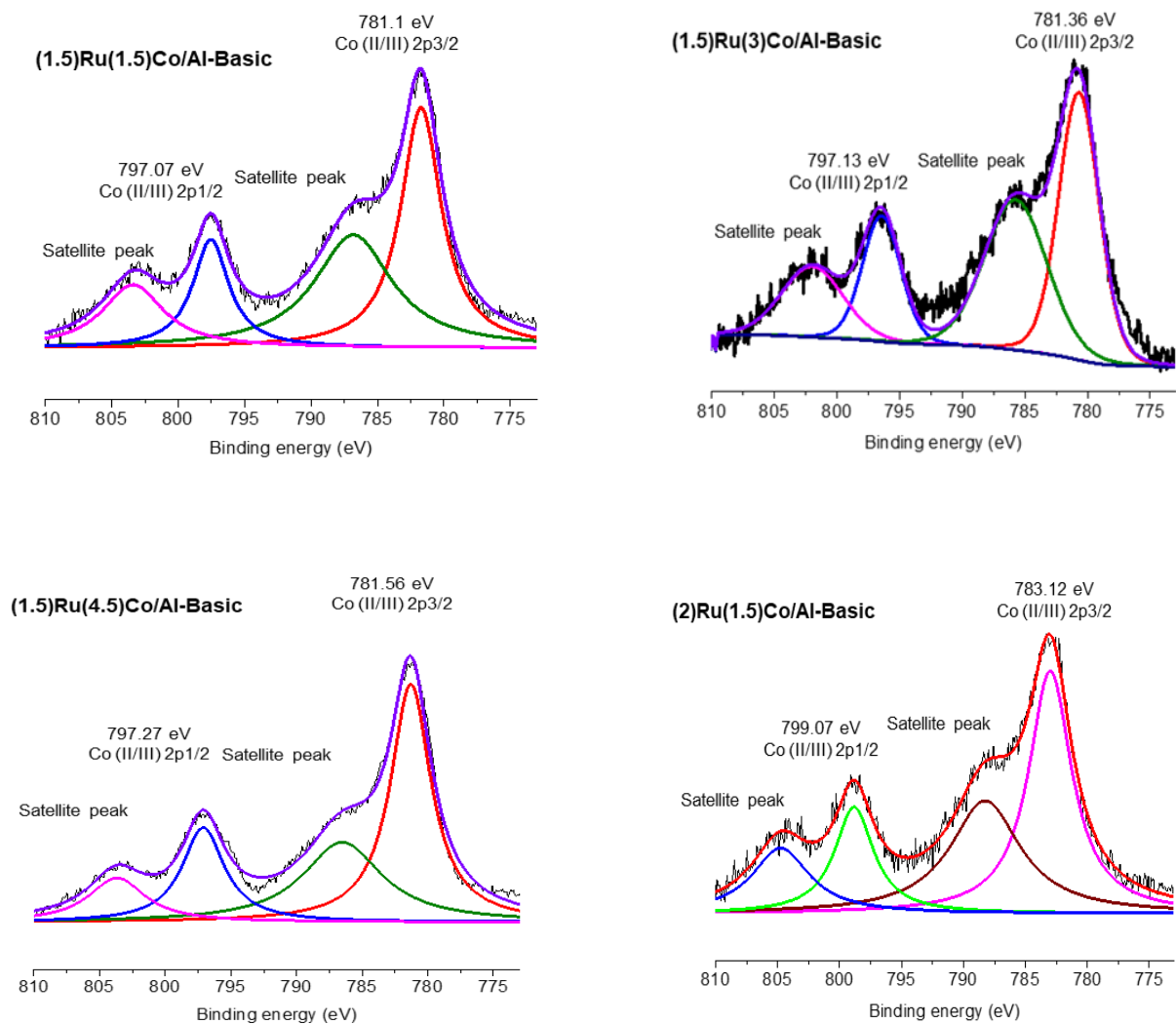


Figure 2.9. XPS spectra of Al-Basic supported monometallic Co catalysts at Co 2p core level

XPS spectra of Ru monometallic and bimetallic catalysts (Figure 2.10 and Figure 2.11) shows Ru (Ru 3p) spectrum with peaks at binding energies of 460 eV to 463 eV and 482 eV to 485 eV attributed to the Ru present in (0) (metallic state) and (IV) (oxide state). These results imply that in monometallic and bimetallic catalysts Ru is mainly found in a metallic form while Co is present in a higher oxidation state. These results are expected with hypothesis and in agreement with the reactions results.

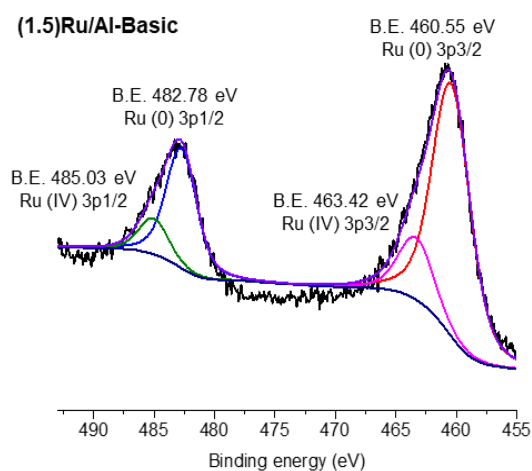


Figure 2.10. XPS spectra of Al-Basic supported monometallic Ru catalysts at Ru 3p core level

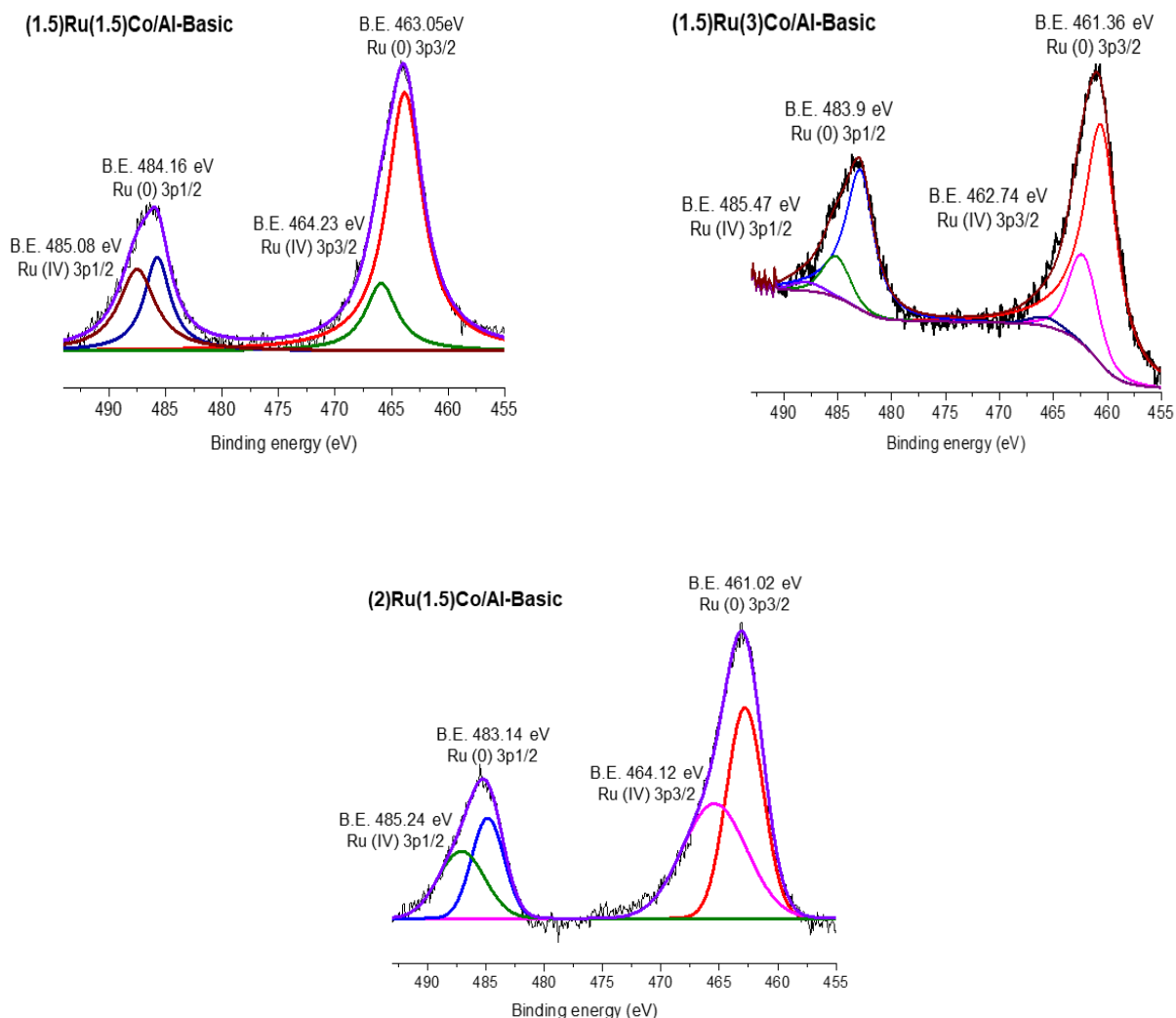


Figure 2.11. XPS spectra of Al-Basic supported bimetallic Ru catalysts at Ru 3p core level

2.3.2.3. N₂ sorption analysis:

N₂ sorption analysis was carried out to determine the physicochemical properties of supports and synthesized materials. The pore volume and particular surface area of different Al₂O₃ (Al) supports like Al-Acidic, Al-Basic and Al-Neutral and synthesized Al supported metal catalysts are listed in Table 2.2. The surface area of all the support alumina Al-Acidic,

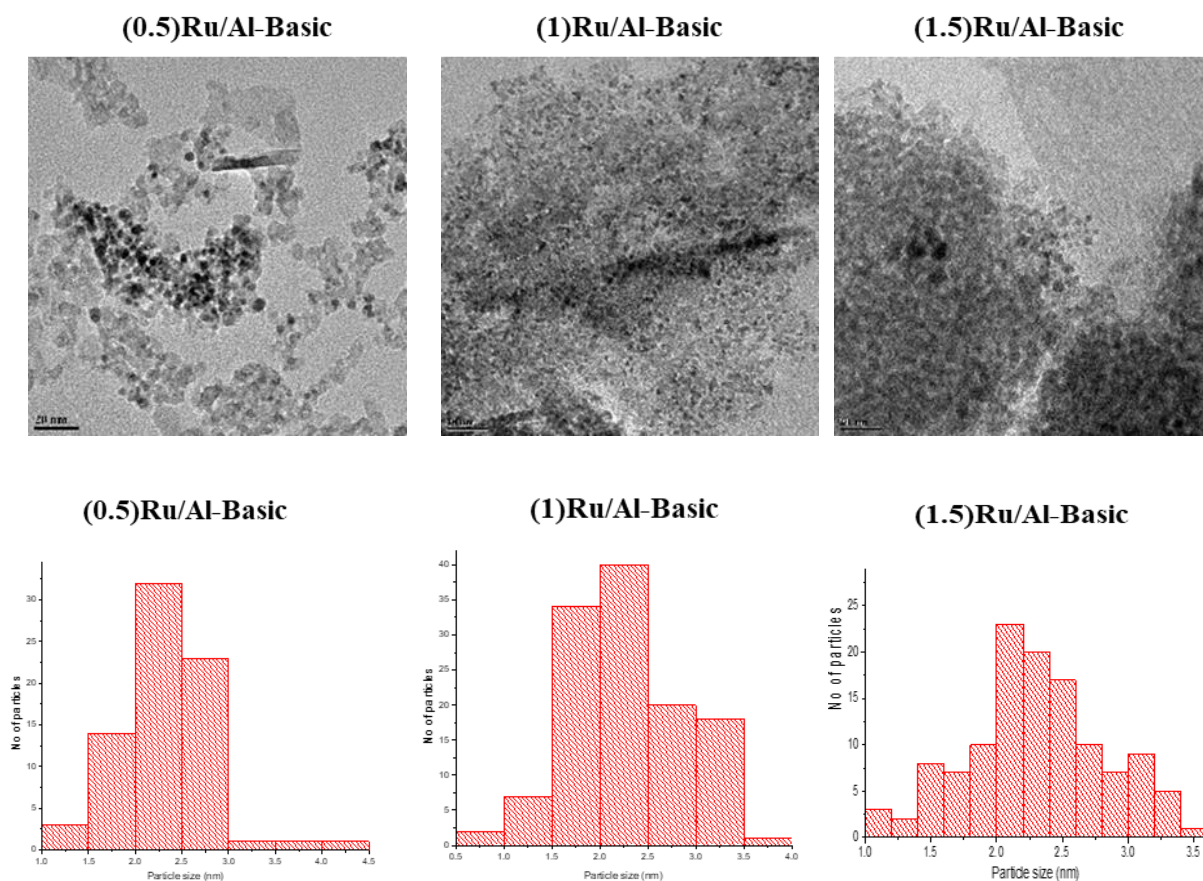
Al-Basic and Al-Neutral was determined to be $240 \text{ m}^2 \text{ g}^{-1}$, $246 \text{ m}^2 \text{ g}^{-1}$ and $242 \text{ m}^2 \text{ g}^{-1}$ respectively, as indicated in Table 2.2. The information gives in the Table 2.2 makes it evident that once metal is impregnated on a support, the specific surface area and pore volume of material decreases. It clearly shows that the particular surface area of catalyst material decreases as a result of deposit of Ru and Co metal on the surface of support. After the metal has been impregnated on support, the metal particles block the portion of its pores which causes decrease in surface area.

Table 2.2. Structural properties of the catalysts

Sr. No.	Catalyst	Surface area (m^2/g)	Pore volume (cc/g)
1.	Al-Basic	246	0.30
2.	Al-Acidic	240	0.40
3.	Al-Neutral	242	0.35
4.	(1.5)Ru/Al-Basic	210	0.28
5.	(2)Ru/Al-Basic	187	0.27
6.	(3)Ru/Al-Basic	149	0.17
7.	(1.5)Co/Al-Basic	210	0.21
8.	(3)Co/Al-Basic	173	0.26
9.	(1.5)Ru(3)Co/Al-Basic-fresh	219/219	0.29
10.	(1.5)Ru(3)Co/Al-Basic-spent	214	0.24
11.	(1.5)Ru(3)Co/Al-Acidic	207	0.38
12.	(1.5)Ru(3)Co/Al-Neutral	210	0.34
13.	(1.5)Ru(1.5)Co/Al-Basic	227	0.33
14.	(1.5)Ru(4.5)Co/Al-Basic	196	0.28
15.	(2)Ru(1.5)Co/Al-Basic-fresh	210	0.26
16.	(2)Ru(1.5)Co/Al-Basic-spent	201	0.22

2.3.2.4. Transmission electron microscopy (TEM) analysis:

Metal dispersion and metal practical size of synthesised catalysts was determined using TEM analysis. The average metal article size for all of the Ru ad Co metal based monometallic catalysts with the compositions of (0.5)Ru/Al-Basic, (1)Ru/Al-Basic, (1.5)Ru/Al-Basic, (2)Ru/Al-Basic, (3)Ru/Al-Basic, (1.5)Co/Al-Basic and (3)Co/Al-Basic catalysts was determined. Figure 2.12. shows the TEM images and calculated size of particle of all the mentioned monometallic Ru and Co catalysts. The mean particle size of Ru catalysts was found to be 2.2 nm and the particle size of (1.5)Co/Al-Basic and (3)Co/Al-Basic catalysts was found to be 2.2 nm and 4 nm respectively. Figure 2.13. shows the TEM images as well as distribution of metal particle size in bimetallic catalysts. From Figure 2.12 and Figure 2.13 it was seen that the particle size of Ru and Co metal is bigger in monometallic catalysts than the particle size in bimetallic catalysts.



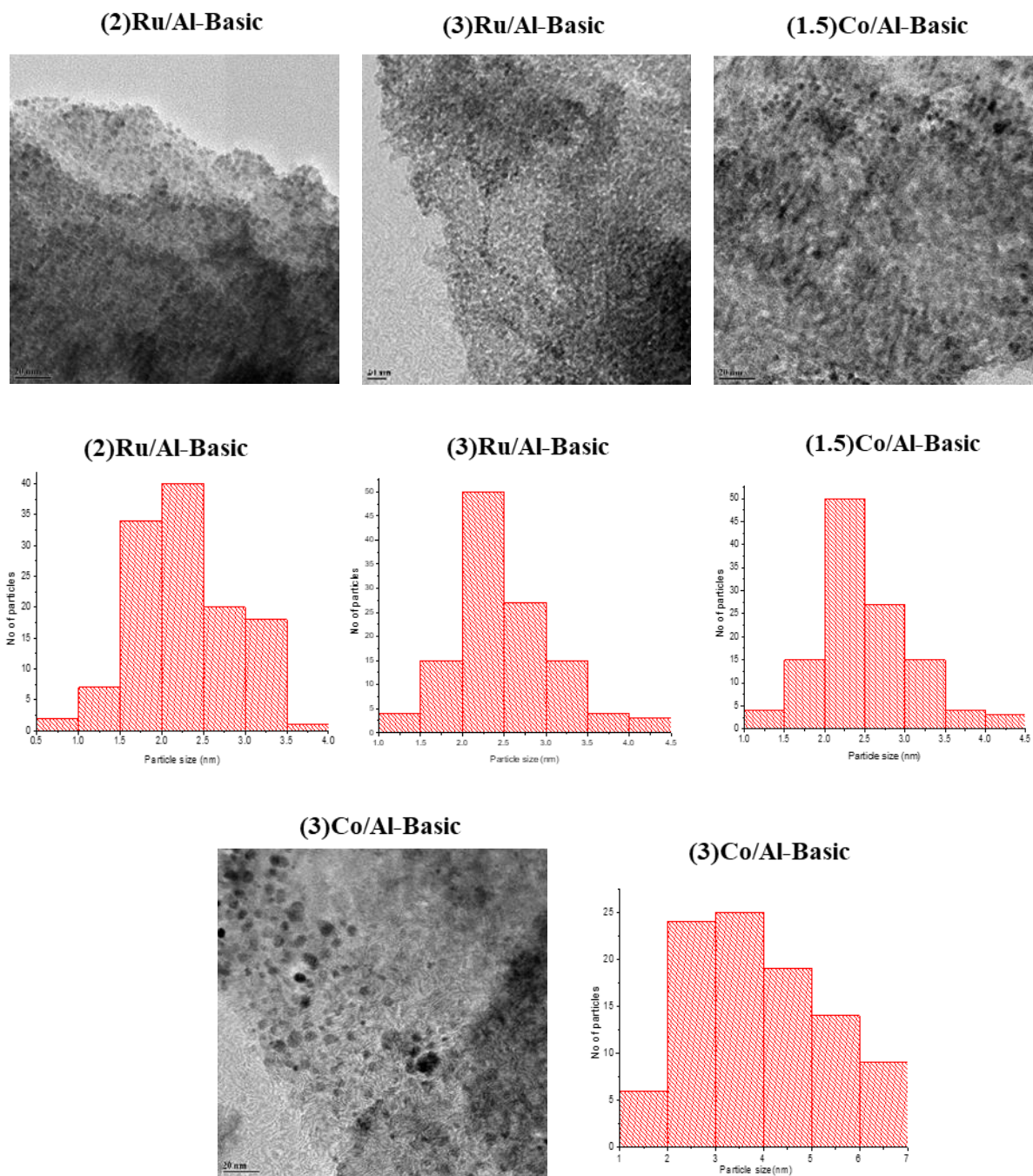


Figure 2.12. TEM images and particle size distribution of monometallic Ru and Co catalysts

According to TEM analysis, the typical metal particle size of Ru and Co in monometallic (1.5)Ru/Al-Basic and (3)Co/Al-Basic catalysts was found to be 2.2 nm and 4 nm respectively. In monometallic catalysts, a large particle size was observed with the formation of aggregates. These results are in agreement with the XRD data, which shows absence of peaks for Ru and Co, which indicates that the metal is well dispersed on support and has smaller particle size. In contrast with monometallic catalysts, bimetallic (1.5)Ru(3)Co/Al-Basic catalyst exhibit well dispersed metal particles with smaller particle size (Figure 2.13). The average particle size of bimetallic (1.5)Ru(3)Co/Al-Basic was found to be an 1.6 nm. After the impregnation of Co, Bimetallic (1.5)Ru(3)Co/Al-Basic catalysts exhibit more metal dispersion with smaller metal particle size when compared to monometallic (1.5)Ru/Al-Basic catalysts. This concludes that, the incorporation of Co prevents the migration of Ru particles during the reduction or calcination, as a result, high metal dispersion with reduced particle size was achieved.

Comparable outcomes for the (2)Ru/Al-Basic, (1.5)Co/Al-Basic, and (2)Ru(1.5)/Al-Basic catalysts were found using TEM analysis (Figure 2.12 and Figure 2.13). The average particle size of 2.2 nm was recorded in the monometallic (2)Ru/Al-Basic and (1.5)Co/Al-Basic catalysts. In contrast, smaller particles with mean particle size of 1.25 nm were seen in the bimetallic (2)Ru(1.5)/Al-Basic catalyst. And in comparison with bimetallic catalysts, the metal particles formed in (2)Ru(1.5)/Al-Basic catalyst are even smaller in size (1.25 nm) than those formed in (1.5)Ru(3)/Al-Basic catalyst (1.6 nm).

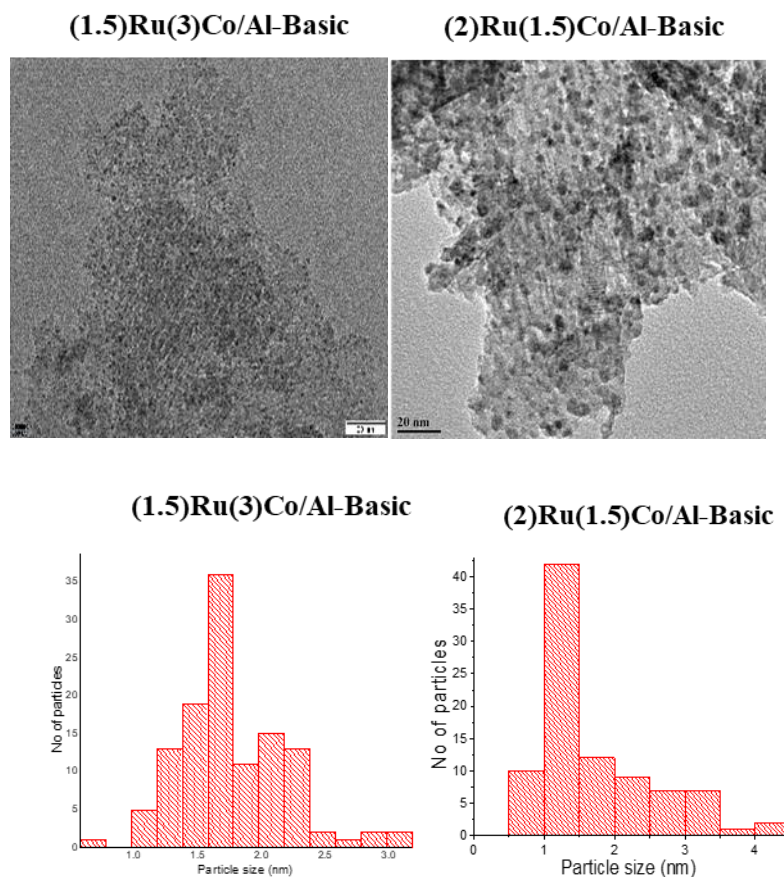


Figure 2.13. TEM images and particle size distribution of bimetallic Ru and Co catalysts

Similarly metal particle size of catalyst with varying Co loading such as (1.5)Ru(1.5)Co/Al-Basic and (1.5)Ru(4.5)Co/Al-Basic was also calculated from TEM analysis (Figure 2.14). It was observed that at lower Co loading (1.5%), the particle size of (1.5)Ru(1.5)Co/Al-Basic catalyst (around 1.6 nm) is similar to the particle size of (1.5)Ru(3)Co/Al-Basic catalyst (1.6 nm). While increasing Co loading to 4.5% in (1.5)Ru(4.5)Co/Al-Basic catalyst, bigger particle size (3-4 nm) was observed.

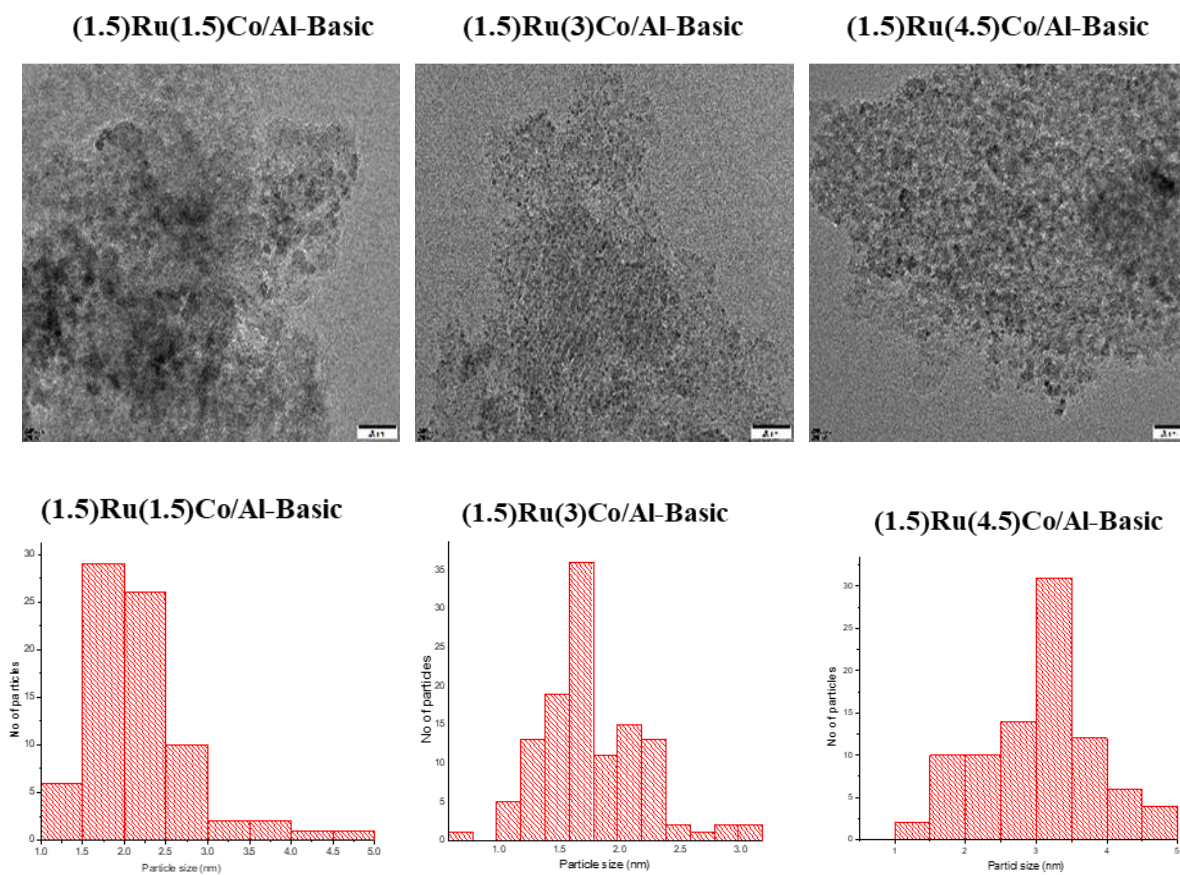


Figure 2.14. TEM images and particle size distribution of bimetallic catalysts with different Co loading

From HRTEM analysis, the d-lattice spacing of bimetallic (1.5)Ru(3)Co/Al-Basic catalysts was calculated. As shown in Figure 2.15, it was found that the metal particles formed on the Al-Basic support had a lattice spacing of 0.21 nm,⁹ which is in line with previous findings in the literature.

Elemental mapping of (1.5)Ru(3)Co/Al-Basic catalysts was also performed and from elemental mapping analysis it was confirmed that both the metals (Ru and Co) present in the catalysts are uniformly distributed on the support (Figure 2.16).

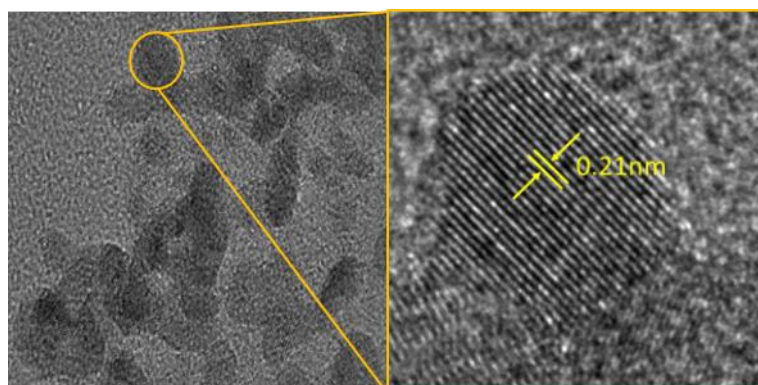


Figure 2.15. HRTEM images of bimetallic (2)Ru(1.5)Co/Al-Basic catalyst

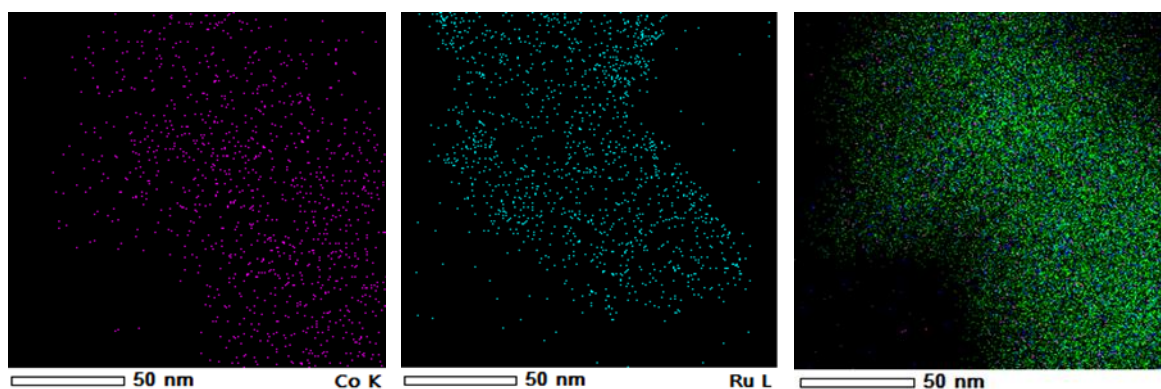


Figure 2.16. Elemental mapping images of (1.5)Ru(3)Co/Al-Basic catalyst

2.3.2.5. Inductively Coupled Plasma-Optical emission spectroscopic (ICP-OES) analysis:

The exact loading of Ru and Co metal in synthesised catalysts has been determined using ICP-OES analysis. The Table 2.3 displays the theoretical and ICP-OES and metal content of synthesized catalysts. The metal content of all the synthesised catalysts has been found to be within a range of theoretical values.

Table 2.3. Summary of results obtained from ICP-OES analysis

Sr. No.	Catalyst	Theoretical Ru wt%		Practical Ru wt%	
		Ru	Co	Ru	Co
1.	Al-Basic	-	-	-	-
2.	(1)Ru-Al-Basic	1	-	1.1	
3.	(1.5)Ru/Al-Basic	1.5	-	1.63	-
4.	(2)Ru-Al-Basic	2	-	1.82	-
5.	(3)Ru-Al-Basic	3	-	2.7	
7.	(1.5)Co/Al-Basic	-	1.5	-	1.63
8.	(3)Co/Al-Basic	-	3	-	3.2
9.	(1.5)Ru(3)Co/Al-Basic	1.5	3	1.23	2.5
10.	(2)Ru(1.5)Co/Al-Basic	2	1.5	1.8	1.49
11.	(1.5)Ru(3)Co/Al-Acidic	1.5	3	1.31	2.63
12.	(1.5)Ru(3)Co/Al-Neutral	1.5	3	1.3	2.5

2.4. Conclusion:

In order to hydrogenate sugars, furfural and furfuryl alcohol, different supported monometallic as well as bimetallic catalysts were developed and synthesized. The wet impregnation method was used to synthesize all the catalysts. The synthesised catalysts were analysed using a range of characterisation technique including XRD, XPS, N₂ sorption, ICP-OES etc. XRD analysis of all the catalysts showed absence of diffraction patterns for Ru and Co because of their low metal content and the formation of highly dispersed smaller nano particles. According to the XPS analysis, in both monometallic and bimetallic catalysts, Co is found in (II) and (III) oxidation states and Ru is present in (0) and (IV) oxidation states. The slight shift towards higher B. E. were observed in bimetallic catalysts is due to the interactions between Ru and Co metal particles. Furthermore, BET Analysis was carried out and the results

of BET analysis indicated that a small reduction in surface area of catalysts after the impregnation of metal on support was seen. The slight decrease in surface area after the impregnation of metal confirms the higher dispersion of metal particles on support. TEM analysis concludes that metal particles are well dispersion on support with the formation of smaller particle size (1.5-3.5 nm) which contributes to an increase the catalysts surface area and ultimately enhances the catalyst activity. The actual metal content present in catalysts was confirmed by ICP-OES analysis and it showed that the metal content of all the synthesized catalysts is approximately near to the expected metal content. The catalyst's activity could be controlled by its physicochemical properties and as discussed above physicochemical properties of catalysts are determined by various factors including type of support, metal and promoter used. In next chapters, the impact of various physicochemical properties of different catalysts for the hydrogenation of sugars, furfural and furfuryl alcohol has been examined.

2.5. References:

1. A. A. Dabbawala, D. K. Mishra, J. -S. Hwang, *Catalysis Today*, 2016, **265**, 163–173.
2. M. Audemar, W. Ramdani, T. Junhui, A. Raluca Ifrim, A. Ungureanu, F. Je'ro'me, S. Royer and K. de Oliveira Vigier, *ChemCatChem*, 2020, **12**, 1973–1978.
3. Y. Fu, L. Ding, M. L. Singleton, H. Idrissi and S. Hermans, *Applied Catalysis B*, 2021, **288**, 119997.
4. M. Hronec, K. Fulajtarová, *Catalysis Communications*, 2012, **24**, 100–104.
5. M. Hronec, K. Fulajtarová, T. Liptaj, *Applied Catalysis A: General*, 2012, **437–438**, 104–111.
6. M. Zhou, J. Li, K. Wang, H. Xia, J. Xu, J. Jiang, *Fuel*, 2017, **202**, 1-11.
7. P. Bhaumik and P. L. Dhepe, *RSC Advances.*, 2013, **3**, 17156–17165.
8. H. Can, S. Can, R. Ebiri and Ö. Metin, *New J. Chem.*, 2022, **46**, 12120–12131.
9. K. Kusada, H. Kobayashi, T. Yamamoto, S. Matsumura, N. Sumi, K. Sato, K. Nagaoka, Y. Kubota and H. Kitagawa, *J. Am. Chem. Soc.*, 2013, **135**, 5493–5496

Chapter 3.

Hydrogenation of sugars to sugar alcohols

Chapter 3A.

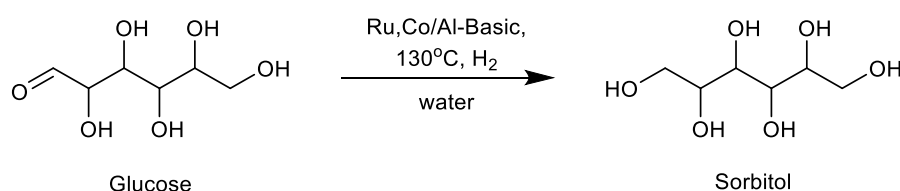
Hydrogenation of glucose to sorbitol

3A.1. Introduction:

Due to the rising energy demand, utilizing lignocellulosic biomass to generate alternative chemicals and fuels has drawn a lot of attention.¹⁻³ A highly versatile sugar alcohol, D-Sorbitol, finds wide applications in the food (low calorie sweetener), cosmetic (moisturizer), polymer, and pharmaceutical industries and numerous other industrial uses.^{4,5} Sorbitol, obtained from the hydrogenation of glucose, is the most commonly used polyol as a sweetener. Besides this, it can also be served as a starting material for the production of isosorbide,^{6,7} ascorbic acid,⁸ glycerol,⁹ and lactic acid.¹⁰ Sorbitol is one of the most important bio-derived chemicals and has been listed as one of the top 12 bio-derived chemicals, according to the U. S. Department of Energy.¹¹ As is known, the transformation of sugars to sugar alcohols can be performed using enzymatic, microbial or chemical methods and amongst all, the biological method shows lower sugar conversions and lower sugar alcohol yields and also requires longer reaction times. Thus, it is implied that the chemical production of sugar alcohols is more efficient than the biological method and hence is commercially practiced. Industrially sorbitol is produced using the RANEY[®] nickel catalyst because of its low cost and earth abundant nature. However, hydrogenation over the RANEY[®] nickel catalyst takes place under very high H₂ pressures such as 40–150 bar.¹²⁻¹⁵ Though being commercially used, the catalyst has a main drawback – it easily gets deactivated because of metal leaching, metal sintering or deposition of carbon on active sites.¹³ Additionally, the leached metal forms a complex with the sugar alcohols, which adds up a step to purify the product. As alternatives to nickel catalysts, various catalysts made up of noble metal (Ru, Pt, Pd and Rh) have been reported by researchers for the hydrogenation of sugars to sugar alcohols.^{14,16} It has been observed that the hydrogenation ability of catalysts decreases in the order Ru > Rh > Pd.¹⁷ It means amongst all of them, supported ruthenium catalysts would be very active in sugar hydrogenation compared to other metal catalysts. In view of this, various Ru-based catalysts are reported with different supports such as SiO₂, AC, Al₂O₃, Nb₂O₅, MCM-48, etc.¹⁷ Besides this, (2.5)Ru–ZrO₂–SBA-15 and amine-functionalized nanoporous polymer (AFPS) supported (5)Ru/AFPS catalysts are also reported for the hydrogenation of sugars. Both these catalysts show high activity and selectivity towards sorbitol formation but typically the reactions that occur require high H₂ pressures (40–55 bar).^{18,19} Although noble metal-based catalysts show good activity, due to the high cost of

precious metals, the substitution of those (at least partially) with non-noble metals has become an interesting research area. Various catalysts based on non-noble metal, such as Ni/NiO,²⁰ (8.33)Fe(8.33)Ni/CB,²¹ (13)Ni(2)Ru@PCS,²² Ni-Co-HZSM-5,²³ (5)Cu/ SiO₂ and (5)Ni/Al₂O₃,²⁴ are reported for the conversion of glucose to sorbitol. However, compared to noble metal-based catalysts, these catalysts show lower selectivity towards sorbitol formation, and active metal sintering, leaching and recycling are the problems associated with these catalysts.

As is evident from the literature, a huge body of work is done on the conversion of sugars to sugar alcohols; however, either a high loading of Ru (2–5%) or the use of severe reaction conditions (>30 bar H₂ pressure) is reported to achieve better yields. In view of the above, it is difficult to use these catalytic systems on the industrial scale and specifically to replace the already existing commercial catalysts. Considering this, the objective of this work was to design an effective recyclable catalytic system having a lower noble metal loading, which could function at lower temperatures and lower H₂ pressures for the conversion of glucose to sorbitol than those reported in the literature. In this chapter, the activity of various supported metal monometallic as well as bimetallic catalysts has been investigated for the hydrogenation of glucose to sorbitol (Scheme 3A.1). Effects of different promoters, metals and supports as well as the effects of different reaction parameters including temperature, H₂ pressure, time, catalyst quantity etc. were also examined in order to maximize conversion and yield. Additionally, recycling study of catalyst was also conducted to examine its stability under optimal reaction condition.



Scheme 3A.1. Hydrogenation of glucose to sorbitol

3A.2. Experimental:

3A.2.1. Materials: Sorbitol (99%) was purchased from Sigma-Aldrich chemicals, USA. Glucose (99%, AR), fructose (99%, AR), mannose (99%, AR), galactose (99%, AR) and galactitol (99%, AR) were bought from Loba Chemie, India. Mannitol (99%, AR) and ethylene glycol (99%) were purchased from s.d. fine chemicals. Before using all the chemicals, no additional treatment was applied.

3A.2.2. Catalyst synthesis:

Monometallic catalysts were prepared using wet impregnation method and bimetallic catalysts were synthesized using co-impregnation method. Evaluation of synthesized catalysts was done to convert sugars into sugar alcohols. The complete procedure for catalyst synthesis is given in chapter 2 (Refer section 2.2.2.).

3A.2.3. Reaction set-up and analysis of reaction mixtures:

Catalytic activity of all the catalysts were measured in a 50 mL batch mode reactor (Amar Equipment's make batch reactor). Typically, for the reaction, 0.35g substrate, 0.1g catalyst and 35mL water were charged in the reactor. The reactor was purged three or four times with low pressure hydrogen to get a ride of air and then pressurized with required H₂ pressure (10-18 bar). The reactions were conducted at desired temperature (120-140°C) for desired reaction time. During the heating, first stirring speed was set at 300 rpm and increased to 900 rpm after attaining the set reaction temperature. After the reaction completion, reactor was cooled down at ambient temperature and reaction mixture taken out.

Using centrifugation, the catalysts was separated from reaction mixture. Collected solution was filtered through a 0.22µm syringe filter before being subjected to analysis. Obtained reaction mixture was analysed by High Performance Liquid Chromatography (HPLC; Agilent technologies, 1200 infinity series, USA) equipped with an RID detector (Agilent Technologies, 1200 infinity series) and HC-75 Pb⁺² column (Hamilton, 7.8mm × 300mm). Column temperature was maintained at 80°C and refractive index detector temperature was maintained

at 40°C. HPLC grade water with 0.5mL·min⁻¹ flow rate was used as an eluent. External Standard method was used for the quantitative determination of each product.

3A.2.4. Calculations:

Conversion (C) of substrate and yield (Y) of products were calculated as follows:

$$\text{Conversion (C)\%} = \left\{ \frac{[(\text{Initial moles of substrate}) - (\text{Final moles of substrate})]}{\text{Initial moles of substrate}} \right\} * 100$$

$$\text{Yield (Y)\%} = \left\{ \frac{\text{Moles of product formed}}{\text{Theoretical moles of product formed based on the moles of substrate converted}} \right\} * 100$$

3A.3. Result and discussion:

The results for the hydrogenation of glucose to sorbitol are included in this section. Various monometallic and bimetallic Ru and Co metal-based catalysts with various supports were prepared and examined for the hydrogenation of glucose to sorbitol. Optimization of reaction variables including time, H₂ pressure, temperature, S/C ratio etc. (S/C ratio is the ratio between substrate and Ru). was carried out to attend maximum yield possible, for the transformation of glucose to sorbitol.

3A.3.1. Effect of different supports:

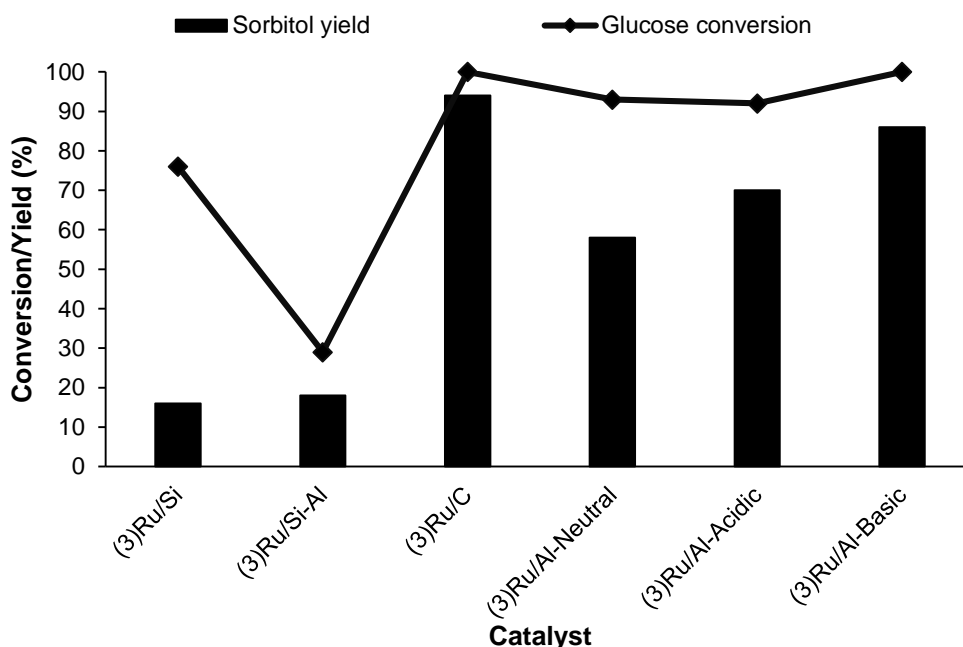


Figure 3A.1. Effect of different supports on glucose hydrogenation.

Reaction conditions: Glucose, catalyst, S/C (98 mol/mol), Water (35mL), 10 bar H₂ at R.T., 100°C, 5 h.

All the reactions are done at least three times and the obtained results are within the error of $\pm 1\%$ -2.5 % range.

To look into the impact of different supports for the hydrogenation of glucose to sorbitol, Different Ru based catalyst were synthesized using different supports like Al₂O₃ (Al) (acidic, basic, neutral), SiO₂ (Si), SiO₂-Al₂O₃ (Si-Al), Carbon (C) and tested for the reaction at 100°C, 10 bar H₂ at R.T. for 5h reaction time. Figure 3A.1 illustrated that, different supports exhibit different activity in catalysts. Initially reactions were done with (3)Ru/Si catalyst and achieved 76% conversion with only 16% sorbitol yield. Further activity of (3)Ru/Si-Al catalyst

was checked and very less amount of sorbitol production (18%) was seen at 29% glucose conversion. Furthermore, activity of (3)Ru/C catalyst was checked and observed that this catalyst is showing highest glucose conversion 100% with 94% sorbitol formation. Further different alumina supports (acidic, basic and neutral) were evaluated for glucose to sorbitol reaction. Following the testing of different alumina supports, it was found that the basic alumina (Al-Basic) support possessed superior activity (conv-100%, yield 86%) over both the acidic (Al-Acidic) (conv-92%, yield 70%) and neutral (Al-Neutral) (conv-93%, yield 58%) alumina. To understand the reason behind this, UV-Vis analysis of a water solution of glucose with base NaOH and without base was performed. As seen from Figure 3A.2, the water solution of glucose in the absence of base did not show any absorbance in the UV spectrum while after the addition of base (NaOH) to the glucose solution, an absorbance peak at $\lambda_{\text{max}} = 270$ nm was seen. The said peak is assigned to the $-\text{CHO}$ group ($\text{C}=\text{O}$), which proves that, in the presence of the basic alumina support, there is an open chain form of glucose is present. Along with a peak at $\lambda_{\text{max}} = 270$ nm, there was an extra peak at $\lambda_{\text{max}} = 310$ nm was also observed which can be corresponds to the enediol anion as reported in literature.²⁵ To understand this further, the pH of different alumina supports (acidic, basic, and neutral) in water was measured. As expected, neutral alumina when suspended in water showed a pH of 6.6 and when acidic alumina was suspended in water, a pH of 3.9 was observed. Interestingly the pH of water after the addition of basic alumina was observed to be 8.7. According to the Lobry de Bruyn–Alberda van Ekenstein mechanism, sugars are mostly present in an open chain form in basic media, while in the case of neutral and acidic media, sugars are typically present in a cyclic form.²⁶ Because, under our reaction conditions, in presence of basic alumina support, the pH of the reaction mixture was around 8.2, glucose was present in the open-chain form and this would help in enhancing the hydrogenation of the exposed carbonyl group.

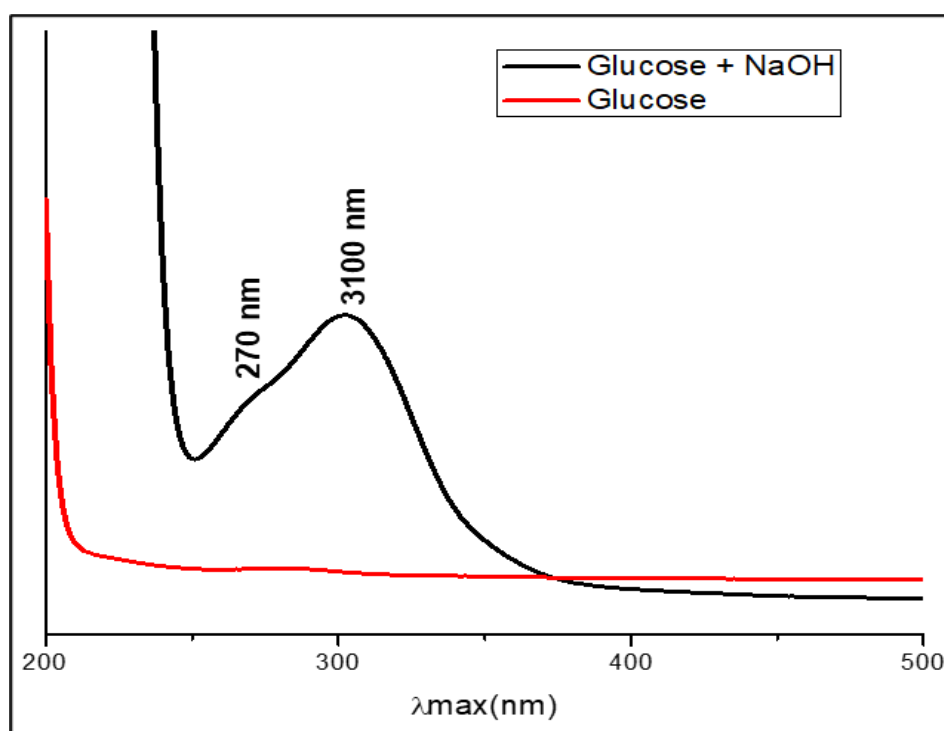


Figure 3A.2. UV-Vis analysis of glucose solution in water

So, in contrast with all the above mentioned supports, activated carbon (C) support provides maximum conversion and yield demonstrating that C is the best support for the conversion of glucose to sorbitol. However, there are significant drawbacks with carbon support. Recovery of carbon supported catalyst in batch mode reaction is difficult due to its amorphous light nature. Additionally, making of carbon pellets is more challenging and these pellets are less stable at high pressure, which limits the use carbon supported catalyst in continuous flow mode reactors. These drawbacks of carbon limit the use of carbon supported catalysts in industry. Following carbon, basic alumina (Al-Basic) support exhibits superior activity for the reaction. So, I decided to use Al-Basic as a support to convert glucose into sorbitol.

3A.3.2. Effect of Ru metal loading:

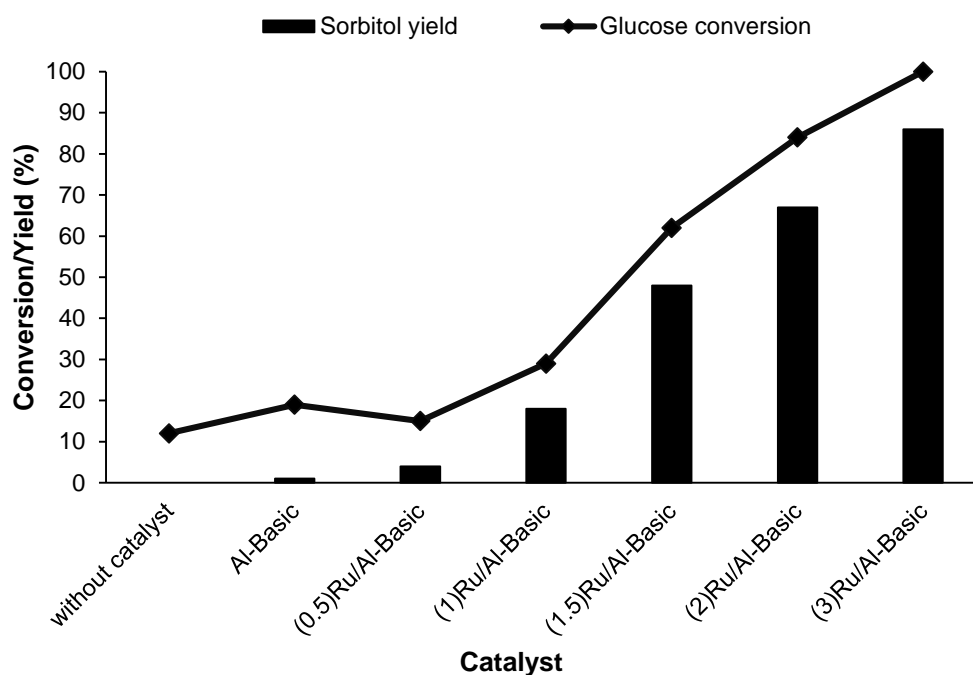


Figure 3A.3. Effect of Ru loading for the conversion of glucose to sorbitol:

Reaction conditions: Glucose 0.35g, catalyst 0.1g, water (35mL), 10 bar H₂ at R.T., 100°C, 5 h.

All the reactions are done at least three times and the obtained results are within the error of $\pm 1\%$ -2.5 % range.

In order to understand the effect of Ru loading for the conversion of glucose into sorbitol, Al-B supported monometallic catalyst with varying Ru loading were synthesized. Earlier results (section 3A.3.1) showed better performance of (3)Ru/Al-Basic catalyst (100% conv and 86% yield). In order to minimize the Ru loading, catalysts with lower Ru loading ranging from 0.5 to 3 wt%, were synthesized and the catalytic activity was checked for the conversion of glucose to sorbitol at 100°C, 10 bar H₂ for 5 h reaction time. As shown in Figure 3A.3, it was seen that increasing the Ru loading led to an increase in catalyst activity. This is

quite apparent because there are more active metal sites in catalysts with higher metal content. As a result, substrate molecules can find the active sites with ease, producing better results.

With the (0.5)Ru/Al-Basic catalyst, achieved 17% conversion and 4% yield of sorbitol. When comparing the activity of (0.5)Ru/Al-Basic and (1)Ru/Al-Basic catalyst, it was found that a 0.5% increase in metal concentration resulted in a 14% increase in sorbitol production. So with (1)Ru/Al-Basic catalyst, 29% conversion and 18% sorbitol yield was achieved. Likewise, 30% increase in sorbitol production was seen using (1.5)Ru/Al-B catalyst compared to (1)Ru/Al-Basic catalyst. Furthermore, despite a 0.5% and 1% increase in Ru loading in (2)Ru/Al-Basic and (3)Ru/Al-Basic catalyst, only 19% improvement in sorbitol yield was observed. Maximum improvement of yield of sorbitol over (1.5)Ru/Al-Basic catalyst compared to other catalysts emphasizes the fact that (1.5)Ru/Al-Basic catalyst is better catalyst for converting glucose to sorbitol.

3A.3.3. Effect of Co metal loading:

As previously mentioned, good yield of sorbitol is obtained over (1.5)Ru/Al-Basic catalyst, however, there is a definite scope of improvement in the sorbitol yield at least to a certain point. It is widely known that the addition of promoter to supported metal catalyst can enhance the catalyst activity. Therefore, in this study effect of Co as a promoter on (1.5)Ru/Al-Basic catalyst to convert glucose to sorbitol was studied with different Co loading. In order to study the impact of different Ru:Co ratio on the catalyst's catalytic activity, a set of catalysts were prepared with fixed Ru (1.5 wt%) loading and varying Co (1.5, 3, 4.5 wt%) loading. The catalytic activity of all the catalysts were tested at 130°C, 15 bar H₂ for 6 h time.

The activity of (1.5)Ru(1.5)Co/Al-Basic and (1.5)Ru(3)Co/Al-Basic catalysts were tested for the conversion of glucose to sorbitol reactions. These activities were compared with the monometallic (1.5)Ru/Al-Basic catalyst. Figure 3A.4. presents the obtained results for glucose conversion from both monometallic and bimetallic catalysts. Figure 3A.4 depicted that using (1.5)Ru(1.5)Co/Al-Basic catalyst, 80% sorbitol yield was obtained compared to 73%

with monometallic (1.5)Ru/Al-Basic catalyst. This suggests that, addition of Co promoter in (1.5)Ru/Al-Basic catalyst enhances the catalyst activity for the transformation of glucose to sorbitol. This prove that Co is also contributes to convert glucose into sorbitol. This means both Ru and Co are playing complementary roles.

Additionally, with (1.5)Ru(3)Co/Al-Basic catalyst the highest 91% sorbitol yield was achieved with complete conversion of glucose. To quantify the gap in activities of bimetallic and monometallic catalysts, the TOF of both the catalysts was calculated within 1 h of the reaction. It was seen that the bimetallic (1.5)Ru(3)Co/Al-Basic catalyst has a higher TOF (143 h^{-1}) compared to the monometallic (1.5)Ru/Al-Basic catalyst (93 h^{-1}) in addition to an increase in selectivity towards sorbitol formation. This proves that the bimetallic catalyst has a higher efficiency to hydrogenate glucose into sorbitol than the monometallic catalyst. However, further increase in Co loading to 4.5%, decrease in sorbitol yield was observed. This could be because of an increase in Co loading, the extra Co metal particle covers the active Ru sites and reduces the accessibility of active Ru site to the H_2 molecule. Additionally, a rise in mannitol production was seen with increasing Co loading. It implies that glucose isomerizes into fructose at increased Co loading, which then transforms into mannitol. Therefore, a rise in mannitol yield was noted at higher Co loading. When the activity of monometallic (3)Co/Al-Basic and (1.5)Ru/Al-Basic catalyst was compared and it was observed that the (3)Co/Al-Basic catalyst showing only 12% conversion and 2% sorbitol yield, which is negligible in comparison with (1.5)Ru/Al-Basic catalyst. This proves that, (3)Co/Al-Basic catalyst is not able to activate a H_2 molecule and hence showing poor results compare to monometallic (1.5)Ru/Al-Basic catalyst. To further investigate this difference in the activities, the correlation between catalyst characterization and activity was found.

As seen from the XPS analysis (Chapter 2, section 2.3.2.2), in the (1.5)Ru(3)Co/Al-Basic catalyst, cobalt is present in a higher oxidation state (+2 and +3) and thus it behaves as an Lewis acid site. During the reaction, as shown in Figure 3A.5, Co will accept the electron pair from the O atom of the C=O group of substrates and can possibly activate the C=O group by making carbonyl carbon more electrophilic; thus, this will facilitate the addition of hydrogen

across the double bond. In view of this, compared to monometallic catalysts, an increased catalytic activity was seen in bimetallic catalysts after the addition of Co.

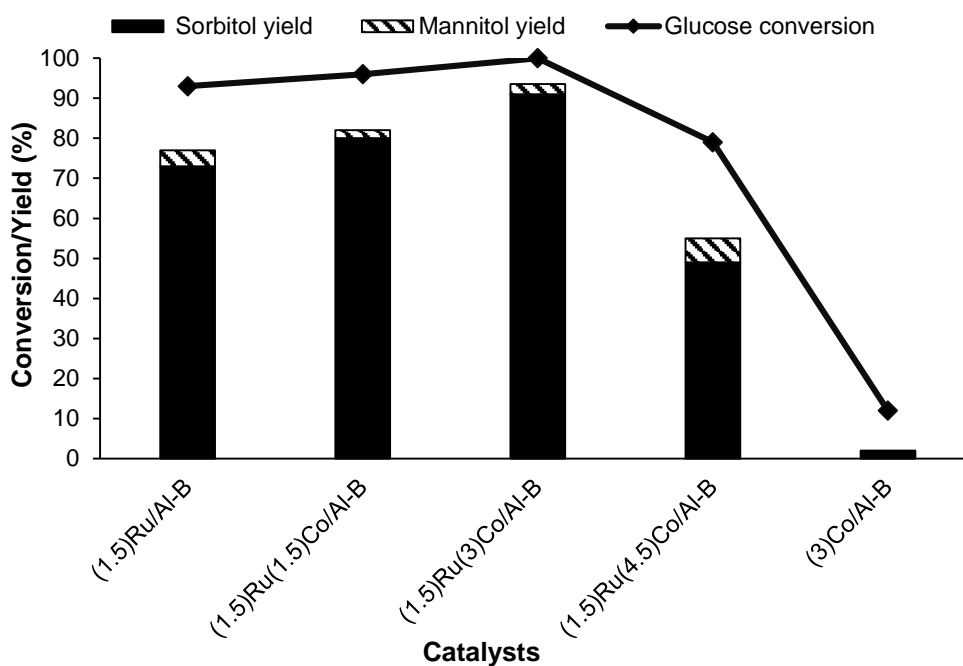


Figure 3A.4. Effect of Co loading on glucose hydrogenation.

Reaction conditions: Glucose, catalyst, S/C (169 mol/mol), Water (35mL), 15 bar H₂ at R.T., 130°C, 6 h.

All the reactions are done at least three times and the obtained results are within the error of $\pm 1\%$ -2.5 % range.

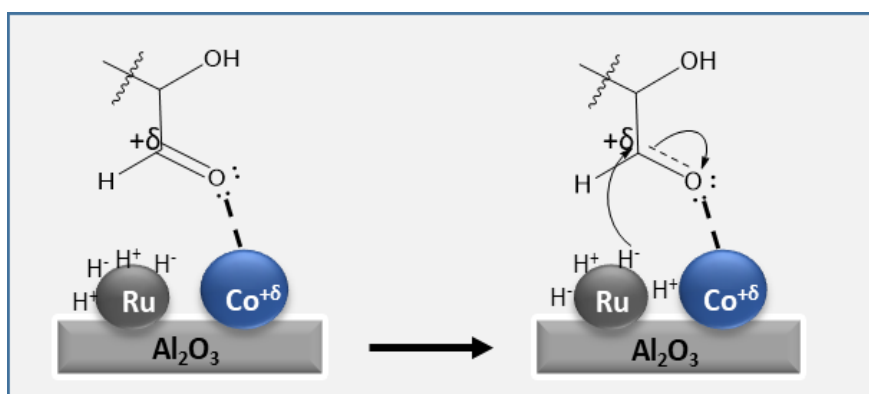
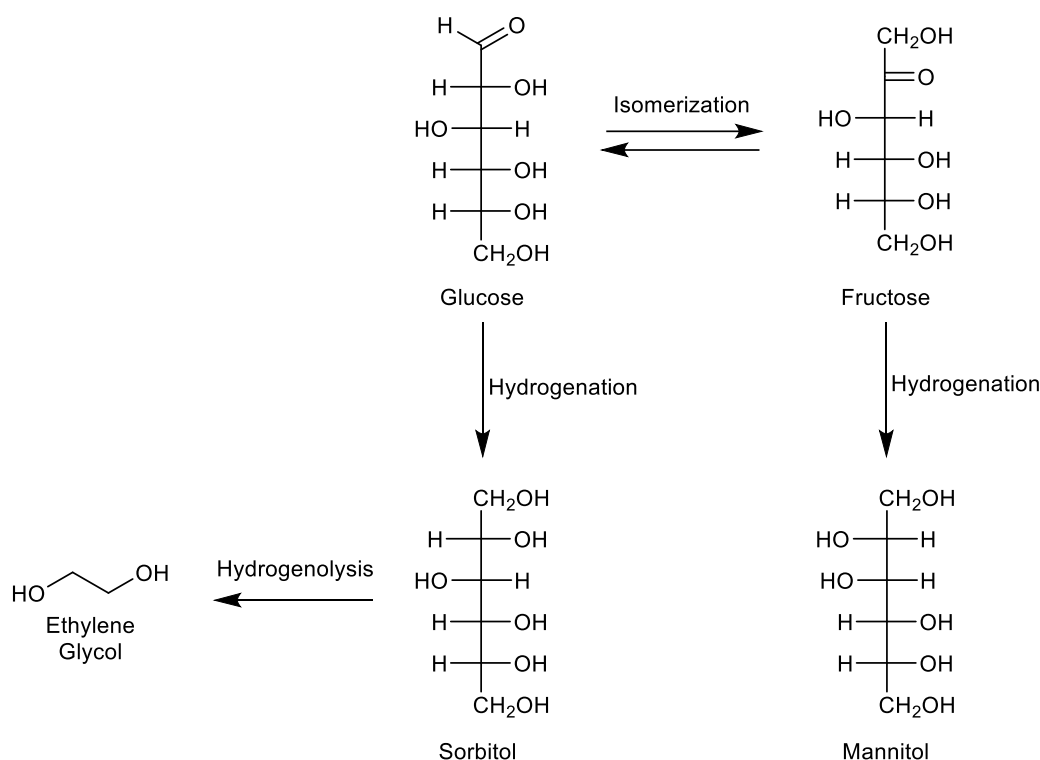


Figure 3A.5. Glucose-Cobalt interactions.

Additionally, in addition to sorbitol, fructose, mannitol and ethylene glycol (E.G.) are also generated during the conversion of glucose to sorbitol, along with sorbitol some other products including. Scheme 3A.2 illustrated the pathways for the formation of these side products. Fructose is an isomerized product of glucose. It is well-known that glucose isomerizes to fructose in presence of Lewis acid. As mentioned before, In (1.5)Ru(3)Co/Al-Basic catalyst, Co provides a Lewis acid sites during the reaction and facilitates glucose hydrogenation to fructose. By hydrogenation, fructose further converted to mannitol and through the hydrogenolysis process, sorbitol is converted to ethylene glycols.



Scheme 3A.2. Glucose to fructose isomerization.

3A.3.4. Effect of different reaction parameters:

Effect of temperature:

The impact of reaction temperature on selectivity and conversion of glucose to sorbitol over (1.5)Ru(3)Co/Al-Basic catalyst was studied at different reaction temperature ranging from 110°C to 140°C. Since it is always preferable to carry out reactions at lower temperatures, the initial reactions were conducted at 100°C under 15 bar H₂ pressure for 6 h. As shown in Figure 3A.6, the yield of sorbitol was reported 60% at 100°C. At this temperature along with sorbitol, 6% fructose and 4% mannitol were also detected like fructose and mannitol. It shows that glucose isomerizes at lower temperature and forms undesired products. When temperature was increased from 100°C to 130°C, subsequent increase in conversion and yield was observed. At 120°C and 130°C, glucose conversion was 92% and 100% with 78% and 91% yield towards sorbitol, respectively. Further increase

in temperature to 140°C did not show much of improvement in the selectivity. Resultantly, 130°C temperature was chosen to be optimized temperature for the catalytic hydrogenation of glucose to sorbitol at 15 bar H₂ pressure for 6h reaction time. Based on the temperature study, the reactions activation energy was calculated and found to be -18.336 kJ mol⁻¹.

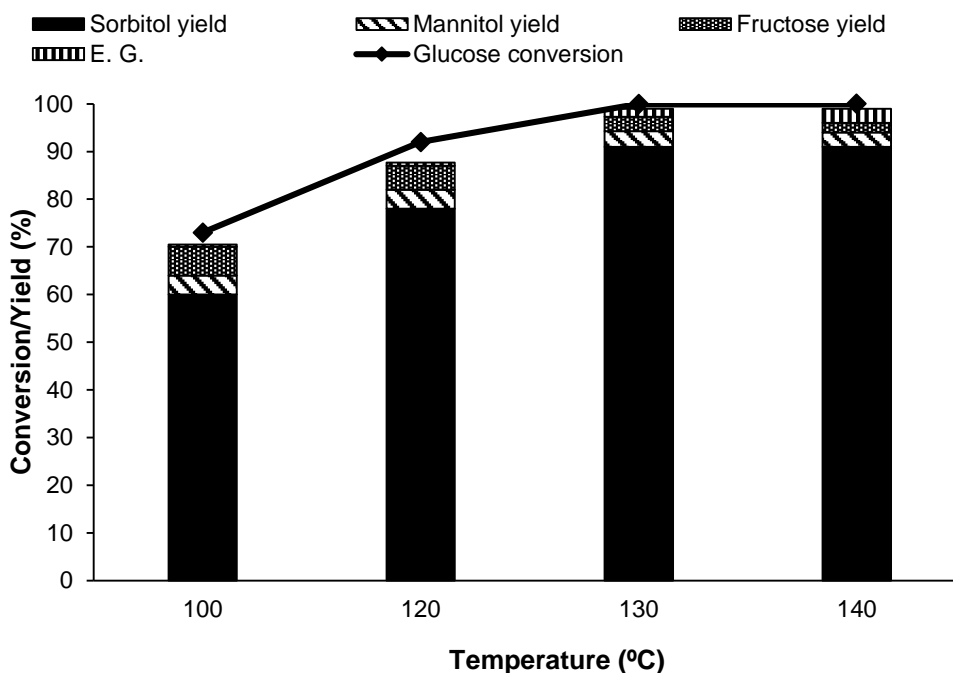


Figure 3A.6. Effect of temperature on glucose hydrogenation over (1.5)Ru(3)Co/Al-Basic catalyst.

Reaction conditions: Glucose, (1.5)Ru(3)Co/Al-Basic catalyst, S/C (169 mol/mol), Water (35mL), 15 bar H₂ at R.T., 6 h.

All the reactions are done at least three times and the obtained results are within the error of ± 1%-2.5 % range.

Effect of H₂ pressure:

To check the influence of H₂ pressure, reactions were done at different hydrogen pressure such as 10, 15 and 18 bar (Figure 3A.7). At 10 bar H₂ pressure, 90% conversion and 70% sorbitol yield with 78% selectivity was achieved however with increase in H₂ pressure to 15 bar, 91% yield was achieved at complete glucose conversion. This resulted in the conclusion that increase in pressure shows positive effect towards conversion and yield. This might be due to the increase in H₂ solubility in solvent under high pressures. Further even rise in H₂ pressure to 18 bar showed no substantial positive change in the conversion and sorbitol formation was observed. This is because, despite the fact that the solubility of H₂ may have improved with a rise of pressure, but the number of active sites accessible to H₂ molecule activation remained constant.

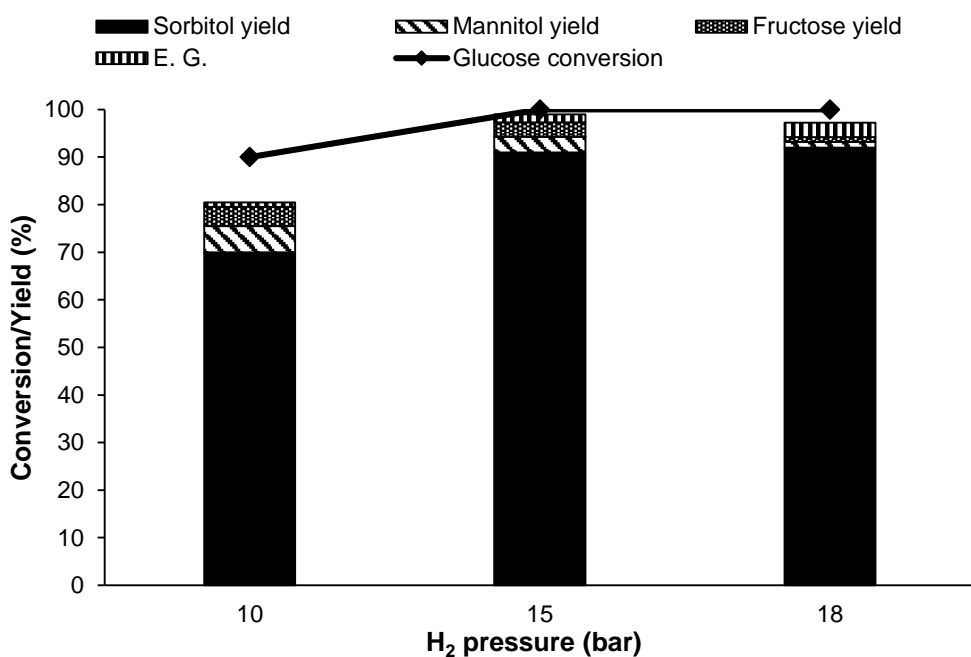


Figure 3A.7. Effect of H₂ pressure on glucose hydrogenation over (1.5)Ru(3)Co/Al-Basic catalyst.

Reaction conditions: Glucose, (1.5)Ru(3)Co/Al-Basic catalyst, S/C (169 mol/mol), Water (35mL), 130°C, 6 h.

All the reactions are done at least three times and the obtained results are within the error of $\pm 1\%$ -2.5 % range.

Effect of time:

The impact of reaction time on the conversion of glucose to sorbitol was examined in the time range between 5 h to 7 h at 130°C and 15 bar H₂ pressure. From Figure 3A.8, it can be said that selectivity towards sorbitol increases with time while the conversion is constant. The maximum conversion 100% and yield of sorbitol 91% was achieved within 6 h. Further rise in reaction time to 7 h, conversion and yield was constant. Therefore, the optimal reaction time for the conversion of glucose to sorbitol would be 6 h.

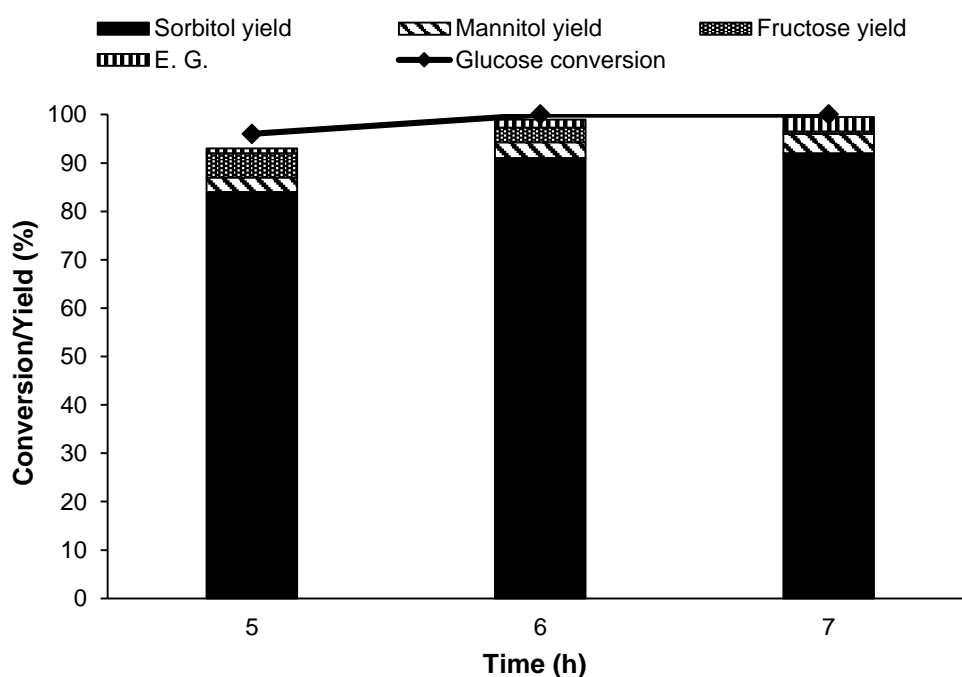


Figure 3A.8. Effect of time on glucose hydrogenation over (1.5)Ru(3)Co/Al-Basic catalyst.

Reaction conditions: Glucose, (1.5)Ru(3)Co/Al-Basic catalyst, S/C (169 mol/mol), Water (35mL), 15 bar H₂ at R.T., 130°C.

All the reactions are done at least three times and the obtained results are within the error of ± 1%-2.5 % range.

Effect of S/C ratio:

In order to get lowest catalyst loading with the higher substrate to catalyst ratio, catalyst loading was optimized (Figure 3A.9). For the optimization reactions were run for 6 h at 130°C and 15 bar H₂ pressure with (1.5)Ru(3)Co/Al-Basic catalyst. All the reactions were carried out by using fixed amount of substrate (0.35g) with varying amount of catalyst (S/C= 197, 157 and 131) (S/C ratio is the ratio of substrate and Ru). At S/C= 197, only 84% conversion and 50% sorbitol yield (with 59% sorbitol selectivity) was achieved. In addition to sorbitol, 7% mannitol was also detected at this S/C ratio. Lower conversion and yield at high S/C raio was might be because of the presence of inadequete active sites of catalyst, which might not be suffucient for the reaction under given reaction conditions. In light of this, the catalyst quantity was increased further, and at S/C= 169, complet glucose converstion was achieved along with highest 91% sorbitol yield and 3.3% mannitol yield. This is because at this S/C ratio, there might be suffucient active metal is available, which improves the interactions between catalyst and H₂ molecule and promotes H₂ molecule spitting. Further increase in catalyst quantity (S/C=131), there was no significantt improvemennt in conversion and yield was observed because even thogh at this S/C ratio, active sites are more but the number of H₂ and substrate molecules present in reaction mixtre are constant. In light of this, all the studiese were conducted using S/C= 169 ratio, because it demonstrated nearly complete glucose conversion with a higher yield of sorbitol.

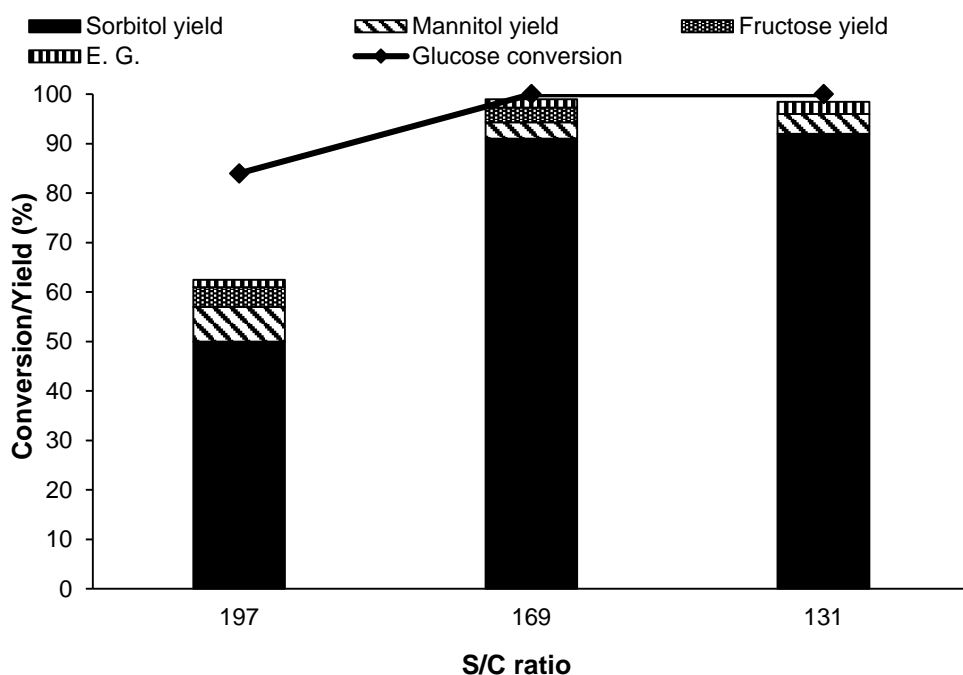


Figure 3A.9. Effect of S/C ratio on glucose hydrogenation over (1.5)Ru(3)Co/Al-Basic catalyst.

Reaction conditions: Glucose, (1.5)Ru(3)Co/Al-Basic catalyst, Water (35mL), 15 bar H₂ at R.T., 130°C, 6 h.

All the reactions are done at least three times and the obtained results are within the error of $\pm 1\%$ -2.5 % range.

Effect of glucose concentration:

To make the process industrially feasible, reactions were done at different glucose concentrations (1 wt%, 7 wt% and 20 wt%) (Figure 3A.10). Under same reaction conditions, with 1 wt% to 7 wt% glucose concentration, constant results were achieved (conv-100%, sorbitol yield-91%, Mannitol yield-3.3%). Nevertheless, further increase in glucose concentration to 20 wt%, showed decrease in yield (82%). Increase in glucose concentration increases amount of mannitol formation (8%) and decrease selectivity towards sorbitol formation was observed. Scale up of the reaction in 1 liter reactor with 1wt% glucose solution was also done and achieved 100% glucose conversion and 86% sorbitol yield.

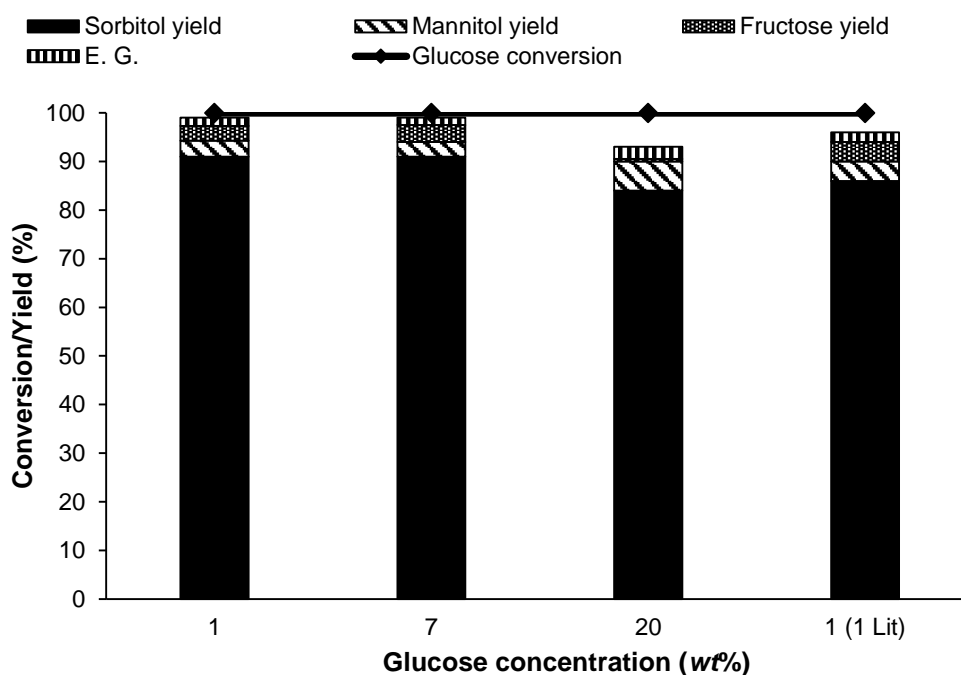


Figure 3A.10. Effect of glucose concentration on glucose hydrogenation over (1.5)Ru(3)Co/Al-Basic catalyst.

Reaction conditions: Glucose, (1.5)Ru(3)Co/Al-Basic catalyst, S/C (169 mol/mol), Water (35mL), 130°C, 15 bar H₂ at R.T., 6 h.

All the reactions are done at least three times and the obtained results are within the error of $\pm 1\%$ -2.5 % range.

3A.3.5. Hydrogenation of different C6 sugars:

To generalize the catalytic system developed for glucose hydrogenation, the catalytic activity of the (1.5)Ru(3)Co/Al-Basic catalyst was checked for the different C6 (glucose, mannose, and galactose) sugars. Reactions of C6 sugars were carried out under optimized reaction parameters of glucose (130°C, 15 bar H₂ at R.T., 6 h). It was observed that the catalyst shows 100% conversion of all the sugars and $\geq 91\%$ yield of corresponding sugar alcohols. Hence, it can be safely assumed that the catalyst is highly active for the hydrogenation of different sugars (Figure 3A.11).

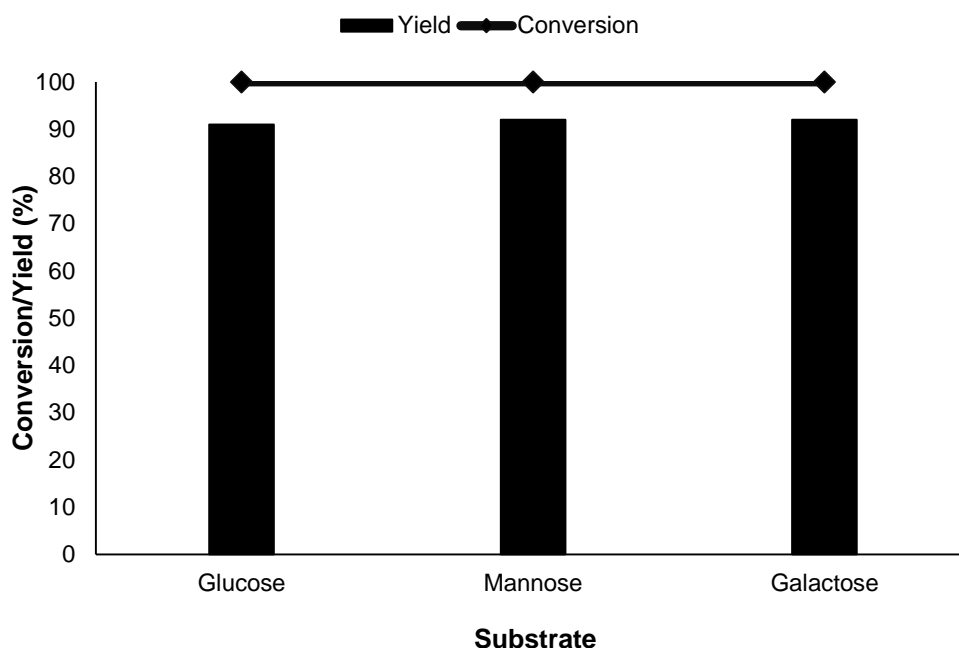


Figure 3A.11. Hydrogenation of different C6 sugars over (1.5)Ru(3)Co/Al-Basic catalyst.

Reaction conditions: Substrate, (1.5)Ru(3)Co/Al-Basic catalyst, S/C (169 mol/mol), Water (35mL), 130°C, 15 bar H₂ at R.T., 6 h.

All the reactions are done at least three times and the obtained results are within the error of $\pm 1\%$ -2.5 % range.

3A.3.6. Recycle study:

From an economic perspective, stability and reusability of catalyst is very important in heterogeneous reactions. To explore the catalyst reusability for the catalytic hydrogenation of glucose to sorbitol, initially reactions were carried out with 20 wt% glucose solution at 130°C under 20 bar H₂ pressure for 6 h time. After the first run, reaction mixture was centrifuged to separate the catalyst from reaction solution. The recycled catalyst was thoroughly washed with distilled water to remove any adsorbed products that had not been converted. Then catalyst was

dried at 60°C for overnight and used for the next run without any further reactivation under similar reaction conditions. During the study of effect of glucose concentration on product yield, it has been seen that with 20 wt% glucose solution catalyst was showing 100% conversion and 84% yield which is less than that of a 1 wt% glucose solution (91% yield). Therefore, in order to enhance the yield of sorbitol with a 20 wt% glucose solution, a first recycle study was done at higher H₂ pressure (20 bar) and results showed that sorbitol yield was observed 70% at 20 bar H₂ pressure, compared to 84% at 15 bar H₂ pressure. Three recycle runs was carried out with 20 bar H₂ pressure and observed that catalyst showed constant sorbitol yield (70%). After that a 4th recycle was conducted at 15 bar H₂ pressure and at this H₂ pressure 84% sorbitol yield was observed. It indicates that regain in catalyst activity was seen when reaction was done at 15 bar H₂ pressure. Consideration of this, further recycle study was conducted with 15 bar H₂ pressure. Further recycle study was conducted up to 6 runs and catalyst exhibits consistence activity up to 6 runs (Figure 3A.12) indicates that (1.5)Ru(3)Co/Al-Basic catalyst has good catalytic stability under the reaction conditions.

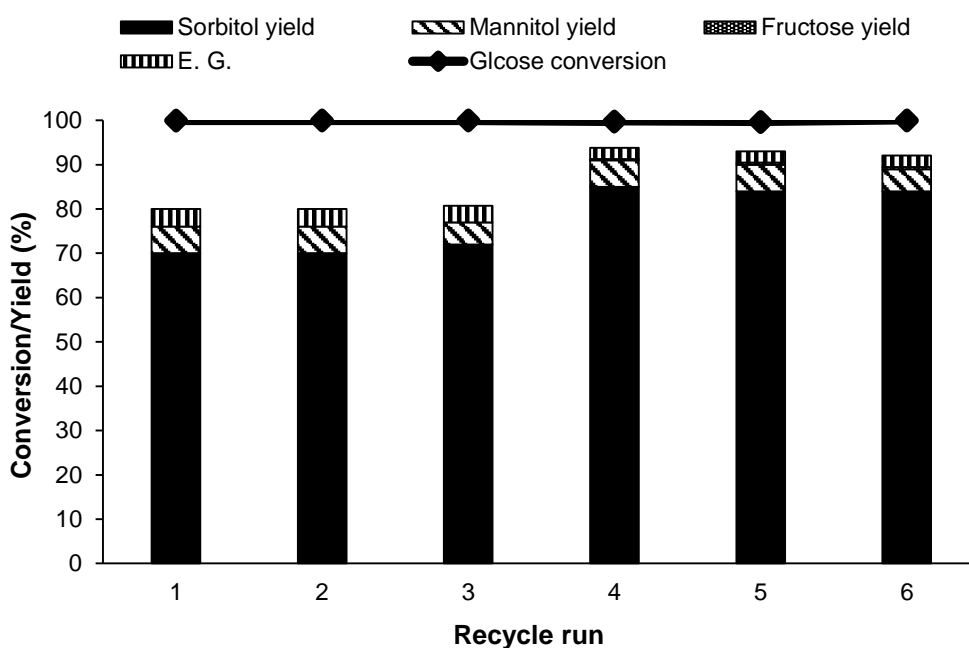


Figure 3A.12. Recycle study of (1.5)Ru(3)Co/Al-Basic catalyst.

Reaction conditions: Glucose, (1.5)Ru(3)Co/Al-Basic catalyst, S/C (169 mol/mol), Water (35mL), 130°C, 20 & 15 bar H₂ at R.T., 6 h.

(1st to 3rd – reactions were done under 20 bar H₂ pressure, 4th to 6th reactions were done under 15 bar H₂ pressure.)

3A.3.7. Spent catalyst characterization:

To find out the impact of reaction parameters on the catalyst's physical and chemical properties, further characterization of spent catalyst was done. TEM images showed similar particle size of fresh and spent catalyst (1-2nm) (Figure 3A.13). This indicates that no metal particle agglomeration or sintering of occurred during the reaction. N₂-sorption analysis showed that no significant changes in surface area of both fresh and spent catalysts was observed (surface area of fresh catalyst is 219 m²/g and spent catalyst is 214 m²/g).

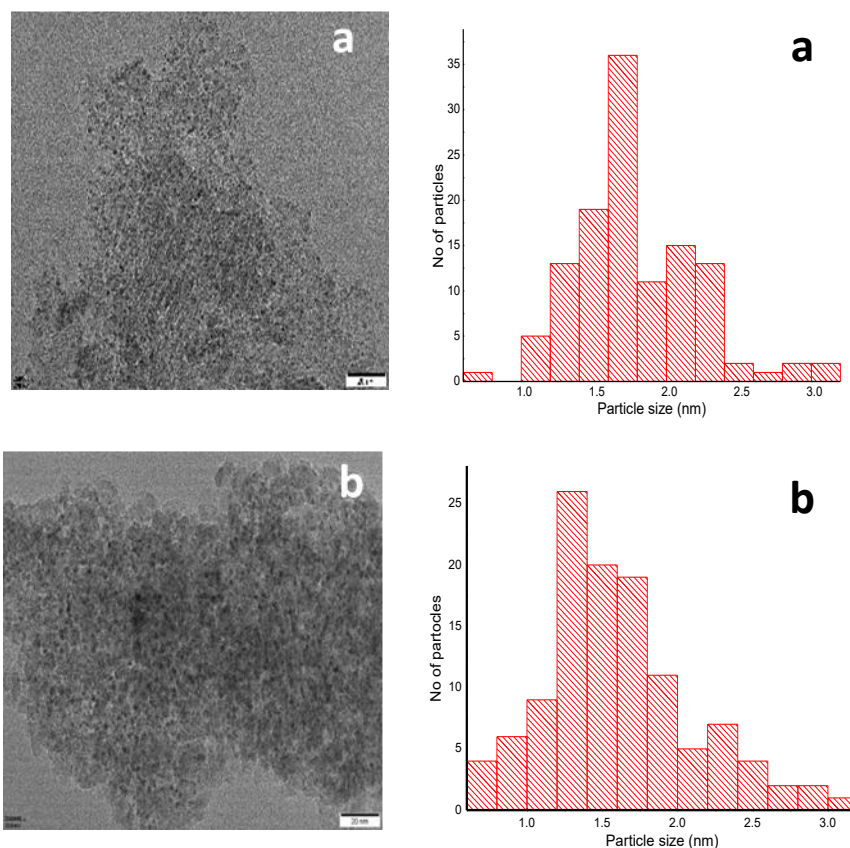


Figure 3A.13. TEM image and particle size distribution of (1.5)Ru(3)Co/Al-Basic (a) fresh and (b) spent catalyst

3A.3.8. Reaction in flow mode reactor:

From above discussions it is observed that (1.5)Ru(3)Co/Al-Basic catalyst efficiently hydrogenate glucose into sorbitol with highest conversion and yield in batch mode reactor. Additionally, for the industrial demonstration of traditional methods, it is preferable to build the process in continuous flow mode reactor because compared to batch mode reactions, continuous flow mode reactions provide more efficient, safe and controlled method for chemical synthesis, which makes them more popular.

Hydrogenation of glucose to sorbitol was carried out in a stainless-steel cylindrical reactor operating in downflow mode with a continuous flow of reactant and H₂ gas. The cylindrical reactor was situated inside the two-zone split furnace (13 mm

inner diameter, Geomechanique, France). For a particular reaction, 1 gm of catalyst in mesh form (mesh size of 0.5mm) was loaded in cylindrical reactor. The catalyst bed was located in between the two layers of glass beads inside the reactor. Prior to the reaction, activation of catalyst was done in presence of H₂ gas at 300°C for 2 h with a H₂ flow of 10 mL·min⁻¹. The high precision syringe pump was used to pump the reactant into the reactor at a desired flow rate. The optimization of reaction parameters like temperature, H₂ pressure, H₂ flow rate, reactant flow etc. was done to achieve maximum conversion and yield. The optimized reaction condition for the transformation of glucose to sorbitol in continuous flow mode reactor is 140°C, 25 bar H₂ pressure, reactant flow 0.15 mL·min⁻¹ and H₂ flow of 10 mL·min⁻¹. From Figure 3A.14, shows that under optimum reaction conditions, a catalyst exhibits an average 85% conversion of glucose and a 74% sorbitol yield over a continuous 270 h run.

During the continuous formation of product, both gas and liquid fluid was cooled down and collected in the gas-liquid separator which is located at the reactor's outlet. After that the collected liquid was analyzed using HPLC technique. For more details regarding instrument and analysis procedure please refer section 3A.2.3.

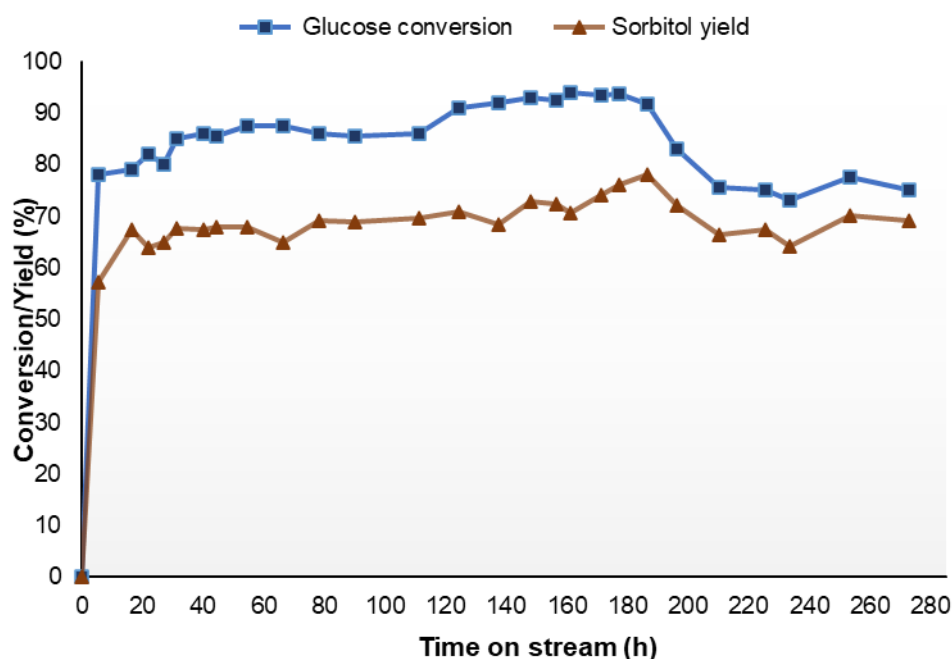


Figure 3A.14. Continuous flow mode reaction for glucose hydrogenation over (1.5)Ru(3)Co/Al-Basic catalyst.

Reaction conditions: Glucose (20 wt%) (glucose flow-0.15 mLmin⁻¹), (1.5)Ru(3)Co/Al-Basic catalyst, 140°C, 25 bar H₂, 10 mLmin⁻¹ H₂ flow.

3A.3.9. Purification of sorbitol:

For the purification of obtained sorbitol, after the reaction, catalyst was separated out from the reaction mixture. The resulting reaction mixture containing sorbitol was concentrated by removing solvent (water) by rotavap and was then subjected to purification to remove impurities. The product was purified simply by crystallization method. For the purification of sorbitol an organic solvent was added in concentrated reaction mixture. Then the solution was heated at certain temperature to obtain clear supernatant solution. Then the solution was cooled

at certain temperature to obtain crystals. The obtained crystals of purified sorbitol were analyzed using various analysis techniques including HPLC, ^1H NMR and HRMS and the outcomes are presented in the Figure 3A.15 and 3A.16 respectively. According to the HPLC analysis the purity level of purified sorbitol is 96% respectively.

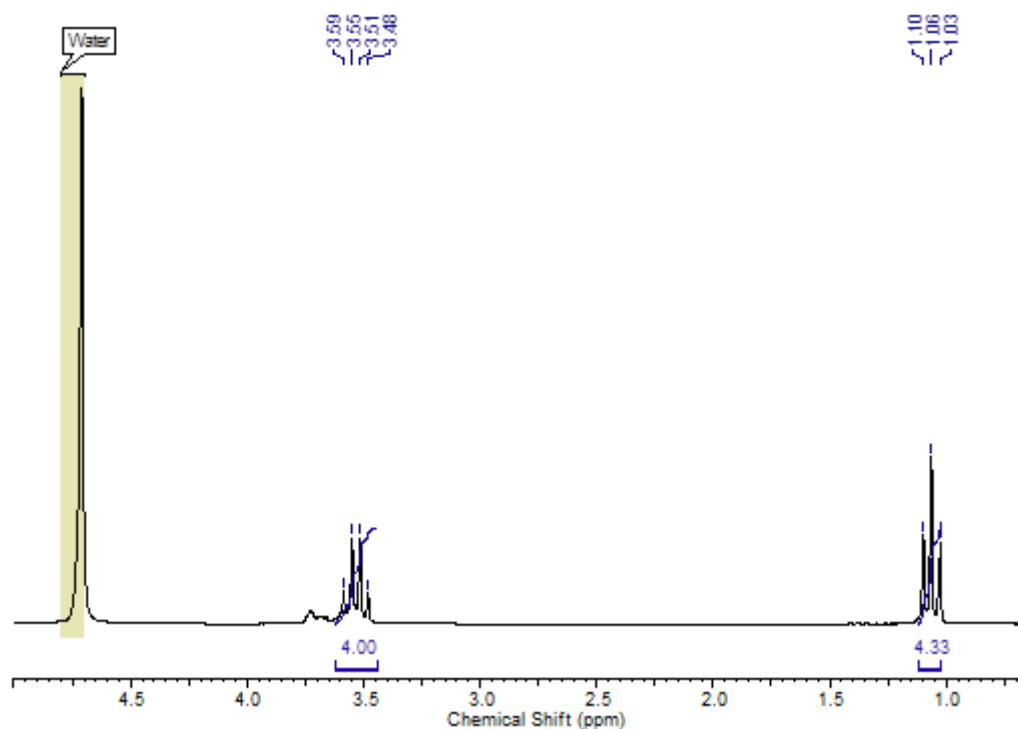


Figure 3A.15. ^1H NMR profile of purified sorbitol.

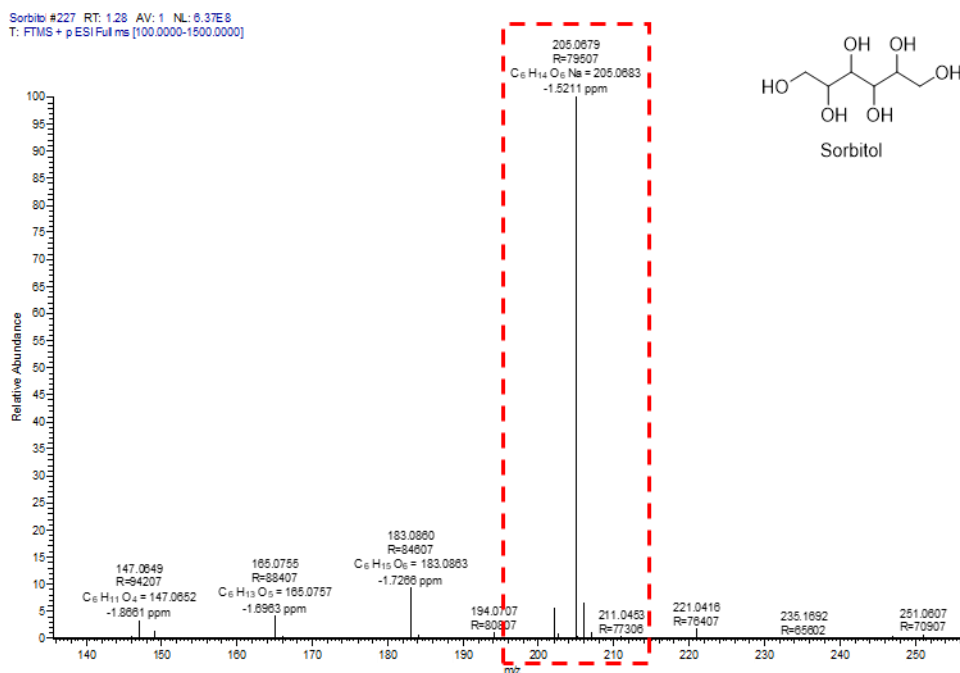


Figure 3A.16. HRMS profile of purified sorbitol.

3A.4. Conclusion:

A range of different monometallic and bimetallic catalysts with distinct metal ratios were prepared using a simple wet impregnation method and employed for the hydrogenation of sugars to sugar alcohols. The effect of different supports like Si, C, Al, Si-Al were also studied and among all the synthesized monometallic catalyst, (3)Ru/C and (3)Ru/Al-Basic exhibits excellent catalytic activity. But considering the drawbacks of carbon support discussed above, (3)Ru/Al-Basic used as a best catalyst to convert glucose into sorbitol. Effect of Co metal as a promoter was studied in order to decrease the Ru loading and increase the product yield. Among synthesized bimetallic Ru,Co catalysts, the (1.5)Ru(3)Co/Al-Basic catalyst demonstrated better catalytic activity for the hydrogenation of glucose with a low Ru loading

(1.5 wt%). Compared to monometallic catalysts, bimetallic catalysts show better activity attributed to the synergistic effect of cobalt and ruthenium. To increase the yield of sorbitol, several reaction variables, including temperature, S/C ratio, time, H₂ pressure etc. were optimized. It was found that (1.5)Ru(3)Co/Al-Basic catalyst exhibits the highest activity at lower H₂ pressure 15 bar and temperature 130°C within 6 h reaction period. Along with glucose, other C₆ sugars (galactose and mannose) also show 100% conversion and >90% sugar alcohol yield at 130°C and 15 bar H₂ pressure. Compared to the reported catalysts, the synthesized (1.5)Ru(3)Co/Al-Basic catalyst is stable, active for different sugar hydrogenation reactions and shows better activity for high concentration reactions also. According to recycle study (Section 3A.3.6.), catalyst shows significant stability and recyclability. Glucose hydrogenation to sorbitol was also done in continuous flow mode reactor at 150°C, 25 bar H₂ pressure with the flow rate of 10 mL·min⁻¹ and achieved 85% conversion with 74% sorbitol yield. Purification of the product is also performed and achieved 96% sorbitol purity.

3A.5. References:

1. W. Deng, Q. Zhang, Y. Wang, *Catalysis Today*, 2014, **234**, 31–41.
2. X. Han, Y. Guo, X. Liu, Q. Xia, Y. Wang, *Catalysis Today*, 2019, **319**, 2–13.
3. H. Cui, X. Tong, L. Yu, M. Zhang, Y. Yan, X. Zhuang, *Catalysis Today*, 2019, **319**, 100–104.
4. B. Zada, M. Chen, C. Chen, L. Yan, Q. Xu, W. Li, Q. Guo and Y. Fu, *Science China Chemistry*, 2017, **60**, 853–869.
5. J.A. Melero, et al, *Molecular Catalysis*, 2020, **484**, 110802.
6. J. M. Robinson, A. M. Wadle, M. D. Reno, R. Kidd, S. R. Barrett Hinsz and J. Urquieta, *Energy Fuels*, 2015, **29**, 6529–6535.
7. M. He, J. Guo, X. Wang, Y. Song, S. Liu, H. Wang and C. Li, *New Journal of Chemistry*, 2020, **44**, 10292–10299.
8. P. Gallezot, P. Cerino, B. Blanc, G. Fleche and P. Fuertes, *Journal of Catalysis*, 1994, **146**, 93–102.
9. A. A. Kirali, S. Sreekantan and B. Marimuthu, *New Journal of Chemistry*, 2020, **44**, 15958–15965.
10. C. A. Ramírez-Lopez, J. R. Ochoa-Gómez, S. Gil-Río, O. Gómez-Jime'nez-Aberasturi and J. Torrecilla-Soria, *Journal of Chemical Technology and Biotechnology*, 2011, **86**, 867–874.
11. T. Werpy and G. Petersen, Top value added chemicals from biomass: volume I—results of screening for potential candidates from sugars and synthesis gas, National Renewable Energy Lab., Golden, CO (US), 2004.
12. B. Hoffer, E. Crezee, F. Devred, P. Mooijman, W. Sloof, P. Kooyman, A. Van Langeveld, F. Kapteijn and J. Moulijn, *Applied Catalysis A*, 2003, **253**, 437–452.

13. D. Shi, R. Wojcieszak, S. Paul and E. Marceau, *Catalysts*, 2019, **9**, 451.
14. J. Wisniak, M. Hershkowitz and S. Stein, *Product Research and Development*, 1974, **13**, 232–236.
15. T.-t Gao, Y.-g Sun, Y.-b Zhu, F. Lin, Y.-d Zhong, Y.-y Li, W.-x Ji and Y.-l Ma, *New Journal of Chemistry*, 2022, **46**, 16058–16067.
16. M. Makkee, A. P. Kieboom and H. van Bekkum, *Carbohydrate Research*, 1985, **138**, 225–236.
17. B. J. Arena, *Applied Catalysis A*, 1992, **87**, 219–229.
18. J. Melero, J. Moreno, J. Iglesias, G. Morales, J. Fierro, R. Sa´nchez-Va´zquez, A. Cubo and B. Garcı´a, *Molecular Catalysis*, 2020, **484**, 110802.
19. A. A. Dabbawala, D. K. Mishra and J.-S. Hwang, *Catalysis Today*, 2016, **265**, 163–173.
20. H. Singh, A. Rai, R. Yadav and A. K. Sinha, *Molecular Catalysis*, 2018, **451**, 186–191.
21. Y. Fu, L. Ding, M. L. Singleton, H. Idrissi and S. Hermans, *Applied Catalysis B*, 2021, **288**, 119997.
22. R. Xi, Y. Tang, R. L. Smith, X. Liu, L. Liu and X. Qi, *Green Energy Environment.*, 2022, DOI: 10.1016/j.gee.2022.04.003.
23. B. Zada, L. Yan and Y. Fu, *Science China Chemistry*, 2018, **61**, 1167–1174.
24. L. Silvester, F. Ramos, J. Thuriot-Roukos, S. Heyte, M. Araque, S. Paul and R. Wojcieszak, *Catalysis Today*, 2019, **338**, 72–80.
25. G. de Wit, C. de Hann, A. P. G. Kieboom and H. van Bekkum, *Carbohydrate Research*, 1980, **86**, 33–41.
26. J. C. Speck, in *Advances in Carbohydrate Chemistry*, ed. M. L. Wolfrom, Academic Press, vol. 13, 1958, pp. 63–103.

Chapter 3B.

Hydrogenation of xylose to xylitol

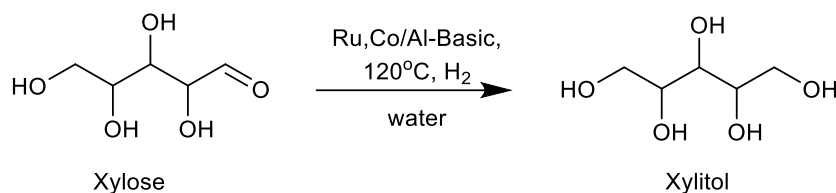
3B.1. Introduction:

According to recent trends in chemical industry, researchers are putting lot of efforts to developing an appropriate method for the transformation of renewable feedstock's to chemicals with added value.¹ According to the US Department of Energy report lists xylitol is among top twelve value added compounds derived from biomass.² Xylitol, obtained from the hydrogenation of xylose, is optically inactive,³ highly soluble in water and is used as an artificial low-calorie sweetener.⁴ It is used to prevent dental and other infections because of its antimicrobial properties.⁵ Additionally, xylitol can be utilized to generate an extensive range of high-value chemicals, including ethylene glycol, propylene glycol, xylaric acid, and so on.⁶ Xylose is produced by hydrolysis of hemicellulose. There are several methods to valuing xylose, among them one is the conversion of xylose to xylitol by hydrogenation.⁷

In industries commonly used metallic catalyst for the conversion of xylose to xylitol is Raney nickel catalyst. This catalyst showing excellent activity and selectivity towards xylitol formation, however, the major drawback of this catalyst is, during the reaction this catalyst undergoes Ni leaching, which causes it to rapid deactivation.⁸⁻¹⁰ xylose hydrogenation to xylitol is also reported over supported metal catalysts.¹¹ The influence of various supports (NiO, SiO₂, TiO₂, AC, KLTL zeolite, Al₂O₃, etc.) on the conversion of xylose to xylitol is also studied in detail by various researchers. A new type of NiO-modified TiO₂ support for anchoring Ru ((1)Ru/NiO–TiO₂) (120°C, 55 bar, conv: 100%, yield: 99%) with different Ru (1 and 5%) and NiO (1, 5 and 10%) loadings is reported and it is shown that incorporation of NiO into a modified NiO–TiO₂ support decreases the yield of arabitol and increases the selectivity toward xylitol formation.^{4,12} But since the recycle study of the catalyst is not performed, it remains to be seen whether this catalyst can be used on a commercial scale. Furthermore, zeolite Y (HYZ-80) supported Ru nanoparticle (1)Ru/HYZ-80 (120°C, 55 bar, conv: 62%, yield: 61%) and (5)Co/SiO₂ (140°C, 50 bar, conv: 100%, yield: 98%) catalysts were synthesized and examined to hydrogenate xylose into xylitol with high selectivity to xylitol formation (98%).^{13,14} But the use of a high H₂ pressure and growth of metal particles in the spent catalyst show a negative impact on the catalytic reactivity and recyclability. The (3.5)Pt/Al₂O₃ catalyst (60°C, 16 bar)

with hydrotalcite as a base was reported for the xylitol and sorbitol production with 79% xylitol and 54% sorbitol yield.¹⁵

The (1.5)Ru(3)Co/Al-Basic catalyst has not yet been reported for the conversion of xylose to xylitol. In this chapter the activity of the synthesized (1.5)Ru(3)Co/Al-Basic catalyst was evaluated for xylose hydrogenation to xylitol (Scheme 3B.1). For the transformation of xylose to xylitol, additional reaction parameter optimization including temperature, H₂ pressure, time was also investigated.



Scheme 3B.1. Hydrogenation of xylose to xylitol

3B.2. Experimental:

3B.2.1. Materials: Xylose (99%, AR), xylitol (99%, AR), arabinose (99%, AR) and arabitol (99%, AR) were bought from Loba Chemie, India. Ethylene glycol (99%) was obtained from s.d. fine chemicals. No additional treatment was applied before using all the chemicals.

3B.2.2. Catalyst synthesis:

Monometallic (1.5)Ru/Al-Basic and (3)Co/Al-Basic and bimetallic (1.5)Ru(3)Co/Al-Basic catalysts were synthesized and assessed for the production of xylitol from xylose. Chapter 2 (Refer section 2.2.2.) provides specific details on synthesis procedure and material used for the synthesis of catalyst.

3B.2.3. Reaction set-up and analysis of reaction mixtures:

A batch reactor made by Amar Equipment with 50 ml volume was used to evaluate the catalytic activity of all the synthesized catalysts. In a typical reaction, reactor was charged with

0.35g of substrate, 0.1g of catalyst and 35 mL of water. To remove the air, the reactor was purged three to four times with low pressure hydrogen. The reactor was then pressurized with the required H₂ pressure (10 bar to 15 bar). The reactions were conducted between 100°C to 130°C for the suitable reaction time. After gaining the required temperature, the stirring speed was raised from 300 rpm to 900 rpm during the heating process. Once reaction was complete, reactor was cooled down to room temperature and reaction mixture has been collected. The centrifugation of reaction mixture was done to separate the catalyst. The collected reaction mixture was filtered using 0.22mm syringe filter before analysis. The reaction mixture was analysed using high performance liquid chromatography (HPLC) equipped with a RID detector (Agilent Technologies, 100 infinite series, 40°C) and HC-75 Pb⁺² column (Hamilton, 7.8mm × 300mm, 80°C). The refractive index detector was kept 40°C while the column temperature was kept 80°C. Eluent HPLC grade water is utilized with a flow rate of 0.5 mL·min⁻¹. For the quantitative determination of each product, External standard method was applied.

3B.2.4. Calculations:

Conversion (C) of substrate and yield (Y) of products were calculated as follows:

$$\text{Conversion (C)\%} = \left\{ \frac{[(\text{Initial moles of substrate}) - (\text{Final moles of substrate})]}{\text{Initial moles of substrate}} \right\} * 100$$

$$\text{Yield (Y)\%} = \left\{ \frac{\text{Moles of product formed}}{\text{Theoretical moles of product formed based on the moles of substrate converted}} \right\} * 100$$

3B.3. Result and discussion:

The catalytic performance of the synthesized (1.5)Ru(3)Co/Al-Basic catalyst was also checked for the hydrogenation of xylose to xylitol. The reaction parameters including temperature, H₂ pressure etc. were optimize to achieve highest xylose conversion and xylitol yield.

3B.3.1. Effect of monometallic and bimetallic catalyst:

The catalytic activity of the synthesized (1.5)Ru(3)Co/Al-Basic catalyst was checked as well for the hydrogenation of xylose to xylitol. Effect of monometallic and bimetallic catalyst for the hydrogenation of xylose to xylitol was studied at 120°C, 15 bar H₂ at R. T. for 3 h and results are shown in Figure 3B.1. With both monometallic (3)Co/Al-Basic catalyst and Al-Basic support, only 12% conversion and 2% yield was obtained and with (1.5)Ru/Al-Basic catalyst 89% conversion and 72% xylitol yield was achieved. This proves that, (3)Co/Al-Basic and Al-Basic support perform poorly compare to (1.5)Ru/Al-B catalyst, since these are unable to activate a H₂ molecule (As discussed in chapter 3A, section 3A.3.3.). Moreover, results with bimetallic (1.5)Ru(3)Co/Al-Basic catalyst are significantly improved, yielded 100% xylose conversion and 93% xylitol yield. From this it has been concluded that bimetallic (1.5)Ru(3)Co/Al-Basic catalyst shows highest activity for the conversion of xylose to xylitol. Further optimization study was done to improve the conversion and yield of xylitol.

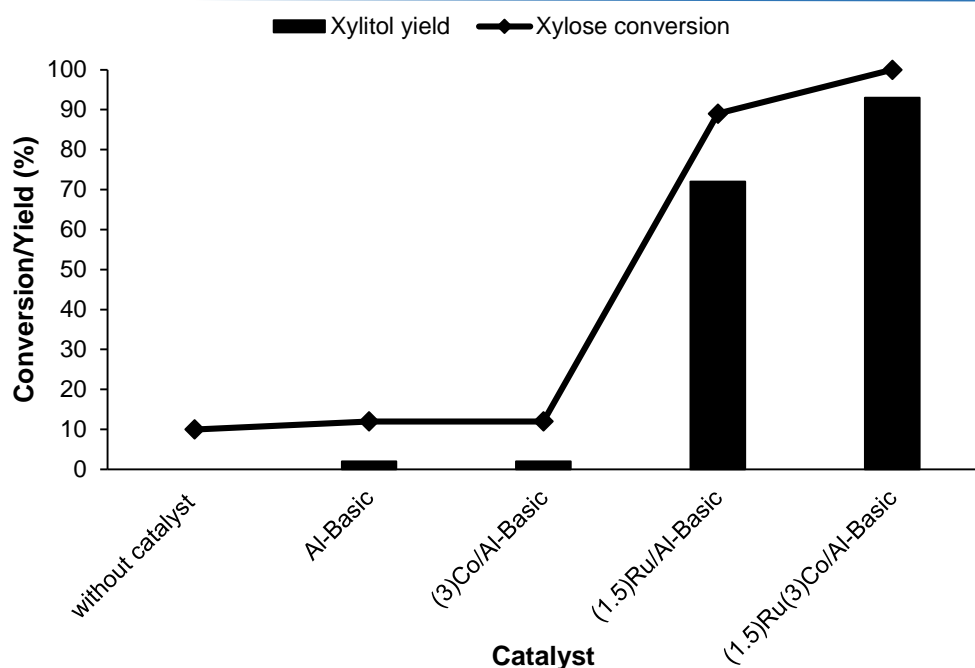


Figure 3B.1. Effect of monometallic and bimetallic catalyst on xylose hydrogenation.

Reaction conditions: Xylose, catalyst, S/C (169 mol/mol), Water (35mL), 15 bar H₂ at R.T., 120°C, 3 h.

All the reactions are done at least three times and the obtained results are within the error of $\pm 1\%$ -2.5 % range.

3B.3.2. Effect of different reaction parameters:

Effect of temperature:

To evaluate the impact of temperature on xylose conversion to xylitol, reactions were carried out at 15 bar H₂ for 3 h at various reaction temperatures ranging from 100°C to 130°C (Figure 3B.2). At 100°C, catalyst showed 72% conversion and 62% yield, as shown in Figure 3B.2, Improvement in yield to 93% with 100% conversion of xylose was seen with rise in temperature up to 120°C. Further increasing the temperature to 130°C, a slight decrease in xylitol yield from 93% to 91% was observed, this might be because at higher reaction temperature unknown product formation was observed. In this investigation the maximum xylitol yield (93%) was achieved at 120°C, hence the optimal 120°C temperature was used to examine further parameters.

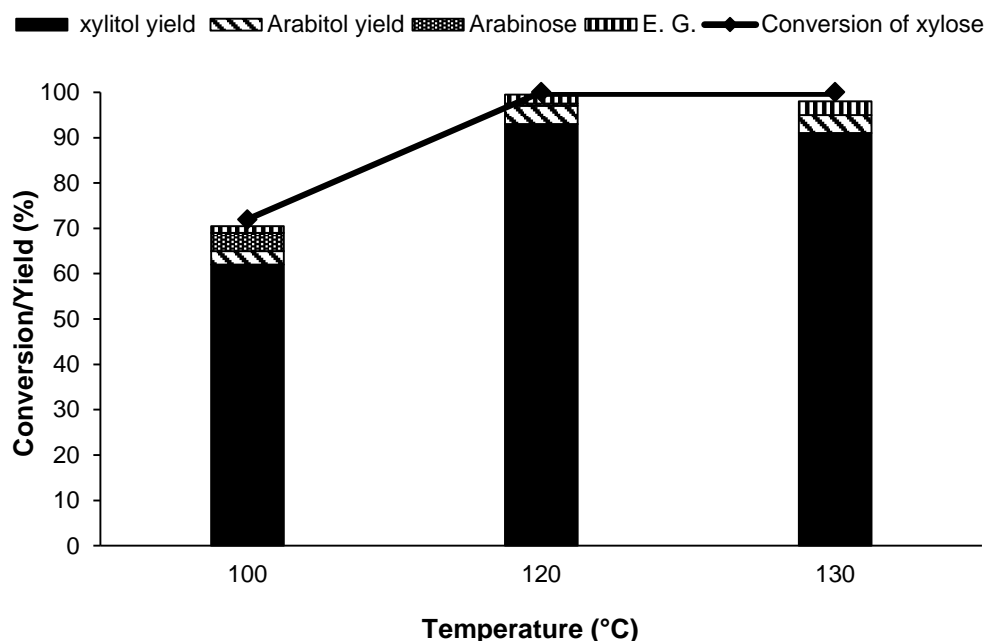


Figure 3B.2. Effect of temperature on xylose hydrogenation over (1.5)Ru(3)Co/Al-Basic catalyst.

Reaction conditions: Xylose, (1.5)Ru(3)Co/Al-Basic, S/C (169 mol/mol), Water (35mL), 15 bar H₂ at R.T., 3 h.

All the reactions are done at least three times and the obtained results are within the error of $\pm 1\%$ -2.5 % range.

Effect of H₂ pressure:

Effectiveness of the H₂ pressure on the hydrogenation of xylose to xylitol was investigated at 120°C for 3 h. H₂ was charged in reactor at room temperature under various pressures (5, 10 and 15 bar). With increase in H₂ pressure from 5 bar to 15 bar, xylitol yield was drastically improved from 30% to 93%. The finding showed that (Figure 3B.3) the increased H₂ pressure encouraged the conversion of xylose to xylitol. It indicates that H₂ pressure has direct impact on hydrogenation of xylose to xylitol. High pressure facilitates the dissolution of H₂ in water.¹⁶ which results to higher H₂ concentration around the active catalyst surface, which increases the active H⁻ species in the reaction mixture which speed up the xylose

hydrogenation process. Thus, the optimum reaction H₂ pressure for the conversion of xylose to xylitol is 15 bar.

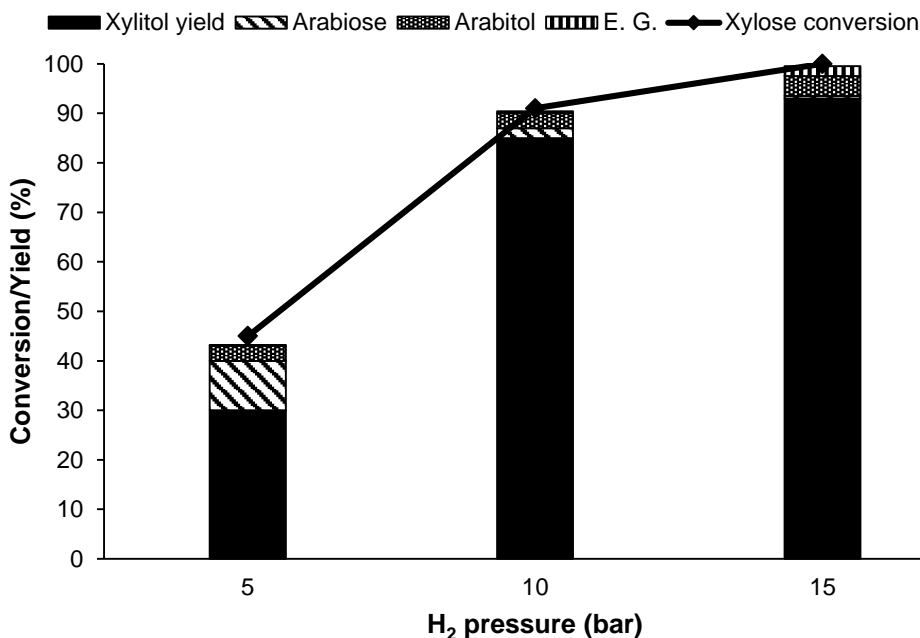


Figure 3B.3. Effect of H₂ pressure on xylose hydrogenation over (1.5)Ru(3)Co/Al-Basic catalyst.

Reaction conditions: Xylose, (1.5)Ru(3)Co/Al-Basi, S/C (169 mol/mol), Water (35mL), 120°C, 3 h.

All the reactions are done at least three times and the obtained results are within the error of $\pm 1\%$ -2.5 % range.

Hydrogenation of concentrated xylose solution:

With 1 wt% xylose solution, (1.5)Ru(3)Co/Al-Basic catalyst showed best activity (93% xylitol yield with 100% xylose conversion) at optimized reaction condition 120°C, 15 bar H₂ pressure, 3 h). In light of the high conversion and yield with 1 wt% xylose concentration, further impact of xylose concentration on their conversion and yield has been studied at optimizes reaction condition. As discussed in chapter 1A, the catalyst exhibits better activity up to a 20

wt% glucose concentration hence it was decided that the activity of catalyst will be tested directly with 20 wt% xylose solution. Figure 3B.4, shows that with 20 wt% xylose concentration catalyst showing 100% conversion and 84% xylitol yield with 5% arabinose formation at optimized reaction condition.

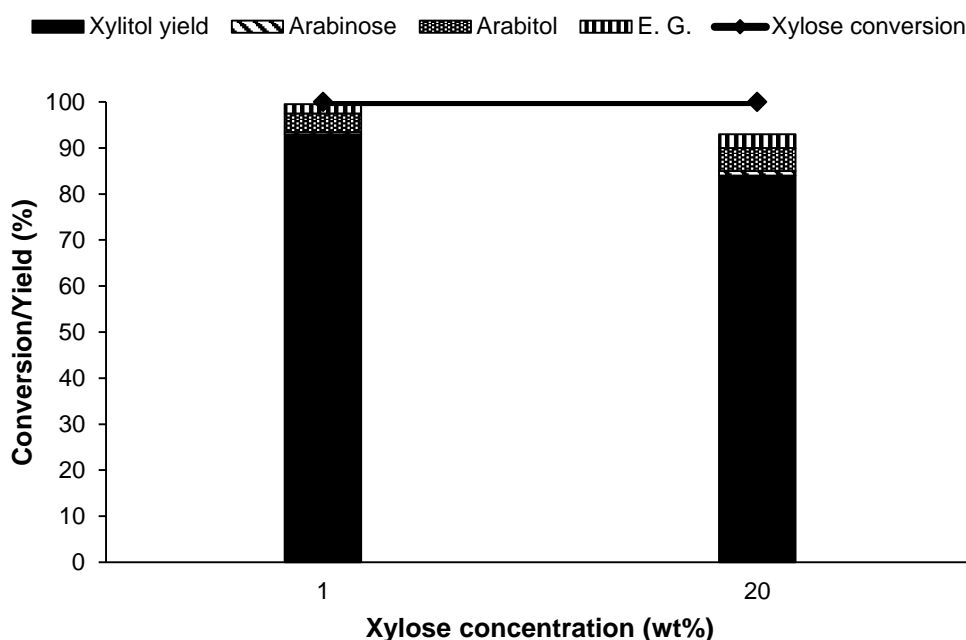


Figure 3B.4. Effect of xylose concentration on xylose hydrogenation over (1.5)Ru(3)Co/Al-Basic catalyst.

Reaction conditions: Xylose, (1.5)Ru(3)Co/Al-Basic, S/C (169 mol/mol), Water (35mL), 120°C, 15 bar H₂ at R.T., 3 h.

All the reactions are done at least three times and the obtained results are within the error of ± 1%-2.5 % range.

3B.3.3. Hydrogenation of different C5 sugars:

The catalytic activity of the (1.5)Ru(3)Co/Al-Basic catalyst was tested for the hydrogenation of different C5 sugars including xylose, arabinose etc. The catalytic reactions were done using optimized reaction conditions which are used for the hydrogenation of xylose

to xylitol (120°C, 15 bar H₂ at R. T., 3 h). It was found that, (1.5)Ru(3)Co/Al-Basic catalyst showing good activity with both xylose and arabinose. It showed collet conversion of sugars with 93% and 91% yield xylitol and arabitol respectively. Hence, from this it can state that the catalyst is exceptionally active for the hydrogenation of different C5 sugars too (Figure 3B.5).

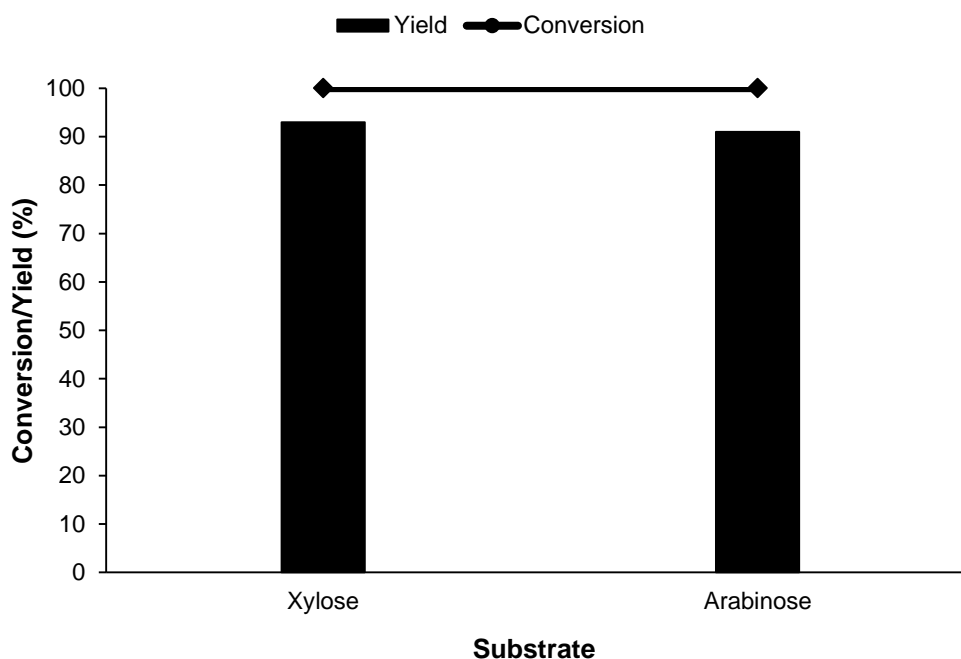


Figure 3B.5. Hydrogenation of different C5 sugars over (1.5)Ru(3)Co/Al-Basic catalyst.

Reaction conditions: Substrate, (1.5)Ru(3)Co/Al-Basic, S/C (169 mol/mol), Water (35mL), 120°C, 15 bar H₂ at R.T., 3 h.

All the reactions are done at least three times and the obtained results are within the error of $\pm 1\%$ -2.5 % range.

3B.3.4. Recycle study:

In addition to having high activity, stability of the catalysts is equally important for the heterogeneous catalysts. To check the stability of the catalyst, recycling test was carried out with 20 wt% xylose solution under optimized reaction condition i.e. 120°C, 15 bar H₂ at R.T., for 3 h time. Recycle study was done by maintaining S/C ratio constant (S/C ratio 169 mol/mol).

After each run, catalyst was retrieved by centrifugation. Then rinsed with water 3 times to remove extra adsorbed impurities, dried at 60°C in lab oven for overnight and used for the next recycle run. As shown in Figure 3B.6, catalyst stability was checked up to 5 runs and it shows that synthesized (1.5)Ru(3)Co/Al-Basic catalyst shows constant activity all over the runs without any distinct loss.

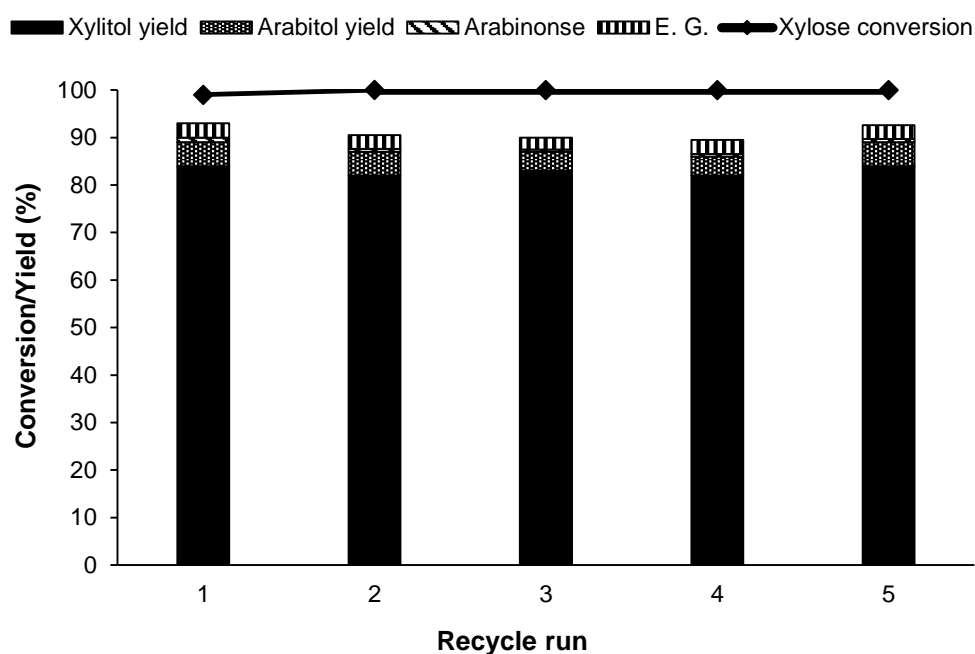


Fig.3B.6. Recycle study of (1.5)Ru(3)Co/Al-Basic catalyst.

Reaction conditions: Xylose, (1.5)Ru(3)Co/Al-Basic, S/C (169 mol/mol), Water (35mL), 120°C, 15 bar H₂ at R.T., 3 h.

All the reactions are done at least three times and the obtained results are within the error of $\pm 1\%$ -2.5 % range.

3B.3.5. Reaction in flow mode reactor:

After achieving good results in batch mode reactor, activity of (1.5)Ru(3)Co/Al-Basic catalyst for the hydrogenation of xylose to xylitol was also checked in continuous flow mode reactor (Figure 3B.7). The flow reactor details, catalyst loading and the reaction procedure is discussed in detail in chapter 3A in section 3A.3.8. For the conversion of xylose to xylitol, optimization of reaction parameters was also done to gain highest conversion and yield. The optimal reaction condition for flow mode reaction is 135°C, 25 bar H₂ pressure, H₂ flow-10 mL·min⁻¹ and reactant flow 0.25 mL·min⁻¹. The obtained average xylose conversion and xylitol yield at optimal reaction condition was 86% and 76% respectively for a continuous reaction of 520 h. The fluctuation in catalyst activity was observed at around 220 h, 350 h and 485 h were because of the rupture disk breaking and power outage. The obtained product was analyzed and quantified using HPLC technique (refer chapter 3A, section 3A.2.3.).

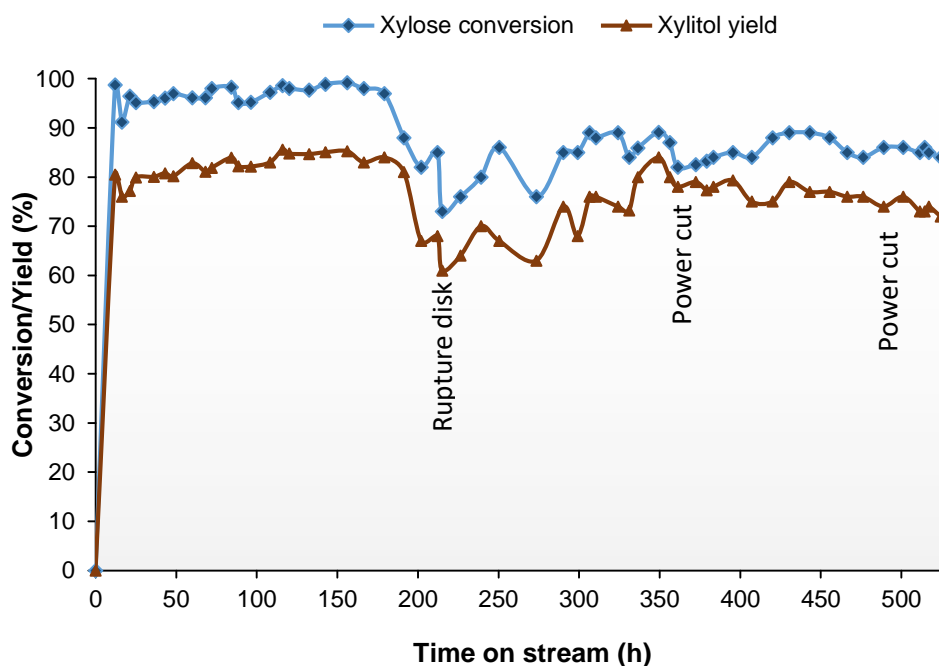


Figure 3B.7. Continuous flow mode reaction for xylose hydrogenation over (1.5)Ru(3)Co/Al-Basic catalyst.

Reaction conditions: Xylose (20 wt%) (xylose flow-0.15 mLmin⁻¹), (1.5)Ru(3)Co/Al-Basic, 150°C, 25 bar H₂, 10 mLmin⁻¹ H₂ flow.

3B.3.6. Purification of xylitol:

Furthermore, purification of xylose was done. For the purification of xylose, after reaction, catalyst was removed from reaction mixture through filtration and the remaining reaction mixture was purified using the crystallization process. For more detailed information about purification refer chapter 3A section 3A.3.9. The purified xylitol was analyzed using different techniques such as HPLC, ^1H NMR and HRMS and the outcomes are shown in the below Figure 3B.8 and Figure 3B.9 respectively. According to the HPLC analysis, refined xylitol has a purity of 98.5%.

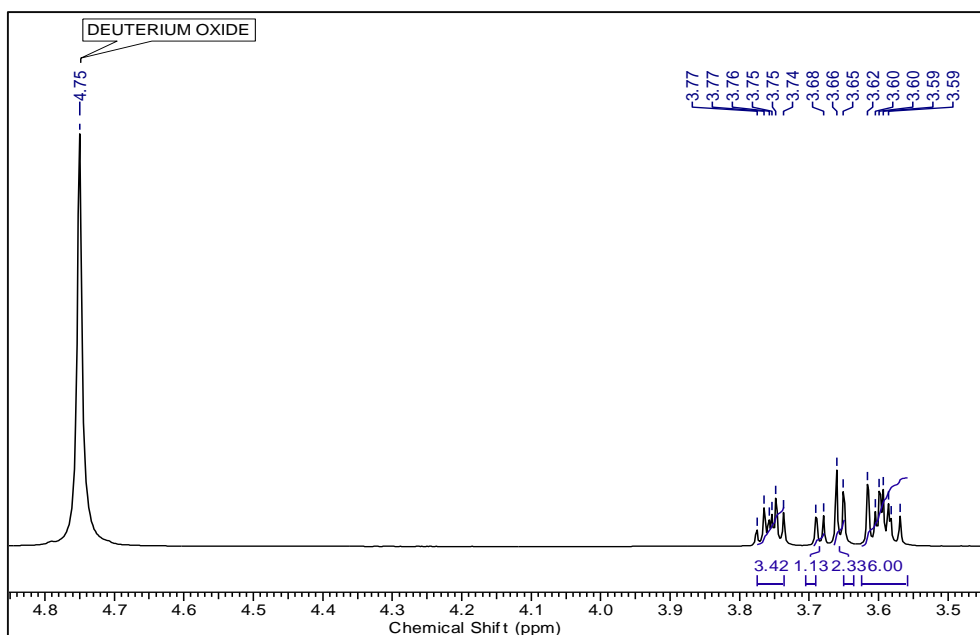


Figure 3B.8. ^1H NMR profile of purified xylitol.

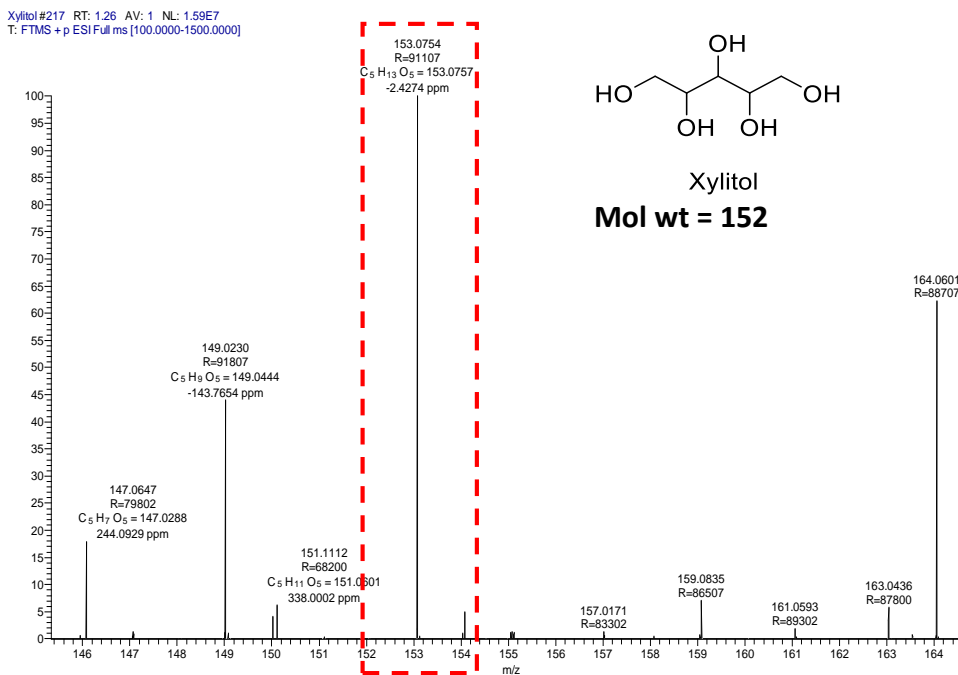


Figure 3B.9. HRMS profile of purified xylitol.

3B.4. Conclusion:

In this work, The hydrogenation of xylose to xylitol was examined using monometallic (3)Co/Al-Basic and (1.5)Ru/Al-Basic catalysts as well as bimetallic (1.5)Ru(3)Co/Al-Basic catalysts. It has been demonstrated that compare to monometallic catalysts, bimetallic (1.5)Ru(3)Co/Al-Basic catalyst have greater activity and selectivity towards xylitol formation. Over (1.5)Ru(3)Co/Al-Basic catalyst, optimization studies of different reaction parameters, including temperature, H₂ pressure etc. have been conducted. Highest xylitol yield (93%) was obtained under 15 bar H₂ pressure at 120°C and 3 h reaction time. Recycle study was conducted up to 5 runs and the catalyst exhibits strong recyclability. As an outcome it can be used as a stable catalyst system for scaling up. Catalyst is also effective for various C5 sugars (xylose, arabinose etc.) hydrogenation and it shows full conversion with a $\geq 91\%$ yield of corresponding sugar alcohols. Flow mode reactions are also carried out and achieved average 86% conversion

and 76% yield at optimal reaction condition. Purification of xylitol was done by an easy crystallization method and 98.5% purity of xylitol was attained.

3B.5. References:

1. T. N. Pham, A. Samikannu, A. R. Rautio, K. L. Juhasz, Z. Konya, J. Wärna, K. Kordas, J. P. Mikkola, *Topics in Catalysis*, 2016, **59**, 1165–1177.
2. A.P. Tathod, P.L. Dhepe, *Green Chemistry*, 2014, **16**, 4944–4954.
3. N.P. Tangale et al, *Microporous and Mesoporous Materials*, 2019, **278**, 70–80,
4. M. Yadav, D. K. Mishra and J.-S. Hwang, *Applied Catalysis A*, 2012, **425**, 110–116.
5. A. Kogje and A. Ghosalkar, *3 Biotech*, 2016, **6**, 1–10.
6. H. Du, X. Ma, M. Jiang, S. Zhao, Q. Fang, X. Liu, and Z. C. Zhang, *ACS Sustainable Chemistry and Engineering*, 2023, **11**, 2115–2126.
7. Dr. M. Audemar, Dr. W. Ramdani, T. Junhui, A. R. Ifrim, Prof. A. Ungureanu, Dr. F. Jérôme, Prof. S. Royer, Prof. K. de Oliveira Vigier, *ChemCatChem*, 2020, **12**, 1973–1978.
8. A. Fehér, C. Fehér, M. Rozbach, G. Rácz, M. Fekete, L. Hegedűs, Z. Barta, *Chemical Engineering & Technology*, 2018, **41**, No. 3, 496–503.
9. Sreedhar Gundekari, Heena Desai, Krishnan Ravi, Joyee Mitra and Kannan Srinivasan, *Frontiers of Chemistry* 2020, **8**, No. 525277.
10. H. Du, X. Ma, M. Jiang, P. Yan, Y. Zhao, Z.C. Zhang, *Catalysis Today*, 2021, **365**, 265–273.
11. L. V. Rao, J. K. Goli, J. Gentela and S. Koti, *Bioresource Technology*, 2016, **213**, 299–310.
12. J. J. Musci, M. Montaña, E. Rodríguez-Castellón, I. D. Lick and M. L. Casella, *Molecular Catalysis*, 2020, **495**, 111150.
13. D. K. Mishra, A. A. Dabbawala and J.-S. Hwang, *Journal of Molecular Catalysis A: Chemical*, 2013, **376**, 63–70.

14. M. Audemar, W. Ramdani, T. Junhui, A. Raluca Ifrim, A. Ungureanu, F. Je'ro^me, S. Royer and K. de Oliveira Vigier, *ChemCatChem*, 2020, **12**, 1973–1978.
15. A. Tathod, T. Kane, E. Sanil and P. L. Dhepe, *Journal of Molecular Catalysis A: Chemical*, 2014, **388**, 90–99.
16. H.A. Pray, C.E. Schweickert, B.H. Minnich, *Industrial and Engineering Chemistry*, 1952, **44**, 1146–1151.

Chapter 4.

Hydrogenative ring rearrangement of furfural (FAL) to cyclopentanone (CPO)

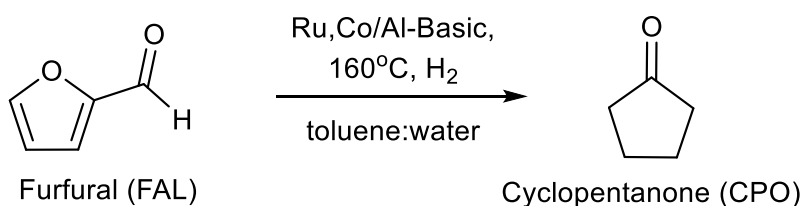
4.1. Introduction:

Because of its plentiful supply and renewability, the transformation of lignocellulosic biomass into fuels and chemicals has become essential to building a sustainable society.¹ Furfural (FAL), produced by acid catalysed dehydration of C5 sugars, is among the most significant compound formed from lignocellulosic biomass. It can be transformed into variety of chemicals with added value, including furfuryl alcohol (FOL), furan, tetrahydrofurfuryl alcohol (THFA), cyclopentanone (CPO), 2-methylfuran (2-MF) etc.^{2,3} The use of cyclopentanone (CPO) is widespread and diverse. It serves as starting ingredient in the synthesis of resins,⁴ fragrance chemicals,⁵ Pharmaceuticals,⁶ can be used as a primary source for the preparation of C15 and C17 fuel precursors.⁷ Typically, CPO synthesis is done by catalytic cyclization of 1,6 hexane diol,⁸ or adipic ester,⁹ and oxidation of cyclopentene.¹⁰ Due to the expensive feedstock's, consumes a lot of energy and produces wastes that is challenging to dispose, these methods are not economically viable and environmentally sustainable. To address these issues, new method for the synthesis of cyclopentanone from biobased molecule furfural had been developed.

Activated carbon (AC) supported noble metal Ru, Pt, Pd based commercial catalysts were explored for the FAL to CPO reactions and found that these metals shows good performance for the selective formation of CPO and cyclopentanol (CPL) and highest yield of CPO (76%) was achieved with (5)Pt/C at 160°C and 80 bar H₂ pressure.¹¹ FAL has been converted to CPO using non precious metal based SBA-15 supported NiCu-50/SBA-15 catalysts at 40 bar H₂ pressure and 160°C and achieved 62% CPO yield and complete FAL conversion.¹² Acidic MOF supported Ru/MIL-101 catalysts was also used at 160°C and 40 bar H₂ pressure resulting 100% conversion of FAL with 96% CPO yield.¹³ Cu-Co catalysts were reported at 170°C, 20 bar H₂ pressure which gives 67% CPO yield.¹⁴ At 10 bar H₂ pressure and 160°C, the (6)Ru/CNT catalyst in aqueous media effectively produces 91% CPO yield. Despite having a substantial amount of metal loading, catalyst is not recyclable.¹⁵ By the addition of metals including Ni, Zn, Mo and Co to the Cu/CNT catalyst, the promoter effect for FAL to CPO reactions was examined. The Cu/CNT catalyst ((17)Cu(3)Zn/CNT) demonstrates the best CPO yield (85%) at 140°C under 40 bar H₂ pressure.¹⁶ At 150°C and 30

bar H₂ pressure, a (5)Pt/NC-BS-500 catalyst was studied and produced 76% CPO yield.¹⁷ Different silica supported Pd catalysts have been developed, and it was determined that at 160°C and 35 bar H₂ pressure, the fumed silica supported (4)Pd/f-SiO₂ catalyst shown optimum performance (100% FAL conversion and 87% yield of CPO).¹⁸ NiFe/SBA-15 catalyst was utilized to study the conversion of FAL to CPO, and it has been found that introducing Fe to Ni catalysts limits the furan ring hydrogenation to THFA and improves the CPO yield. At 160°C under 35 bar H₂ pressure, NiFe/SBA-15 catalyst possessed the best catalytic performance (90% CPO yield).¹⁹ The maximum 93% CPO yield is produced by the Pd/C-BTC catalyst at 40 bar H₂ pressure and 150°C.²⁰ TiO₂ supported Ni based bimetallic (NiCo/TiO₂ and NiFe/TiO₂ with Ni/Co or Ni/Fe molar ratio 3) catalysts have also been studied for FAL to CPO hydrogenation. Under 30 bar pressure and 110°C, very little CPO (27%) yield was reported with these catalysts.²¹ Ni-P-Al₂O₃ catalysts with phosphorus modifications were studied, and results showed 97% FAL conversion and 72% CPO production at 190°C under 30 bar H₂ pressure.²² At 120°C and 30 bar H₂ pressure, the Pd/UiO-66-NO₂ catalyst showed a 94% CPO yield.²³

A number of noble and non-noble metal based catalysts were investigated to convert of FAL to CPO. However, these catalysts either exhibit poor CPO selectivity or make heavy use of precious metals and requires high H₂ pressure (30 to 80 bar). To solve these issues, in this work I have synthesized Ru, Co based supported metal catalysts with low precious metal (Ru) loading and we tested their activity in the accelerating the FAL to CPO reactions. The effects of various Ru/Co ratios and various reaction variables including temperature, pressure, time were thoroughly studied.



Scheme 4.1 Conversion of furfural (FAL) to cyclopentanone (CPO)

4.2. Experimental

4.2.1. Materials: Furfural (FAL) (99%), Pentane-1,2-diol (1,2-PDO) (99%), Pentane-1,5-diol (1,5-PDO) (99%), Pentane-1,4-diol (1,4-PDO) (99%), Pentane-2,4-diol (2,4-PDO) (99%), 2-cyclopentene-1-one (99%) were ordered from Sigma Aldrich. Cyclopentanone (CPO) (99%), cyclopentanol (CPL) (99%) were bought from Lancaster. Furfuryl alcohol (FOL) (99%) was purchased from Loba Chemie, India. Furan (99%) was ordered from Spectrochem, Mumbai, India. 2-methylfuran (2-MF) (99%), 2-methyl tetrahydrofuran (2-MTHF) (99%), tetrahydrofurfuryl alcohol (THFA) (99%) were supplied by Alfa Aesar. Toluene (99%, AR) was purchased from RANKEM, India.

4.2.2. Catalyst synthesis:

Wet impregnation method was used to prepare monometallic catalysts, while co-impregnation method was employed to prepare bimetallic catalysts. The effectiveness of synthesized catalyst was examined for the conversion of FAL to CPO. Chapter 2 (Refer section 2.2.2.) provides a detailed overview of the catalyst synthesis process.

4.2.3. Reaction set-up and analysis of reaction mixtures:

The efficiency of synthesized catalyst for the conversion of furfural (FAL) to cyclopentanone (CPO) was evaluated in 50 mL stainless steel equipped Amar reactor. First, the reactant furfural, solvent (water/toluene (4:3 v/v)) and catalysts together were added to the reactor and then reactor was flushed with low hydrogen pressure to get rid of any remaining air. After that, the reactor was pressurized with 8-13 bar H₂ pressure and heated to 150 to 180°C for a predetermined time while being stirred continuously at 900 rpm. The reactor was cooled down after the completion of reaction and reaction mixture was then collected and subjected to analysis by gas chromatography (GC) and high-performance liquid chromatography (HPLC). Gas chromatography (Agilent GC) with an FID detector was used for the analysis of

the organic solvent reaction mixture. Analysis data obtained from GC were used to calculate the conversion of FAL and the yield of CPO, CPL, FOL etc. GC is equipped with a HP-5 capillary column with dimensions (0.25 $\mu\text{m} \times 0.32 \text{ mm} \times 30 \text{ m}$), and the FID detector carrier gas used was N_2 with a flow rate of 30 mL min^{-1} at 250°C . The oven temperature program is 50°C (1 min hold time) to 200°C (10 min hold time) at the rate of $15^\circ\text{C min}^{-1}$. The temperature of the injector was maintained at 200°C . HPLC equipped with RID detector (Agilent technologies, 1200 infinity series, 40°C) and HC-75 Pb^{+2} column (Hamilton, $7.8\text{mm} \times 300\text{mm}$, 80°C) was used to analyse the water layer. Eluent HPLC grade water was used with a flow rate of $0.5\text{mL}\cdot\text{min}^{-1}$. For the calculating conversion of furfural and the yield of the products, external standard method was used.

4.2.4. Calculations:

The FAL conversion (C) and yield (Y) of products were determined as follows.

$$\text{Conversion (C)\%} = \left\{ \frac{[(\text{Initial moles of substrate}) - (\text{Final moles of substrate})]}{\text{Initial moles of substrate}} \right\} * 100$$

$$\text{Yield (Y)\%} = \left\{ \frac{\text{Moles of product formed}}{\text{Theoretical moles of product formed based on the moles of substrate converted}} \right\} * 100$$

4.3. Results and discussion:

4.3.1. Effect of different catalysts:

In order to convert FAL to CPO, the effects of several bimetallic catalysts have been investigated in a toluene/water 3:4 v/v (35 mL) solvent at 180°C , 13 bar H_2 pressure at R.T., and a 6 h reaction period. The reason behind using biphasic solvent system is the solubility of FAL, FOL and CPO. Previously, the solubility study of FAL, FOL and CPO have been reported in water, toluene and toluene/water biphasic solvent system.²⁴ The study states that a biphasic toluene/water solvent system works well for the conversion of FAL to CPO. Thus, I too have employed the toluene/water biphasic solvent system for the conversion of FAL to CPO.

The findings from an evaluation of the selective hydrogenation and rearrangement to produce CPO from FAL incorporating various supported metal catalysts are shown in Figure 4.1. Initially, the synthesized (1.5)Ru(3)Co/Al-Basic catalyst which was used to produce sugar alcohols from sugars, was evaluated for FAL to CPO conversion. The catalyst exhibited a 90% FAL conversion and 46% CPO yield. Additionally, the performance of Ru and Co based catalysts supported on different supports, including SAPO and ZrO₂ was evaluated. It was observed that, among these (1.5)Ru(3)Co/Al-Basic catalyst showed the highest CPO yield (46%) and FAL conversion (90%), followed by the (1.5)Ru(3)Co/ZrO₂, (1.5)Ru(3)Co/SAPO and (1.5)Ru(3)Co/Al-Basic catalysts. However, (1.5)Ru(3)Co/Al-Basic catalyst showed very less selectivity towards CPO. In order to further boost the CPO selectivity, (2)Ru(1.5)Co/Al-Basic catalyst was synthesised by increasing Ru loading by 0.5% and decreasing Co loading by 1.5%. With (2)Ru(1.5)Co/Al-Basic catalyst under same reaction condition, complete FAL conversion with 53% CPO and 17% CPL yield was achieved (CPO+CPL yield was 70%). Along with CPO and CPL, Other side products were also seen under this scenario.

Since, (2)Ru(1.5)Co/Al-Basic catalyst demonstrated excellent catalytic activity of all the synthesized catalysts, with 100% FAL conversion and 53% CPO and 17% CPL yield, moreover, to obtain maximum CPO yield and minimal side products, different reaction parameters were optimized using (2)Ru(1.5)Co/Al-Basic catalyst.

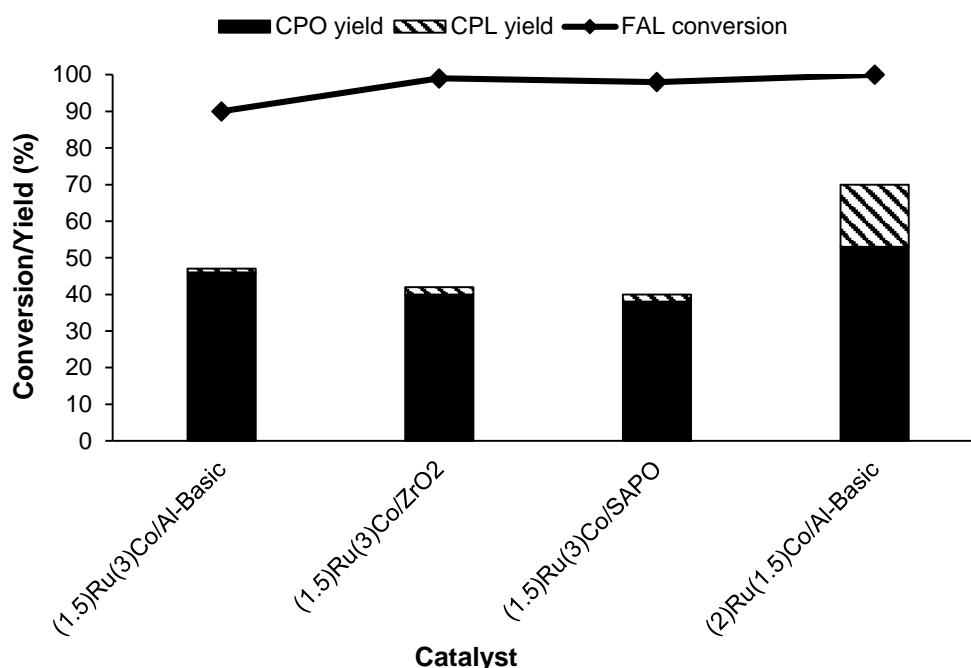


Figure 4.1. Effect of different catalyst for the conversion of FAL to CPO.

Reaction conditions: FAL, catalyst, toluene/water 3:4 v/v (35mL), 13 bar H₂ at R.T., 180°C, 6 h.

All the reactions are done at least three times and the obtained results are within the error of $\pm 1\%$ -2.5 % range.

4.3.2. Effect of monometallic and bimetallic catalysts:

In order to observe the effect of monometallic and bimetallic catalysts for the hydrogenation of FAL to CPO, reactions were carried out at 180°C, 13 bar H₂ for 6 h reaction time using toluene/water 3:4 v/v (35mL) solvent (Figure 4.2). First reactions were done with monometallic catalyst and it was observed that, in contrast to the (1.5)Co/Al-Basic catalyst, which showed 84% FAL conversion and 3% CPO yield, (2)Ru/Al-Basic catalyst is showing 92% FAL conversion and 34% CPO yield along with 5% CPL yield. The reason behind the (2)Ru/Al-Basic catalyst exhibits superior activity as compared to (1.5)Co/Al-Basic catalyst is that H₂ molecule activation will occur on Ru surface, which facilitates the hydrogenation FAL molecule. Because Co lacks the ability to activate the H₂ molecule, it produces less CPO than

the (2)Ru/Al-Basic catalyst. Additionally, Compared to monometallic catalyst, the results of bimetallic (2)Ru(1.5)Co/Al-Basic catalysts was significantly improved, yielding 53% CPO and 100% FAL conversion along with 17% CPL yield. Non catalytic reactions and reactions with Al-Basic support were also performed and it was observed that only 50% of FAL could be converted in the non-catalytic reactions and 70% FAL was converted when the reaction was performed with Al-Basic support. While the CPO formation was unfavourable in both the reactions. It was assumed that in a nonanalytic reaction, some FAL was decomposed, because after the reaction, the dark brown reaction mixture and some brown solid were left behind on the reactor wall.

This demonstrates that compared to monometallic catalysts, a bimetallic (2)Ru(1.5)Co/Al-Basic catalyst is superior for the production of CPO. While taking into account the activity of bimetallic (2)Ru(1.5)Co/Al-Basic catalyst at 180°C under 13 bar H₂ pressure for 6 h reaction time, the reaction parameters were further optimized to achieve highest selectivity towards CPO.

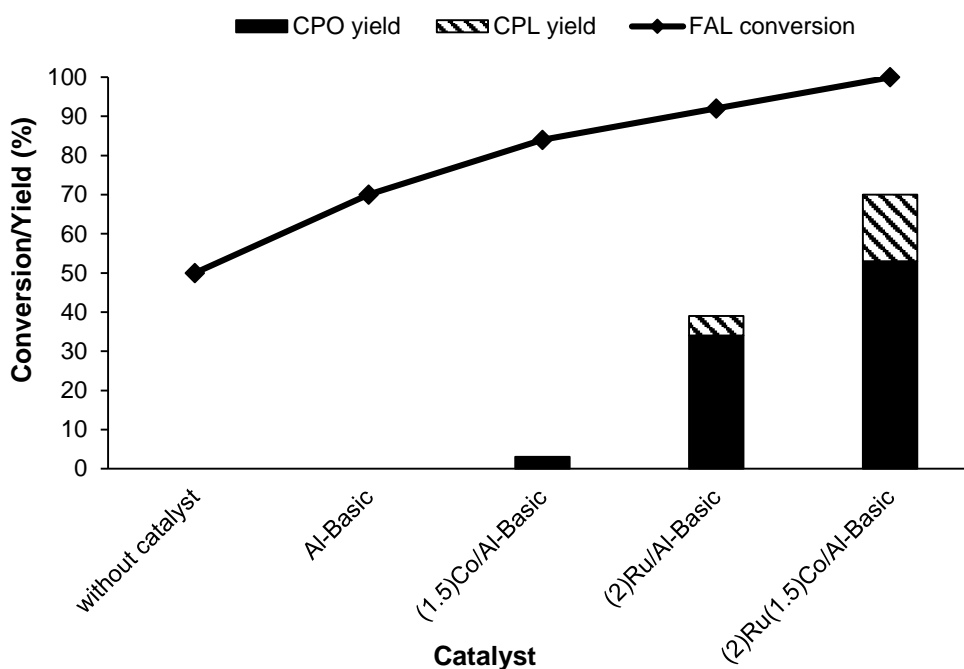


Figure 4.2. Effect of mono and bimetallic catalyst for the conversion of FAL to CPO.

Reaction conditions: FAL, catalyst, S/C (191 mol/mol), toluene/water 3:4 v/v (35mL), 13 bar H₂ at R.T., 180°C, 6 h.

All the reactions are done at least three times and the obtained results are within the error of $\pm 1\%$ -2.5 % range.

4.3.3. Effect of varying Co loading:

How Co metal functions in (2)Ru(1.5)Co/Al-Basic catalyst for the transformation of FAL to CPO was also examined. For the sake of this study different Ru and Co based catalysts were prepared by adjusting the Co loading from 0.5 wt% to 3 wt% while maintaining the Ru loading constant (2 wt%). The effectiveness of each catalyst was evaluated in toluene/water 3:4 v/v (35mL) solvent at 180°C, 13 bar H₂ at R. T. and 6 h reaction time (Figure 4.3.). It was found that FAL conversion and CPO yield was increased with a rise in Co loading from 0.5 to 1.5 wt%. Conversion reached to 100% with 53% CPO yield at 1.5 wt% Co loading. As Co loading increased further to 3 wt%, decline in catalytic activity was

observed. As mentioned in chapter 3, section 3A.3.3, the excess Co may cover the active sites of Ru metals which could be the reason why catalyst activity decreases with increasing Co loading. Therefore, the 1.5 wt% Co loading is the ideal Co loading in order to achieve maximum level of catalytic activity.

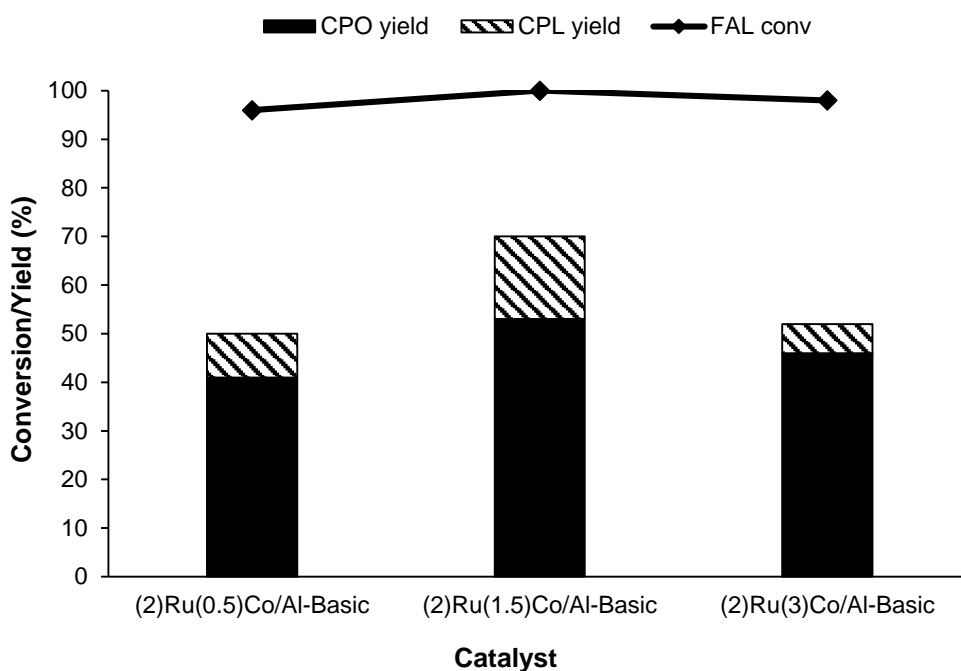


Figure 4.3. Effect of varying Co loading for the conversion of FAL to CPO.

Reaction conditions: FAL, catalyst, S/C (191 mol/mol), toluene/water 3:4 v/v (35mL), 13 bar H₂ at R.T., 180°C, 6 h.

All the reactions are done at least three times and the obtained results are within the error of $\pm 1\%$ -2.5 % range.

4.3.4. Effect of different reaction parameters:

Effect of H₂ pressure:

In order to evaluate the efficiency of (2)Ru(1.5)Co/Al-Basic catalyst for FAL hydrogenation, number of experiments were carried out. As shown in Figure 4.4., first effect of H₂ pressure towards the conversion and yield were examined at 180°C, 6 h reaction time in toluene/water 3:4 v/v (35mL) solvent. At 8 bar H₂ pressure, 78% FAL conversion and 54% CPO yield was attained. CPL formation not seen at 8 bar H₂ pressure but HPLC profile showed the formation of an unknown products with prominent intensity peaks. In addition to increase in H₂ pressure to 10 bar, there was a drop in unknown peak intensities and increase in conversion 96% and 65% CPO were seen. In addition to CPO, 4% CPL formation was also seen under 10 bar H₂ pressure. With increasing H₂ pressure, decrease in unknown product formation and increase in mass balance from 63% to 77.5% was also seen. Further, in order to minimize the side product formation and maximize the CPO yield, pressure was again increased to 13 bar. At 13 bar H₂ pressure conversion reached to 100% with 53% CPO ad 17% CPL yield. According to the Figure 4.4, it was found that the increasing H₂ pressure, both FAL conversion and CPO yield increased. This might be because, H₂ is more soluble at higher pressure, so it dissolved more readily and converts FAL to CPO efficiently. Therefore, at 13 bar H₂ pressure, catalyst exhibited the highest FAL conversion (100%) and CPO yield (53%). Despite this, 17% CPL formation was also seen, which indicates that at high H₂ pressure CPO is getting converted to CPL by the hydrogenation of C=O bond of the CPO. In order to minimize CPL formation, additional optimization study of temperature and time was conducted using a 13 bar H₂ pressure.

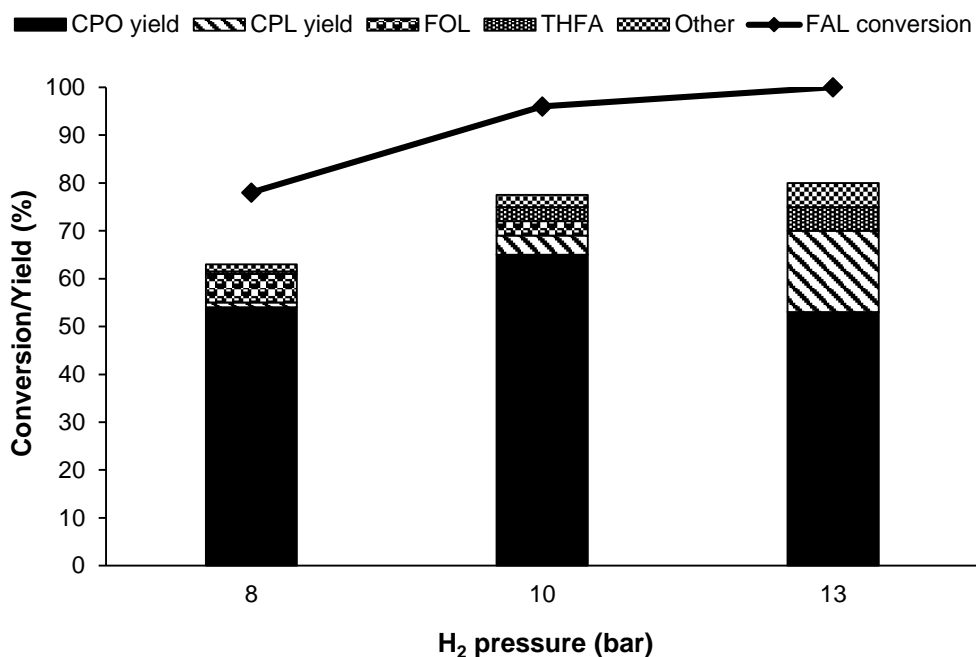


Figure 4.4. Effect of H₂ pressure for the conversion of FAL to CPO.

Reaction conditions: FAL, (2)Ru(1.5)Co/Al-Basic catalyst, S/C (191 mol/mol), toluene/water 3:4 v/v (35mL), 180°C, 6 h.

All the reactions are done at least three times and the obtained results are within the error of $\pm 1\%$ -2.5 % range.

Effect of temperature:

Figure 4.5. illustrates that the effect of temperature changes on the conversion of FAL and yield of CPO. To examine the temperature effect, reactions were carried out at various temperature between 150°C to 180°C under 13 bar of H₂ pressure at R. T. for 6 h reaction time in toluene/water 3:4 v/v (35mL) solvent. As presented in Figure 4.5, at 150°C catalyst exhibited 84% conversion and 50% CPO yield along with 6% FOL. At this temperature, the unknown product was also observed displaying high intensity peak in HPLC. When the temperature was raised from 150°C to 160°C, increase in FAL conversion and decrease in FOL formation was observed. Additionally, a decrease in the peak trend of an unknown product was

also seen with an increase in temperature to 160°C. Highest CPO yields (74%) were attained at 160°C. At 170°C and 180°C, the yield of CPO decreased and more by products (CPL, THFA and diols) were formed. At the same time, C=C hydrogenation was also seen at higher temperature resulting increase in yield of THFA at high temperature. C=O hydrogenolysis was also observed resulting formation of hydrogenized products like 2-methylfuran, 2-methyltetrahydrofuran etc. As a result, 160°C is the ideal temperature that works best for converting FAL to CPO under 13 bar H₂ pressure and 6 h reaction time.

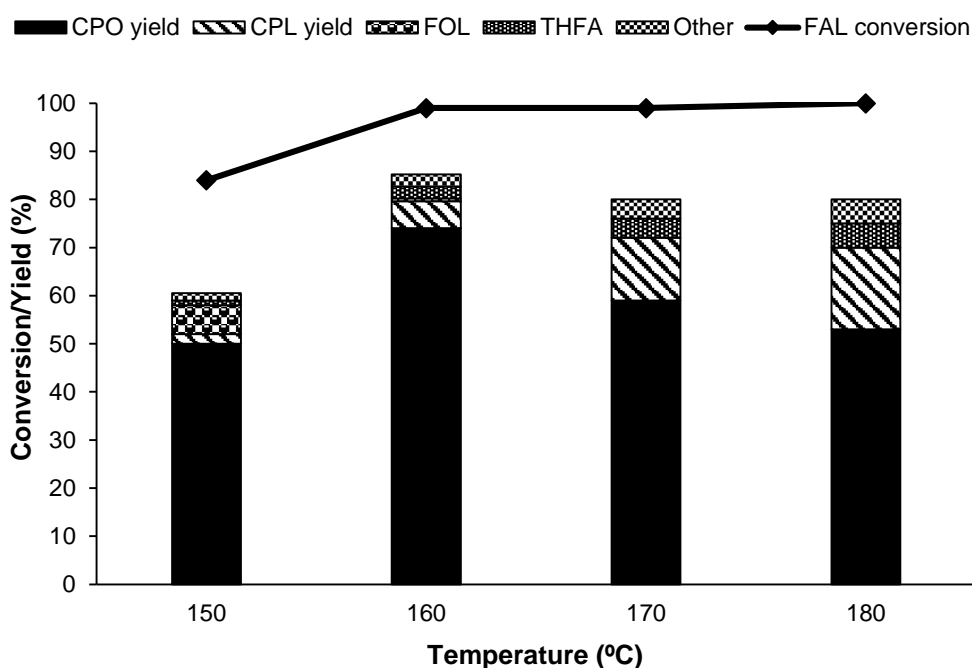


Figure 4.5. Effect of temperature for the conversion of FAL to CPO.

Reaction conditions: FAL, (2)Ru(1.5)Co/Al-Basic catalyst, S/C (191 mol/mol), toluene/water 3:4 v/v (35mL), 13 bar H₂ at R.T., 6 h.

All the reactions are done at least three times and the obtained results are within the error of $\pm 1\%$ -2.5 % range.

Effect of time:

How reaction time affected the conversion of FAL to CPO was investigated under optimal reaction condition (160°C, 13 bar H₂ pressure at R. T., toluene/water 3:4 v/v (35mL) solvent). As seen in Figure 4.6., the catalyst demonstrated 95% conversion and 65% CPO production in 5 h. In addition to CPO, peaks for CPL (2.5%) and FOL (9.3%) were also seen. The obtained FOL is the intermediate product for FAL to CPO reaction. In order to achieve complete FAL conversion and convert the remaining FOL to CPO, we have therefore extended the reaction time to 6 h. As reaction extended to 6 h, CPO yield reached to 74% with 100% FAL conversion and 5.6% CPL yield. The CPO yield dropped to 68% and CPL yield increased to 7% when the reaction time was extended to 7 h. It means that when reaction time was prolonged, the formed CPO get hydrogenated to CPL. It suggests that prolongation of reaction time encourages the hydrogenation of C=O bond of CPO, which boost the generation of CPL. According to the time study, the optimum reaction time for converting of FAL to CPO at 160°C and 13 bar H₂ pressure is 6 h. Along with CPO, side products such as CPL, FOL, THFA, diols, polymers and certain gaseous products (methane, 2-methylfuran, furan) was also seen at the optimized reaction condition. At the reaction conditions, a total carbon balance was attained around 86%.

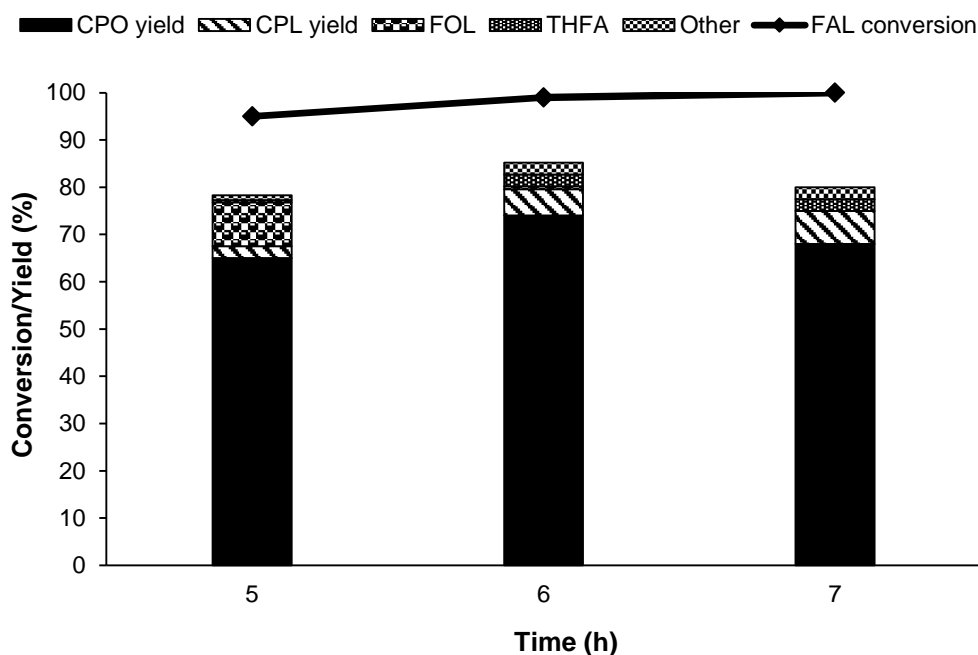


Figure 4.6. Effect of time for the conversion of FAL to CPO.

Reaction conditions: FAL, (2)Ru(1.5)Co/Al-Basic catalyst, S/C (191 mol/mol), toluene/water 3:4 v/v (35mL), 13 bar H₂ at R.T., 160°C.

All the reactions are done at least three times and the obtained results are within the error of $\pm 1\%$ -2.5 % range.

4.3.5. Effect of acetic acid treated (2)Ru(1.5)Co/Al-B catalyst:

Using (2)Ru(1.5)Co/Al-Basic catalyst under optimal reaction conditions (160°C, 13 bar H₂ at R. T., 6 h in toluene/water 3:4 v/v (35mL) solvent), 100% FAL conversion and 74% CPO yield was achieved. Additionally, In order to increase the CPO yield, under the same reaction conditions 160°C, 13 bar H₂ at R. T., 6 h, reactions with acetic acid treated (2)Ru(1.5)Co/Al-Basic catalyst were conducted. With this catalyst only 74% FAL conversion and 14% CPO along with 2% CPL yield was achieved. It denotes that the (2)Ru(1.5)Co/Al-Basic catalyst is being deactivated by acetic acid which lowers the FAL conversion and CPO yield of the reaction.

4.3.6. Recycle study:

In light of the catalysts good activity, further recycle study of (2)Ru(1.5)Co/Al-Basic catalyst for the transformation of FAL to CPO was conducted. Recycle study was conducted under ideal reaction conditions (160°C, 13 bar H₂ at R. T., 6 h in toluene/water 3:4 v/v (35mL) solvent). For the recycle study, the centrifugation was used to remove the catalyst from initial reaction mixture. Following separation, the catalyst was dried at 60 °C overnight and used as it is for the next recycle run. In the recycle study, the second recycle run showed the drop in catalyst activity. 100% FAL conversion and 74% CPO was seen with fresh catalyst, while 70% conversion and 41% CPO yield were seen with spent catalyst (Figure 4. 7). The decrease in catalytic activity may be attributed because of the adsorption of undesired products on the active sited of the catalysts.

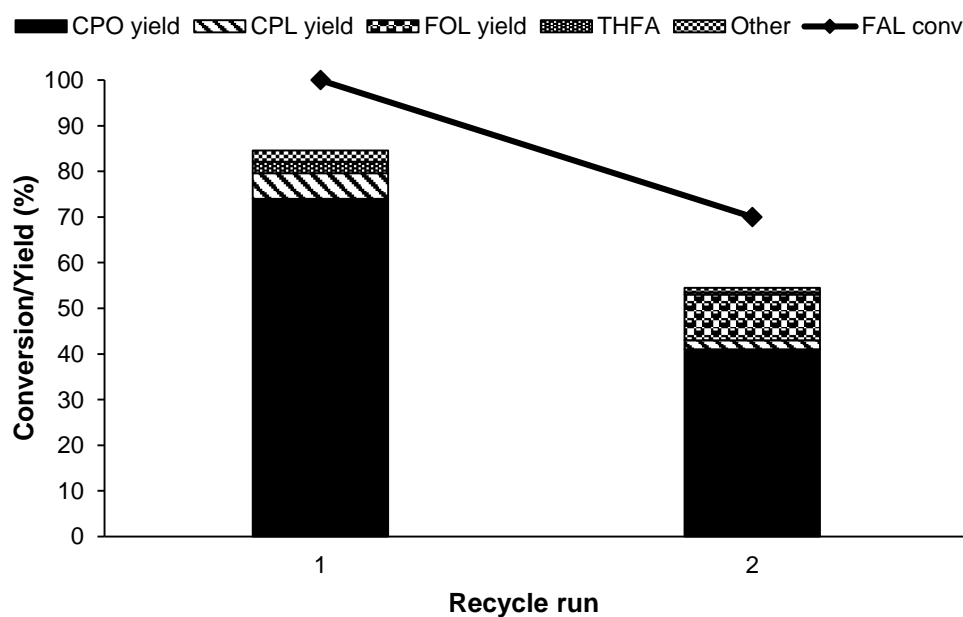


Figure 4.7. Recycle study of (2)Ru(1.5)Co/Al-Basic catalyst for the conversion of FAL to CPO.

Reaction conditions: FAL, (2)Ru(1.5)Co/Al-Basic catalyst, S/C (191 mol/mol), toluene/water 3:4 v/v (35mL), 13 bar H₂ at R.T., 160°C, 6 h.

All the reactions are done at least three times and the obtained results are within the error of $\pm 1\%$ -2.5 % range.

4.4. Conversion of FAL to CPO using commercial (5)Ru/Al catalyst:

As discussed in section above (section 4.3.), the transformation of FAL to CPO employing the (2)Ru(1.5)Co/Al-Basic catalyst produces 100% conversion and 74% CPO yield under optimized reaction conditions (160°C, 13 bar H₂ at R. T., 6 h, S/M (mol/mol)-191 in toluene/water 3:4 v/v (35mL) solvent). Additionally, for the comparison purpose, the hydrogenation reaction of FAL to CPO was also studied using (5)Ru/Al commercial catalyst and compared the activity of commercial (5)Ru/Al catalyst with that of synthesized (2)Ru(1.5)Co/Al-Basic catalyst. For this, initial reactions were conducted over a 6 h reaction period at 160°C and 13 bar H₂ pressure. Under these reaction conditions, (5)Ru/Al catalyst is demonstrating 100% FAL conversion, however it's selectivity to CPO was only 46% and THFA (10%) and CPL (18%) were also detected showing significant selectivity. Considering the target product selectivity is not very high, the reaction conditions were further optimized at various reaction parameters (Temperature, H₂ pressure, time, etc.) using a commercial (5)Ru/Al catalyst.

4.4.1. Effect of reaction parameters for the conversion of FAL to CPO over commercial (5)Ru/Al catalyst:

Effect of temperature:

For the temperature study, as shown in Figure 4.8., first reactions were conducted at 160 °C for 1 hour under 13 bar H₂ pressure. At 160°C, 14% CPO yield and 64% FAL conversion was achieved. With rising temperature there was a rise in conversion of FAL and CPO yield was observed with the catalyst displaying its highest FAL conversion (80%) and highest CPO yield (41%) at 180°C.

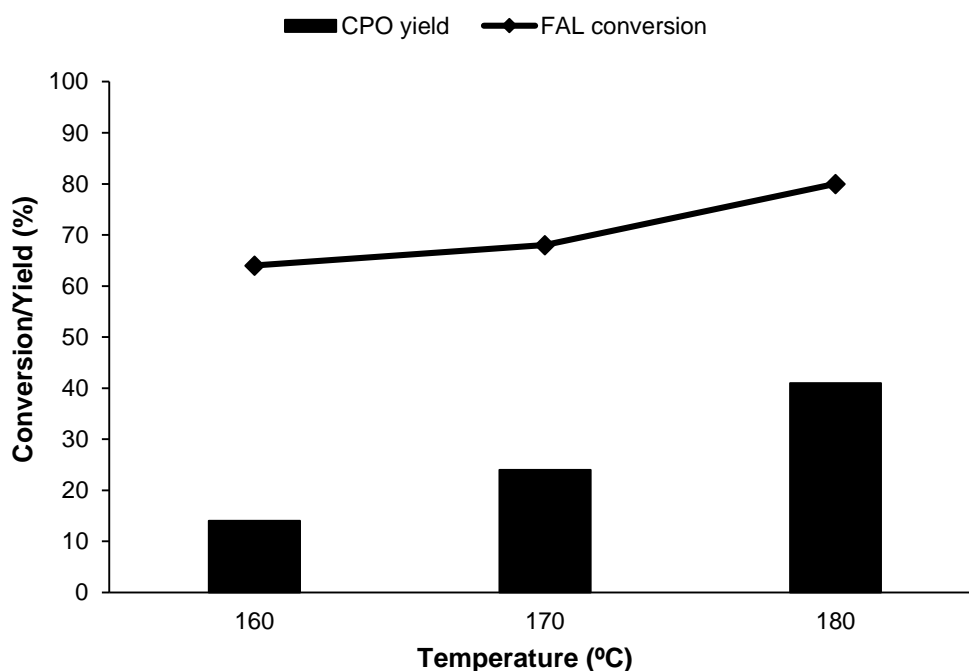


Figure 4.8. Effect of temperature for the conversion of FAL to CPO using commercial catalyst.

Reaction conditions: FAL, (5)Ru/Al catalyst, S/C (191 mol/mol), toluene/water 3:4 v/v (35mL), 13 bar H₂ at R.T., 1 h.

All the reactions are done at least three times and the obtained results are within the error of $\pm 1\%$ -2.5 % range.

Effect of time:

A time study was conducted at 180°C under 13 bar of H₂ pressure for different reaction time ranging from 1 h to 4 h (Figure 4.9.). Within 1h reaction time, only 41% CPO yield was achieved at 64% FAL conversion. Further increase in reaction period to 3 h, 91% FAL conversion and 51% CPO yield were detected. The highest FAL conversion 99% with maximum CPO yield of 62% were attained at 4h reaction time. Therefore, the optimal reaction condition for converting FAL to CPO using (5)Ru/Al commercial catalyst is 180°C, 13 bar H₂ pressure and 4 h.

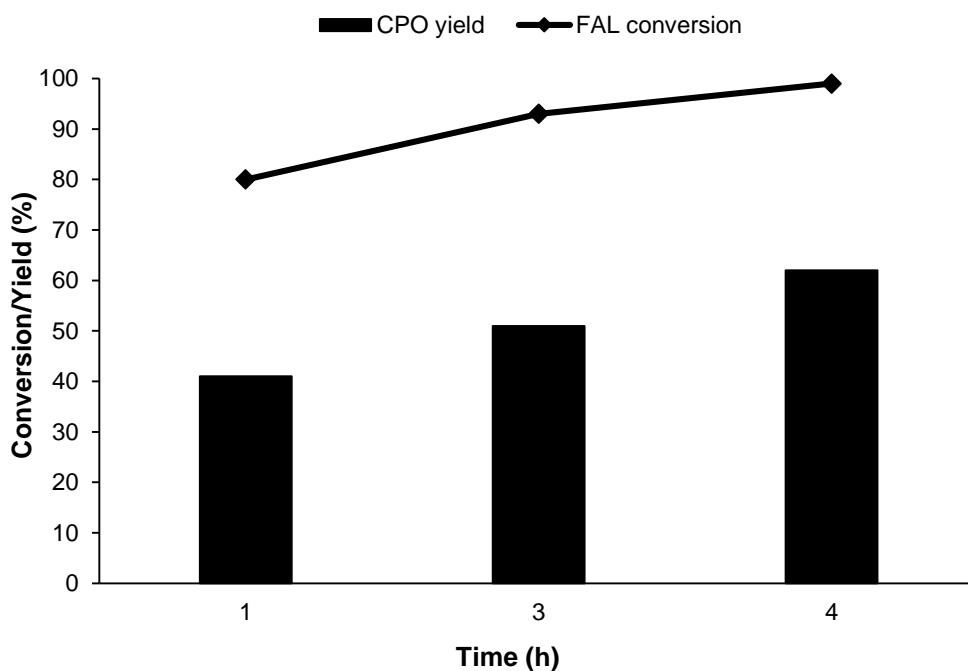


Figure 4.9. Effect of time for the conversion of FAL to CPO using commercial catalyst.

Reaction conditions: FAL, (5)Ru/Al catalyst, S/C (191 mol/mol), toluene/water 3:4 v/v (35mL), 13 bar H₂ at R.T., 180°C.

All the reactions are done at least three times and the obtained results are within the error of $\pm 1\%$ -2.5 % range.

Effect of H₂ pressure:

The impact of H₂ pressure was examined under 10 to 15 bar H₂ pressure with commercial (5)Ru/Al catalyst (Figure 4.10.). Initially, the activity of commercial (5)Ru/Al catalyst was tested at 10 bar H₂ pressure (17 bar at reaction temperature) and found that catalyst exhibiting 97% conversion and 45% CPO yield at this pressure. Under 13 bar H₂ pressure (22 bar at reaction temperature), the highest conversion 99% and CPO yield 62% was attained.

Additionally, pressure increased to 15 bar (25 bar at reaction temperature) had an adverse impact on CPO yield.

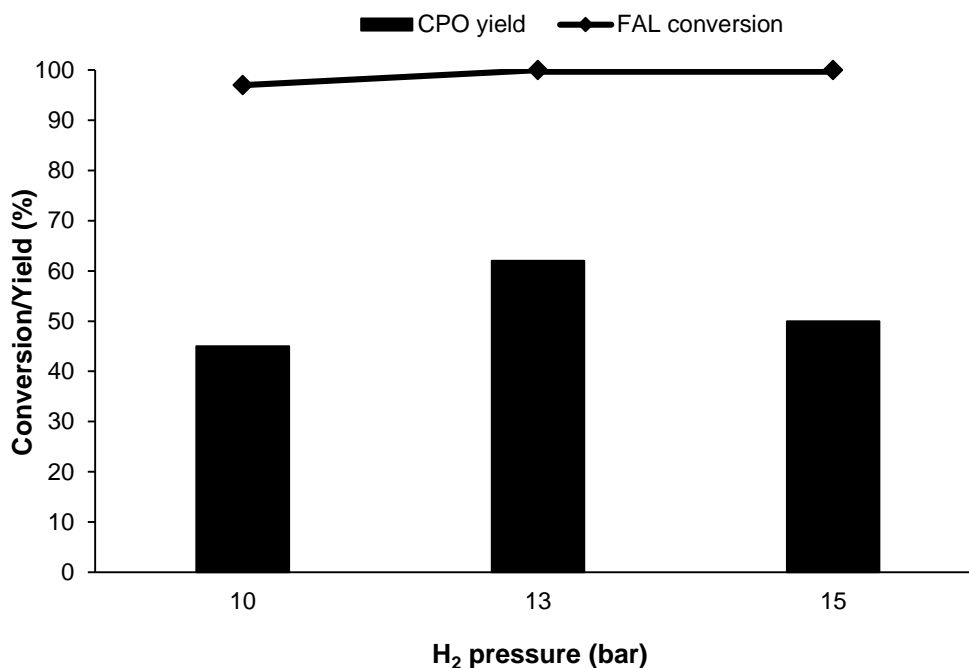


Figure 4.10. Effect of H₂ pressure for the conversion of FAL to CPO using commercial catalyst.

Reaction conditions: FAL, (5)Ru/Al catalyst, S/C (191 mol/mol), toluene/water 3:4 v/v (35mL), 180°C, 4 h.

All the reactions are done at least three times and the obtained results are within the error of $\pm 1\%$ -2.5 % range.

4.5. Reactions with crude FAL:

4.5.1. Synthesis of FAL from hydrolyzed hemicellulose (Industry sample):

To test the activity of synthesized catalyst for the transformation of crude FAL to CPO, I have synthesized in-house FAL using hydrolyzed hemicellulose. We received various hydrolyzed hemicellulose samples from industry with varying xylose concentrations. Using

HPLC technique, first we quantified every received sample (Table 4.1). In addition to xylose, samples also contain additional contaminants such as glucose, arabinose and some solid impurities was also there. The HPLC profile and quantification of several samples is depicted in Figure 4.11. and Table 4.1. respectively.

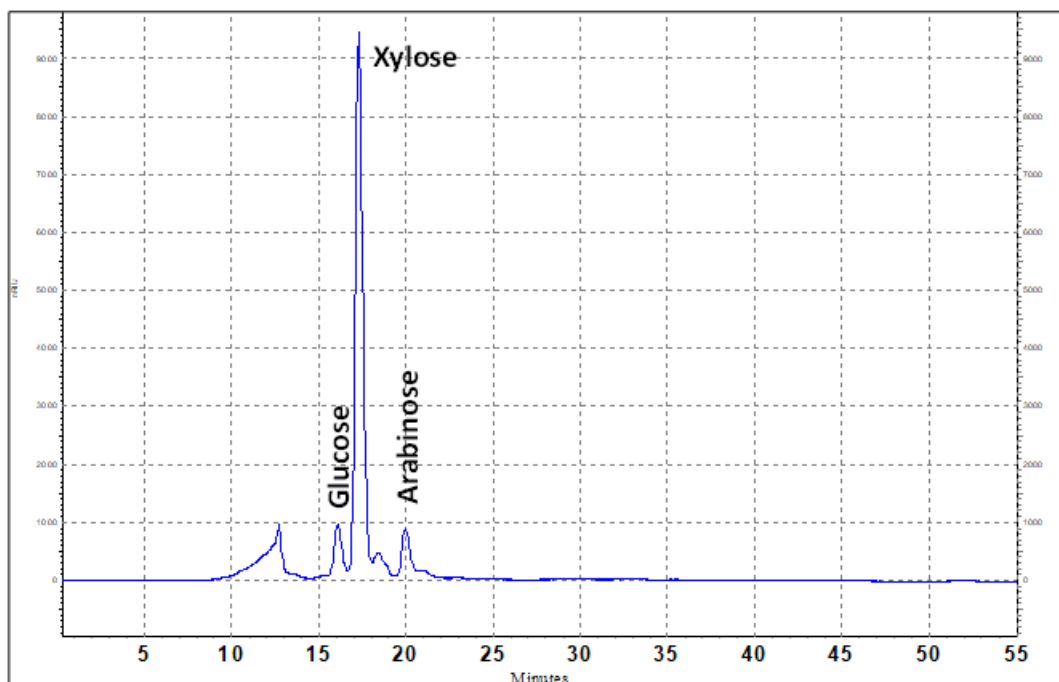


Figure 4.11. HPLC profile of hydrolysed hemicellulose (Industry sample).

Table 4.1. Quantification of hydrolysed hemicellulose (Industry samples).

Sample name	Xylose concentration (wt %)
JK-1	4.4
JK-2	4.9
JK-3	2.6

JK-4	1.7
JK-5	1.6
JK-6	2.1
JK-7	2.3

FAL was synthesized from hydrolyzed hemicellulose using acetic acid as a catalyst in a toluene water biphasic solvent system at 180°C temperatures for varying reaction time. Initially, reaction was run for 4 h and observed that within 4 h, 75% CPO was formed with complete conversion (Figure 4.12.). The reaction was done for prolonged period of time, and within 5 h reaction period, highest FAL yield (82%) was obtained. FAL yield was dropped to 60% with an increase in reaction time to 6h, which may have been caused by the degradation of formed FAL. The conversion of hydrolyzed hemicellulose to FAL was also carried out in 1L reactor. As shown in Figure 4.13., in a 1L reactor, 97% conversion with 78% FAL yield was achieved within 2.5 h time period.

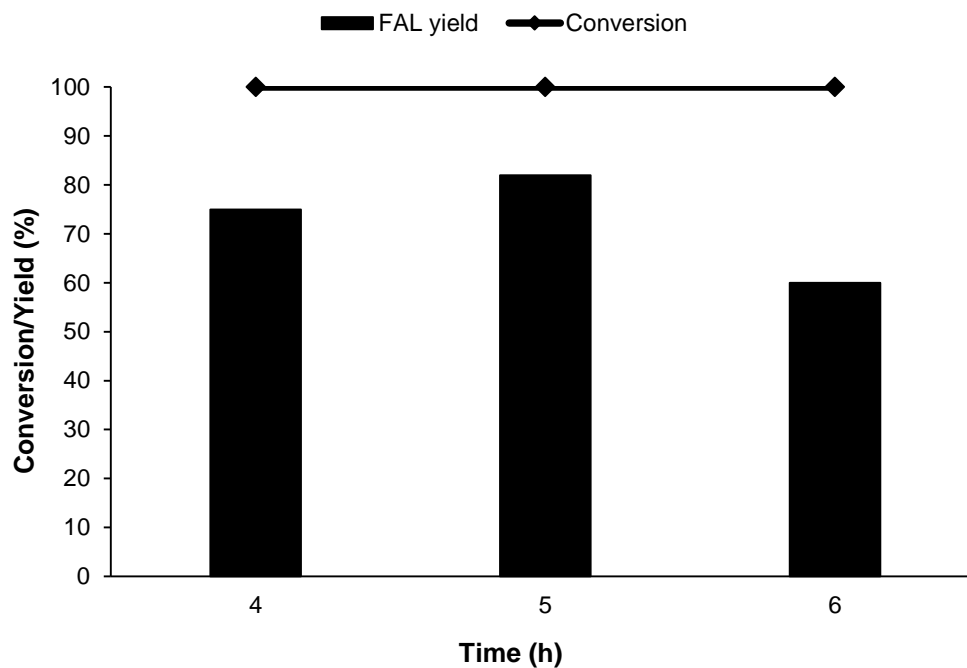


Figure 4.12. Effect of time for the conversion of hydrolysed hemicellulose to FAL in 300mL reactor.

Reaction conditions: FAL, Acetic acid catalyst, toluene/water 3:4 v/v (35mL), 180°C.

All the reactions are done at least three times and the obtained results are within the error of $\pm 1\%$ -2.5 % range.

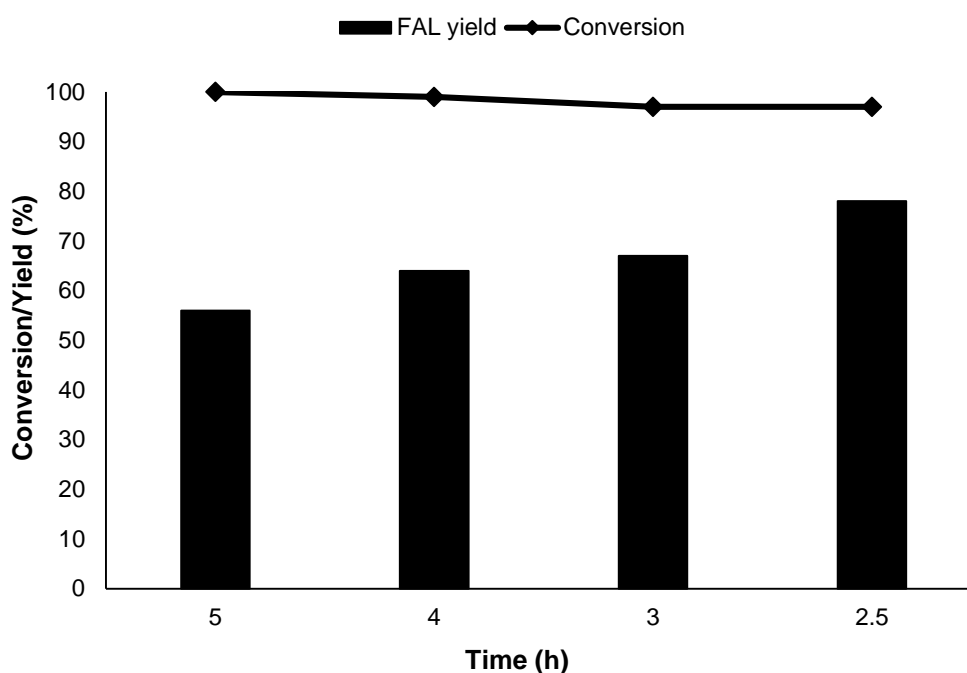


Figure 4.13. Effect of time for the conversion of hydrolysed hemicellulose to FAL in 1L reactor.

Reaction conditions: FAL, Acetic acid catalyst, toluene/water 3:4 v/v (35mL), 180°C.

All the reactions are done at least three times and the obtained results are within the error of $\pm 1\%$ -2.5 % range.

4.5.2. Conversion of crude FAL to CPO:

After the in-house production of FAL, I have tested the performance of our synthesizes (2)Ru(1.5)Co/Al-Basic catalyst for the conversion of synthetic crude FAL into CPO (Figure 4.14.). Following the synthesis of FAL from hydrolyzed hemicellulose, the water and toluene layer were separated. The toluene layer was again quantified and found that it contains 0.5% of FAL. Obtained toluene layer which contains 0.5% FAL was used as it is to convert FAL to CPO. Using commercial FAL, at 160°C under 13 bar H₂ at R. T. within 6 h, (2)Ru(1.5)Co/Al-Basic catalyst exhibits 100% FAL conversion and 74% CPO yield. Furthermore, reactions were conducted using crude 0.5% FAL solution and achieved 100% FAL conversion and 56% CPO

yield at the same reaction conditions (160°C, 13 bar H₂ at R. T., 6 h). Under these reaction conditions, along with the CPO, 2% CPL and 9% diols (1,2-PDO, 1,5-PDO and 1,4-PDO) formation was also noticed. Further reactions were conducted with reduced reaction time (5 h), a small increase in CPO yield (60%) was noted. With a further reduction in reaction time to 4.5 h, the highest 63% CPO formation were accomplished with 98% FAL conversion. When reactions were run for 4.5 h, there was also a decrease in diol formation was observed (6%). Both conversion and CPO yield were dropped as the reaction time was further reduced to 4 h. Therefore, using crude FAL, we were able to produce 63% CPO in 4.5 h at 160°C and 13 bar H₂ pressure. This suggests that the synthesized (2)Ru(1.5)Co/Al-Basic catalyst has the ability to convert of crude FAL as well.

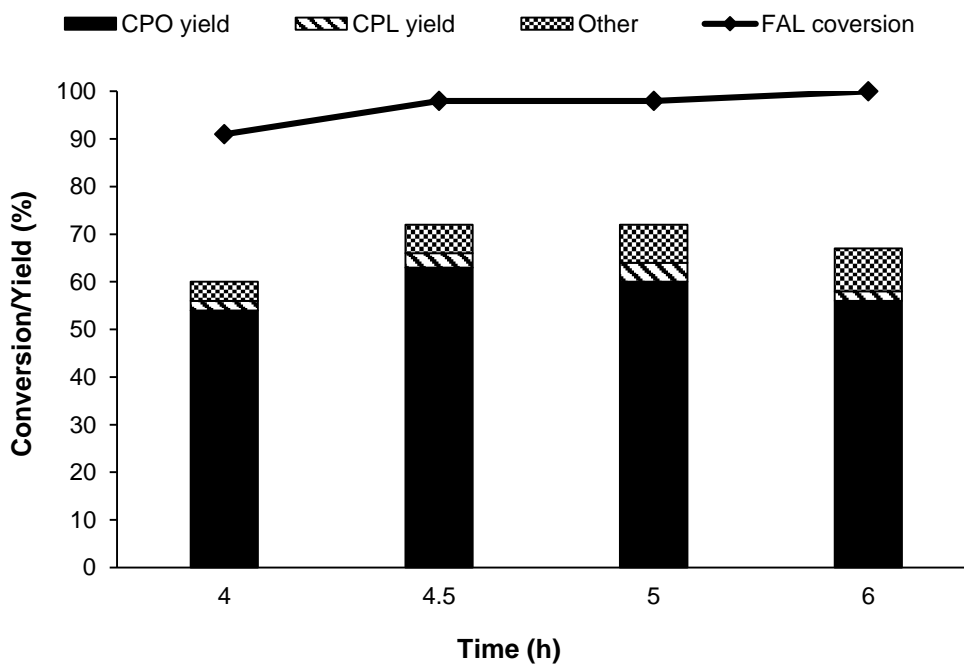


Figure 4.14. Effect of time for the conversion of crude FAL to CPO.

Reaction conditions: FAL, (2)Ru(1.5)Co/Al-Basic catalyst, S/C (191 mol/mol), toluene/water 3:4 v/v (35mL), 13 bar H₂ at R.T., 160°C, 6 h.

All the reactions are done at least three times and the obtained results are within the error of $\pm 1\%$ -2.5 % range.

4.6. Conclusion:

A range of supported Ru and Co metal based catalysts were synthesised using impregnation method and used to convert of FAL to CPO. Out of all the supports, basic alumina (Al-Basic) support demonstrated the best activity and the highest CPO production. Compared to monometallic (2)Ru/Al-Basic and (1.5)Co/Al-Basic catalysts, bimetallic (2)Ru(1.5)Co/Al-Basic catalyst demonstrated better catalytic activity showed 100% FAL conversion and 74% CPO yield in water/toluene 4:3 v/v (35 mL) solvent under optimized reaction conditions (160°C, 13 bar H₂ at R. T., 6 h). Increased selectivity towards CPL and THFA production was seen during high temperature and high H₂ pressure reactions, whereas polymerization of FAL and CPO was considered at low temperature and low pressure reactions. The recycle study revealed that loss of catalyst and adsorption of byproducts onto catalyst's active sites may be the cause of decrease in catalyst activity. At 180°C, 13 bar H₂ pressure and 4 h using water/toluene 4:3 v/v (35 mL) solvent, a commercial (5)Ru/Al catalyst showed 100% FAL conversion and 62% CPO yield. Synthesis of FAL from hydrolysed hemicellulose was also possible in presence of acetic acid catalyst to produce up to 82% FAL yield with 100% conversion over 5 h reaction period at 180°C. Additionally, crude FAL was also hydrogenated using (2)Ru(1.5)Co/Al-Basic catalyst, yielding 63% CPO with 100% FAL conversion.

4.7. References:

1. G. Zhang, T. Chen, Y. Zhang, T. Liu, G. Wang, *Catalysis Letters*, 2020, **150**, 2294–2303.
2. H. Gebre, K. Fisha, T. Kindeya, T. Gebremichal, *International Letters of Chemistry, Physics and Astronomy*, ISSN: 2299-3843, **57**, 72-84.
3. Y. Tang, M. Qiu, J. Yang, F. Shen, X. Wang and X. Qi, *Green Chemistry*, 2021, **23**, 1861-1870.
4. P. Karthikeyan, A. N. Uttaravalli, S. Dinda, *Materials Today: Proceedings*, 2018, **5**, 16313-16318.
5. J. Scognamiglio, L. Jones, C.S. Letizia, A.M. Api, *Food and Chemical Toxicology*, 2012, **50**, S608-S612.
6. A. Duereh, H. Guo, T. Honma, Y. Hiraga, Y. Sato, R. L. Smith, Jr. and H. Inomata, *Industrial and Engineering Chemistry Research*, 2018, **57**, 7331–7344.
7. M. Hronec, K. Fulajtárova, T. Liptaj, M. Štolcová, N. Prónayová, T. Soták, *Biomass and Bioenergy*, 2014, **63**, 291-299.
8. T. Akashi, S. Sato, R. Takahashi, T. Sodesawa, K. Inui, *Catalysis Communications*, 2003, **4**, 411-416.
9. M. Renz, *European Journal of Organic Chemistry*, 2005, **2005**, 979–988.
10. A. Kishi, T. Higashino, S. Sakaguchi and Y. Ishii, *Tetrahedron Letters*, 2000, **41**, 99–102.
11. M. Hronec, K. Fulajtarová, *Catalysis Communications* 2012, **24**, 100–104.
12. Y. Yang, Z. Du, Y. Huang, F. Lu, F. Wang, J. Gao and J. Xu, *Green Chemistry*, 2013, **15**, 1932–1940.
13. R. Fang, H. Liu, R. Luque and Y. Li, *Green Chemistry*, 2015, **17**, 4183–4188.

14. Xing-Long Li, J. Deng, J. Shi, T. Pan, Chu-Guo Yu, Hua-Jian Xu and Yao Fu, *Green Chemistry*, 2015, **17**, 1038–1046.
15. Y. Liu, Z. Chen, X. Wang, Y. Liang, X. Yang and Z. Wang, *ACS Sustainable Chemistry and Engineering*, 2017, **5**, 744–751.
16. M. Zhou, J. Li, K. Wang, H. Xia, J. Xu, J. Jiang, *Fuel*, 2017, **202**, 1–11.
17. X. Liu, B. Zhang, B. Fei, X. Chen, J. Zhanga and X. Mu, *Faraday Discussions*, 2017, **202**, 79–98.
18. N. S. Date, S. E. Kondawar, R. C. Chikate, and C. V. Rode, *ACS Omega*, 2018, **3**, 9860-9871.
19. P. Jia, X. Lan, X. Li and T. Wang, *ACS Sustainable Chemistry and Engineering*, 2019, **7**, 15221–15229.
20. Q. Deng, X. Wen, P. Zhang, *Catalysis Communications*, 2019, **126**, 5–9.
21. M. D. Astuti, D. Kristina, R. Rodiansono, D. R. Mujiyanti, *Bulletin of Chemical Reaction Engineering & Catalysis*, 2020, **15**, 232.
22. G. Gao, Y. Shao, Y. Gao, T. Wei, G. Gao, S. Zhang, Y. Wang, Q. Chen and X. Hu, *Catalysis Science and Technology*, 2021, **11**, 575–593.
23. C. Wang, Z. Yu, Y. Yang, Z. Sun, Y. Wang, C. Shi, Y. Liu, A. Wang, K. Leus and P. Voort, *Molecules*, 2021, **26**, 5736.
24. M. Dohade and P. L. Dhepe, *Catalysis Science and Technology*, 2018, **8**, 5259–5269.

Chapter 5.
**Hydrogenation of furfuryl alcohol (FOL) to
cyclopentanone (CPO)**

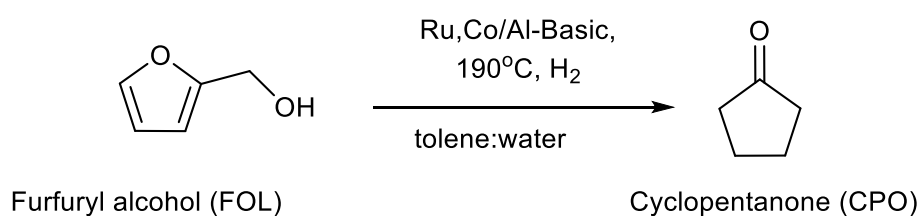
5.1. Introduction:

In the recent years, with the aim of replacing petroleum, transformation of biomass to chemicals has gained more attention. One of the basic compounds, furfural (FAL), is synthesized via acid-catalyzed dehydration of hemicellulose as a starting material.¹⁻⁵ Due to the multifunctional properties of carbonyl (C=O), conjugation (-C=C-C=C-) groups and five membered ring structure of furfural, it is regarded as a significant platform molecule to transform biomass feedstock's into compounds with added values such as furfuryl alcohol (FOL), 2-methyl tetrahydrofuran (2-MTHF), 2-methylfuran (2-MF), furan, tetrahydrofurfuryl alcohol (THFA) etc.^{6,7} Furfuryl alcohol (FOL), which is the primary hydrogenation product of furfural, can be used for the synthesis of lubricants, perfumes, resins, vitamin C, plasticisers, lysine etc., with wide range of potential applications.^{8,9} The C=C bond of furan ring of FOL undergoes hydrogenation produces THFA and hydrogenative rearrangement of FOL produces cyclopentanone (CPO). As discussed in chapter 4 (section 4.1), CPO has wide applications in different fields such as for the synthesis of fungicides, pharmaceuticals, flavour and fragrance chemicals, polyamides⁷, jet fuels etc.¹⁰⁻¹⁶ Until now there is only one literature available for the transformation of FOL into CPO. In this literature they have reported various supported metal as well as bulk catalysts for the transformation of FOL to CPO in aqueous solvent and achieved complete FOL conversion and 88% CPO yield using Ni based G-134 catalyst and acetic acid as an additive at 160°C and 25 bar H₂ pressure.¹⁷ They have also been examined that how temperature, pressure, time, catalysts concentration etc. can affect the product selectivity. They have reported how altering the H₂ pressure or catalyst quantity can affect the selectivity towards either CPO or THFA. Low catalyst concentration and moderate H₂ pressure can selectively produce CPO, while high H₂ pressure and high catalyst concentration can favour the THFA formation.

In previous chapter (chapter 4) conversion of FAL to CPO has been discussed. It has been seen that synthesized (2)Ru(1.5)Co/Al-Basic catalyst showed 100% FAL conversion and 74% CPO yield within 4 h reaction time at 160°C temperature and 13 bar H₂ pressure in water/toluene (4:3 v/v) solvent. Using commercial (5)Ru/Al catalyst, in water/toluene (4:3 v/v) solvent at 180°C, 13 bar H₂ pressure and 4 h reaction time, 100% FAL conversion and 62%

CPO yield has been achieved. Additionally, in chapter 4, using synthesized (2)Ru(1.5)Co/Al-Basic catalyst, crude FAL was hydrogenated as well, yielding 63% CPO with 100% FAL conversion at 160°C and 13 bar H₂ pressure within 4 h using water/toluene (4:3 v/v) 35 mL solvent.

With both the catalysts, conversion was shown to be 100% during the hydrogenative ring rearrangement of FAL to CPO, although CPO yield did not exceed 74%. The production of side products such as THFA, 2-MTHF, Pentane-1,2-diol (1,2-PDO), Pentane-1,4-diol (1,4-PDO), Pentane-1,5-diol (1,5-PDO), Pentane-2,4-diol (2,4-PDO), etc. were also observed during the conversion of FAL to CPO. Along with these products, some unidentified products were also seen. The production of side products may be the cause of the CPO yield not going above 74%. In order to boost the yield of CPO, limiting the amount of side products formation is necessary. Finding the reaction pathways that lead to the development of these products is essential to limiting the formation of side products. In present chapter, the precise reaction mechanism and pathways that lead to the formation of these side products will be covered in detail. To get the maximum CPO yield, optimization of reaction condition for the conversion of FOL to CPO will also be carried out.



Scheme 5.1 Conversion of furfuryl alcohol (FOL) to cyclopentanone (CPO)

5.2. Experimental

5.2.1. Materials: The Pentane-1,2-diol (1,2-PDO) (99%), Pentane-1,4-diol (1,4-PDO) (99%), Pentane-2,4-diol (2,4-PDO) (99%), Pentane-1,5-diol (1,5-PDO) (99%) and 2-cyclopetene-1-one (99%) were purchased from Sigma Aldrich. Cyclopentanone (99%) and cyclopentanol (99%) were obtained from Lancaster. From Loba Chemie, India, furfuryl alcohol (FOL) (99%) was ordered. Furan (99%) was supplied by Spectrochem, Mumbai, India. Alfa Aesar supplied the 2-methylfuran (2-MF) (99%), 2-methyl tetrahydrofuran (2-MTHF) (99%) and tetrahydrofurfuryl alcohol (THFA) (99%). Toluene (99%, AR) was purchased from RANKEM, India.

5.2.2. Catalyst synthesis:

Supported monometallic catalysts were manufactured using wet impregnation method and well researched co-impregnation method was used to synthesise bimetallic catalysts. Earlier descriptions (Refer chapter 2, section 2.2.2.) provides more information on materials and catalyst synthesis process utilized to manufacture supported metal catalysts. All the synthesized catalysts were assessed for the production of CPO from FOL.

5.2.3. Reaction set-up and analysis of reaction mixtures:

Batch mode autoclave with 50 mL capacity were used to perform both catalytic and non-catalytic reactions. Reactions were carried out with 0.35g FAL and 0.04g catalyst using water/toluene (4:3 v/v) as a solvent. Typically, experiments were conducted at the temperature ranging from 160°C to 200°C for varying period of time (1 to 1.3 h) and varying H₂ pressure (10 to 16 bar). The reaction mixture was analysed using gas chromatography (GC) and high-performance liquid chromatography (HPLC). The organic solvent was analysed using GC (Agilent GC) equipped with HP-5 capillary column and FID detector. The HP-5 capillary column used of dimensions 0.25 μm \times 0.32 mm \times 30 m, and the FID detector with N₂ as a carrier gas with a flow rate of 30 mL \cdot min⁻¹ was used at 250°C. The program of oven

temperature was 50°C (1 min hold time) to 200°C (10 min hold time) with the rate of 10°C min⁻¹. The injector temperature was kept constant at 200°C. The water layer was analysed using HPLC equipped with RID detector (Agilent technologies, 1200 infinity series, 40°C) and HC-75 Pb⁺² column (Hamilton, 7.8mm × 300mm, 80°C). HPLC grade water was utilized as an eluent with the flow rate of 0.5mL·min⁻¹.

5.2.4. Calculations:

The external standard method was employed to calculate the FOL conversion and yield of the obtained products. Conversion (C) of FOL and yield (Y) of products have been calculated as below.

$$\text{Conversion (C)\%} = \left\{ \frac{[(\text{Initial moles of substrate}) - (\text{Final moles of substrate})]}{\text{Initial moles of substrate}} \right\} * 100$$

$$\text{Yield (Y)\%} = \left\{ \frac{\text{Moles of product formed}}{\text{Theoretical moles of product formed based on the moles of substrate converted}} \right\} * 100$$

5.3. Results and discussion:

According to the discussions in chapter 4, the catalyst (2)Ru(1.5)Co/Al-Basic operates effectively to convert FAL to CPO, however, the CPO yield was remained restricted at 74% due to the generation of side products. In order to learn more about the reaction pathway for the formation of CPO and side products, the reactions were carried out using FOL as a substrate, which is a primary intermediate in the conversion of FAL to CPO. The effect of reaction parameters for the conversion of FOL to CPO was also studied.

5.3.1. Effect of different reaction parameters:

In order to minimize the side product formation and maximise the yield of CPO, the influence of experimental conditions like temperature, H₂ pressure, reaction time, S/C ratio were studied for the conversion of FOL to CPO.

Effect of H₂ pressure:

To examine the impact of H₂ pressure for the conversion of FOL to CPO, reactions under different H₂ pressure (10 to 16 bar at R.T.) were conducted. As shown in Figure 5.1, all the experiments were conducted at 160°C for 1 h reaction time. 80% of FOL conversion and 57% of CPO yield were detected at 10 bar H₂ pressure (16 bar at reaction temperature). It means that 10 bar pressure is not sufficient for the conversion of FOL to CPO. At 10 bar pressure, 2% CPL, 2.5% THFA and 3% some other products including 1,2-PDO, 1,4-PDO, 1,5-PDO, 2,4-PDO, MTHF, 2-MF etc. were also seen. Along with these products some unknown product formation was also observed at 10 bar pressure. In order to increase the conversion and yield the pressure was raised to 13 bar (21 bar at reaction temperature). When pressure increased to 13 bar both FOL conversion and CPO yield were rose, reaching 92% and 68% respectively. This suggests that FOL conversion and CPO yield are dependent on H₂ pressure, since H₂ solubility increases with H₂ pressure. Since the dissolution of gases in solvent dependent on both temperature and pressure, it is anticipated that with increase in pressure H₂ will get more dissolved in solvent and hence improvement in yield were observed with increase in H₂ pressure. Along with CPO, CPL, THFA and other product formation were also seen at 13 bar H₂ pressure with the yields of 5%, 2% and 2.5% respectively. But at this pressure, the intensity of unknown products peaks is less compared to 10 bar pressure. Considering this positive effect of pressure on the FOL to CPO reactions, further pressure was increased to 16 bar (25 bar at reaction temperature). The highest FOL conversion of 100% was achieved at 16 bar H₂ pressure, however the CPO yield was achieved only 62%. Additionally, it has been found that at high pressure (16 bar), the yield of CPO decreases while the yield of CPL 12%, THFA 5% and other products 4% were increased. This suggests that at higher H₂ pressure C=C

and C=O bond hydrogenation takes place produces CPL and THFA with high yield. It was also noted that if we increase the H₂ pressure, intensities of unknown product peaks were lowered. Despite the fact that the maximum FOL conversion was achieved at 16 bar pressure, maximum CPO yield was achieved at 13 bar pressure. And in terms of selectivity also, maximum CPO selectivity (74%) was observed at 13 bar H₂ pressure compare to 16 bar (62%). Since the catalyst exhibits maximal CPO yield (68%) as well as selectivity (74%) at 13 bar H₂ pressure, indicating it is the ideal H₂ pressure for converting FOL to CPO.

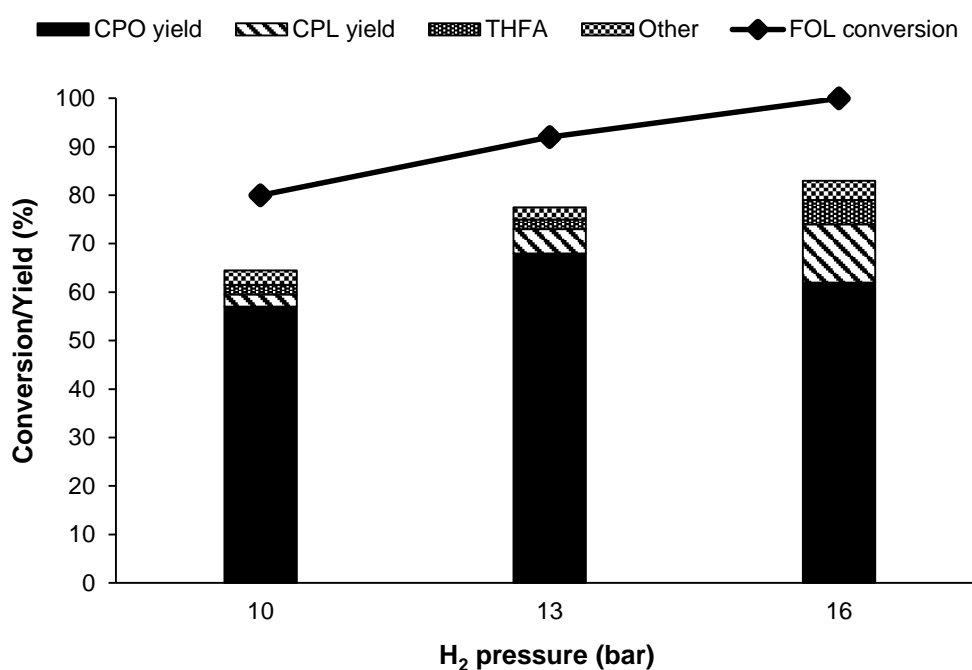


Figure 5.1. Effect of H₂ pressure for the conversion of FOL to CPO.

Reaction conditions: FOL, (2)Ru(1.5)Co/Al-Basic catalyst, S/Ru (714 mol/mol), toluene/water 3:4 v/v (35mL), 160°C, 1 h.

All the reactions are done at least three times and the obtained results are within the error of $\pm 1\%$ -2.5 % range.

Effect of temperature:

The effect of reaction temperature on product distribution over (2)Ru(1.5)Co/Al-Basic was studied for the hydrogenation of FOL to CPO. Evidently, as the temperature raised from 160°C to 200°C, the conversion of FOL improved from 81% to 100%. At lower temperature (160°C), 53% CPO yield was observed, which reached to 68% as temperature raised to 190°C. In addition to increase in temperature to 200°C, reduces the CPO yield to 60%. It suggests that, CPO selectivity is negatively impacted at higher temperature. However, selectivity toward CPL, THFA and other products were increased with increase in temperature as show in Figure 5.2. During the analysis of reaction mixture, it was come to light that when reactions were conducted at lower temperature, many unknown products peaks with prominent intensities were seen in HPLC. When temperature was raised from 160°C to 190°C, there was drop in peak intensities of unknown peaks were observed. It was additionally found that with increase in temperature, mass balance was also increased. It implies that at lower temperature FOL may get polymerize in water medium generating unidentified products and having an adverse impact on CPO selectivity as well as mass balance of the reaction. Furthermore, when temperature rose to 200°C, an increase in CPL, THFA and diols yield was noticed. It implies that, CPO selectivity is negatively impacted at higher temperature. However, increase in selectivity toward CPL, THFA and other products (diols) as well as loss in mass balance was also observed with a rise in temperature. The formation of some gaseous products like, 2-MF, furan etc. was also the cause of this drop in mass balance at 200°C temperature.

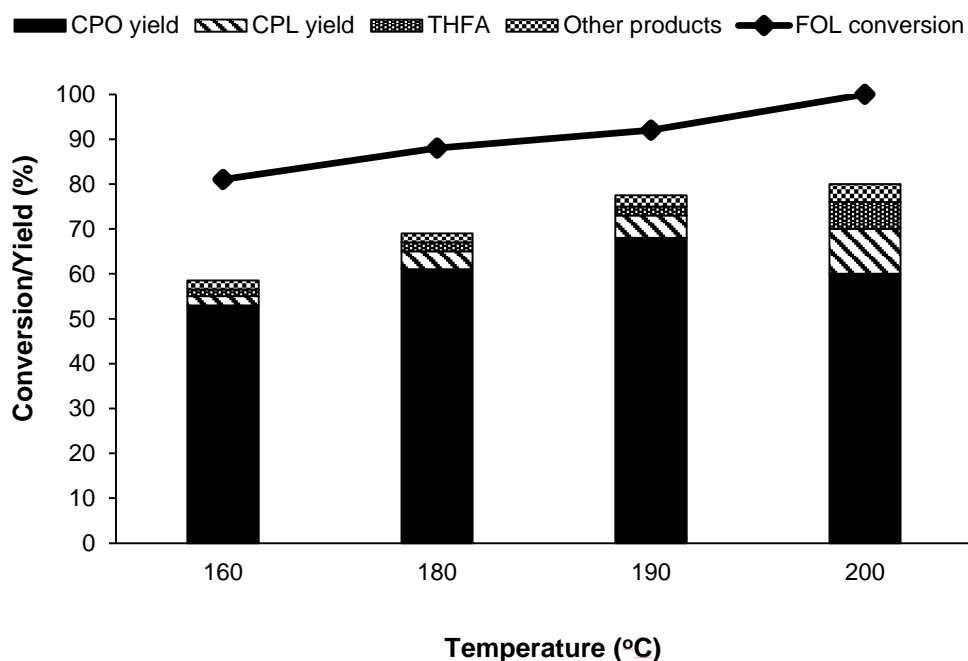


Figure 5.2. Effect of temperature for the conversion of FOL to CPO.

Reaction conditions: FOL, (2)Ru(1.5)Co/Al-Basic catalyst, S/Ru (714 mol/mol), toluene/water 3:4 v/v (35mL), 13 bar H₂ at R.T., 1 h.

All the reactions are done at least three times and the obtained results are within the error of $\pm 1\%$ -2.5 % range.

Effect of time:

The impact of reaction time on the conversion of FOL to CPO under desired reaction conditions (190°C, 13 bar H₂ and water/toluene 4:3 v/v (35mL) solvent) is shown in Figure 5.3. The Figure 5.3 illustrated that at shorter reaction time (1 h), FOL conversion (92%) and CPO yield (68%) was lower. It means that 1 h time is not sufficient for the transformation of FOL to CPO. Further in order to increase the conversion and yield, the reactions were conducted for the extended reaction time i. e. 1.3 h, 99% FOL conversion with 74% CPO yield was achieved. Further, duration of reaction time was extended to 1.5 h, slight decrease in CPO yield along with increase in CPL and THFA yield was observed. According to time study it was seen that,

with the prolongation of reaction time, the yield of CPL and THFA increased steadily. Figure 5.3 shows that highest CPO yield was achieved in 1.3 h reaction time. Therefore 1.3 h is the ideal reaction time to transform FOL into CPO.

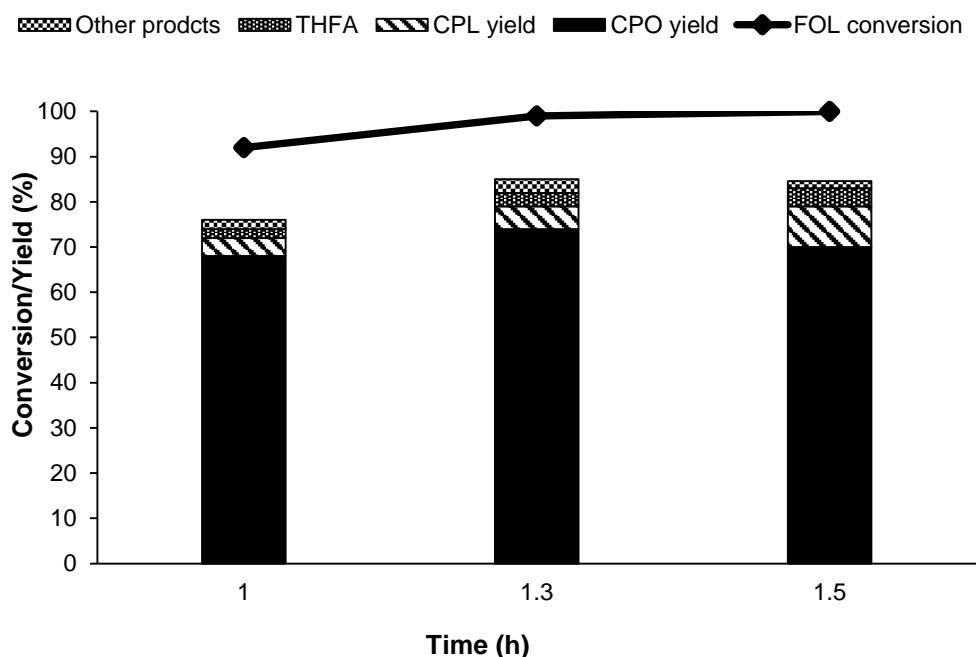


Figure 5.3. Effect of time for the conversion of FOL to CPO.

Reaction conditions: FOL, (2)Ru(1.5)Co/Al-Basic catalyst, S/Ru (714 mol/mol), toluene/water 3:4 v/v (35mL), 13 bar H₂ at R.T., 190°C.

All the reactions are done at least three times and the obtained results are within the error of $\pm 1\%$ -2.5 % range.

Effect of S/C ratio:

For the transformation of FOL into CPO, the impact of S/Ru ratio in the range of 190 to 1516 mol/mol was also studied. Initially, as shown in Figure 5.4, reactions were carried out with lower S/Ru ratio (190) and it was found that FOL was converted completely but the yield towards CPO (38%) was lower than expected. Additionally, along with CPO, 15% CPL, 26%

THFA and 6% other product formation were also observed. It suggests that with higher catalysts concentration, C=C bond of furan ring of FOL and C=O bond of CPO get hydrogenated, produces THFA and CPL exclusively. Additionally, C-C bond cleavage occur at higher catalysts concentration forming undesired products. This could be because at higher catalysts quantity, more active sites of catalysts are available, which encourages the hydrogenation of C=C and C=O bond as well as breaking of C-C bond. In order to maximize the yield and selectivity of CPO and minimize the formation of undesired products, further reactions were conducted with a low S/Ru ratio. With the S/Ru 357 mol/mol, increase in the yield towards CPO (60%) and decrease in THFA (12%), CPL (8%) and other products (5%) yield was observed with 100% FOL conversion. Further, S/Ru ratio was increased to 714 mol/mol and at this S/Ru ratio, maximum CPO yield (74%) and minimum THFA (2%) and CPL (4%) yield was achieved with 92% FOL conversion. Furthermore, increase in the S/Ru ratio to 1516 mol/mol, a drop in FOL conversion and CPO yield was observed. This is because the lack of adequate active sites in catalysts. The maximum selectivity toward CPO was seen at S/Ru ratio 714 mol/mol, therefore, the ideal ratio for the conversion of FOL to CPO is S/Ru 714 mol/mol.

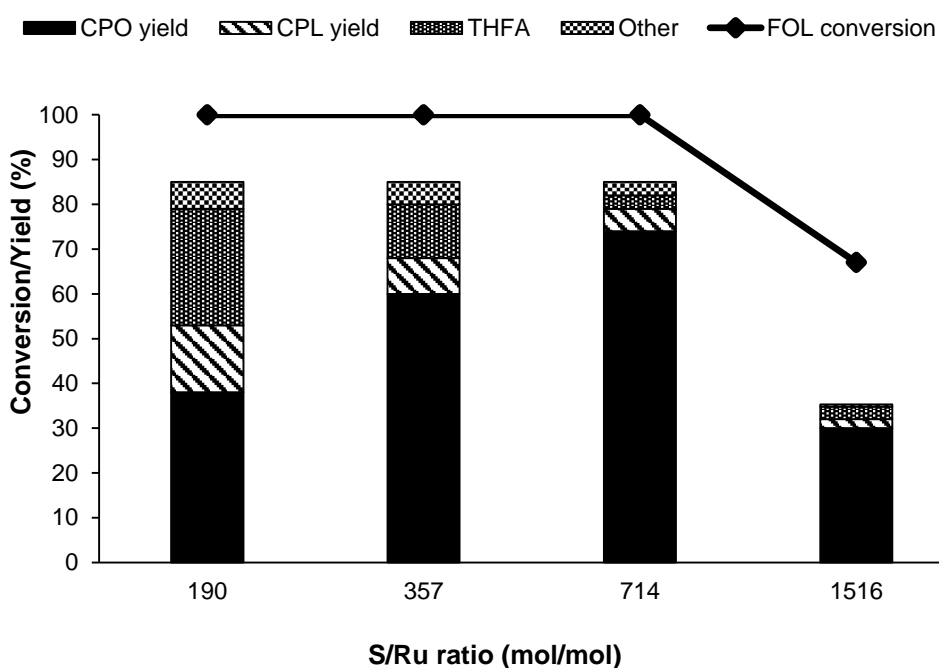


Figure 5.4. Effect of S/Ru ratio for the conversion of FOL to CPO.

Reaction conditions: FOL, (2)Ru(1.5)Co/Al-Basic catalyst, toluene/water 3:4 v/v (35mL), 13 bar H₂ at R.T., 190°C, 1.3 h.

All the reactions are done at least three times and the obtained results are within the error of $\pm 1\%$ -2.5 % range.

5.3.2. Stability of products:

In chapter 4, it was observed that, during the hydrogenative ring rearrangement process of FAL to CPO, it was observed that FAL conversion is 100% but CPO yield was not going beyond 74%. In FOL to CPO reactions, 100% FOL conversion and 74% CPO yield was achieved. In both the reactions, it was seen that CPO yield was not going beyond 74% and the generation of side products (THFA, 2-MTHF, 1,2-PDO, 1,4-PDO, 1,5-PDO, 2,4-PDO and some unidentified products etc.) may be the reason of this. In order to elucidate the reaction pathway to hydrogenate FAL to CPO and FOL to CPO, some controlled experiments were conducted. All the experiments were conducted for 1 h at 160°C, 13 bar H₂ at R. T., which are the optimal reaction conditions to convert FAL to CPO. As illustrated in Table 5.1, if FAL is

used as a substrate, 80% FAL conversion and 41.5% CPO with 14.5% FOL formation were noted in this reaction. In addition, side products like THFA, CPL, 2-MTHF and diols formation were also observed. To determine the cause of the side products (THFA, 2-MTHF, 1,2-PDO, 1,4-PDO, 1,5-PDO, 2,4-PDO etc.) formation, the stability study of products such as CPO, FOL and THFA was carried out. All of the products stability studies were carried out for 1 h time period under optimal reaction conditions (water/toluene 4:3 v/v, 160°C, 13 bar H₂ pressure). Initially, thermal stability of CPO was conducted and it was found that 96.4% CPO converted to 95.5% CPL. As discussed in section 5.3.1, tuning the H₂ pressure and reaction time can reduce the CPL formation. During the stability study of CPO, except CPL, no additional side product formation was observed. This demonstrated that the side products formation during the FAL to CPO reactions are not caused by CPO. Further, reaction was carried out using intermediate FOL as substrate, which showed 98% FOL conversion with 41% CPO, 2.5% CPL and 8% THFA formation. Additionally, if reactions were done with FOL, some unknown product formation was also observed. Further, reaction was conducted using THFA as a substrate, then no CPO and CPL formation was observed and the main product was 2-MTHF (5.2%) with diols (4%) formation was observed at 9.5% THFA conversion. This proves that, as shown in Table 5.1, the intermediate FOL is the cause of side products formation.

In this stability study it was found that if reactions were done with FOL as a substrate resulted in a very low mass balance (65%) when compared to other substrates including FAL (81%), CPO and THFA. This might be due to the polymerization of FOL under reaction conditions. It is reported that FOL undergoes polymerization reactions in an acidic environment (Lewis and Brønsted).¹⁸ In present work, water and toluene are used as a solvent for the reactions. The FOL formed, which is an intermediate of FAL to CPO reactions, is highly soluble in water than toluene. Therefore, it can be said that the FOL formed during the transformation of FAL to CPO is present in aqueous medium. Water has a potential to behave as Brønsted acid, while the Co present in (2)Ru(1.5)Co/Al-Basic catalyst has the ability to act as a Lewis acid. As a result, this water and Co might have been the cause of the FOL polymerization during the reaction. According to the section 5.2.1, yield of CPO is not exceeding beyond 74% and mass balance is not going beyond 85%. This could be due to the polymerization of FOL during the reaction.

Table 5.1. Thermal stability study

Substrates/ products	FAL (%)	CPO (%)	CPL (%)	THFA (%)	FOL (%)	2- MTHF (%)	1,5- PDO (%)	1,2- PDO (%)	1,4- PDO (%)	2,4- PDO (%)
FAL	20	41.5	0.44	1.13	14.5	2.24	0.15	0.28	0.38	0.4
CPO	-	3.6	95.5	-	-	-	-	-	-	-
FOL	-	41	2.5	8	2	3.29	0.9	4.12	2.76	0.34
THFA	-	-	-	90.5	-	5.2	0.4	1.2	2.2	0.2

5.3.3. Reaction pathway for the conversion of FAL to CPO:

Considering the above discussions, the plausible reaction pathway has been suggested for the transformation of FAL to CPO. As illustrated in Figure 5.5, the catalytic hydrogenation of FAL results in the formation of FOL. Then, the C=C bond either get catalytically hydrogenate to form THFA or undergoes hydrogenative ring rearrangement to form CPO. For the formation of CPO, first FOL undergo Piancatelli rearrangement to form 4- hydroxyl-2-cyclopentenone (HCP) intermediate. HCP is an another key intermediate in FAL to CPO reaction. This Piancatelli rearrangement occurs in presence of water.¹⁹ Further the of C=C bond of HCP intermediate get hydrogenated to form 4- hydroxyl cyclopentanone, which is then dehydrated to form 2-cyclopentenone (CEO). The unsaturated C=C bond of CEO undergoes hydrogenation to form CPO. Because CPO contains C=O bond, excessive hydrogenation might take place to form CPL. As discussed in section 5.3.1, the selectivity of CPO or CPL depends upon the reaction conditions used. CPL is formed under harsh reaction conditions (high temperature, high catalyst quantity, high H₂ pressure and prolonged reaction time). The optimal reaction conditions are necessary for the selective formation of CPO.

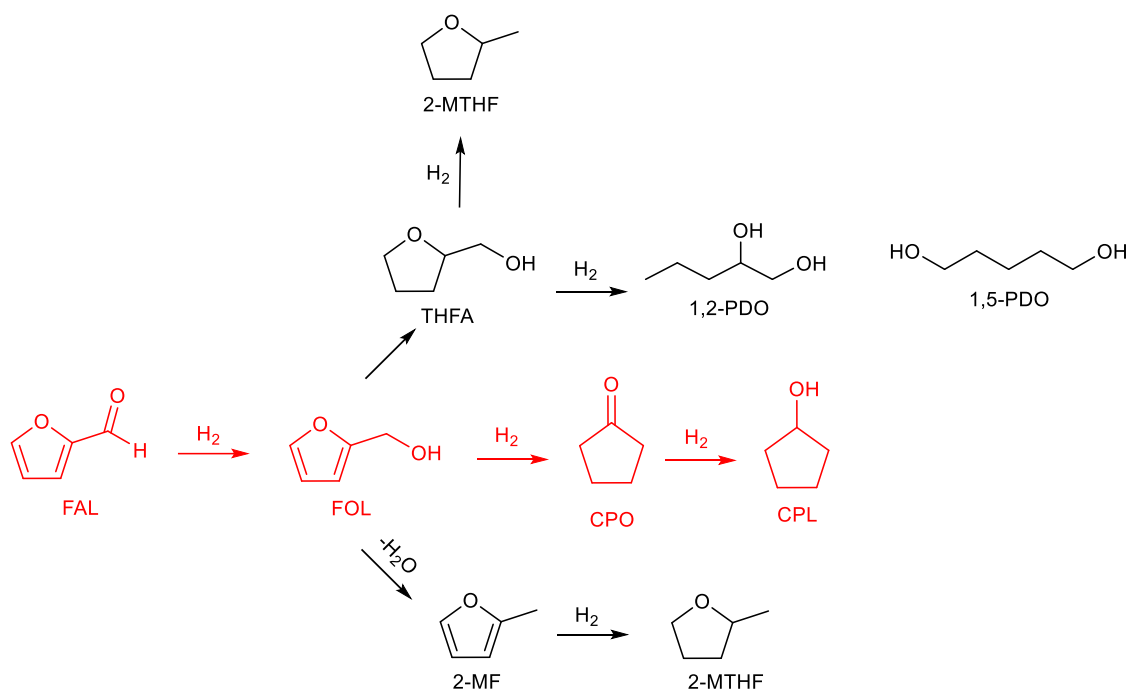


Figure 5.5. Reaction pathway for the conversion of FAL to CPO.

5.4. Conversion of FOL to CPO using commercial (5)Ru/Al catalyst:

As discussed in above section 5.2, (2)Ru(1.5)Co/Al-Basic catalysts is operating efficiently for the transformation of FOL to CPO with 100% FOL conversion and 74% CPO yield at 190°C, 13 bar H₂ at R. T., 1.3 h, S/Ru-714 mol/mol. Moreover, the reactivity of commercial (5)Ru/Al catalyst for converting of FOL to CPO was examined. As illustrated in Figure 5.6, using commercial (5)Ru/Al catalyst, initially reaction was carried out at similar reaction condition (190°C, 13 bar H₂ at R. T., 1.3 h, S/Ru-714 mol/mol), and achieved 100% conversion and 68% CPO yield. At this condition, in addition to CPO generation, 6% CPL and 5% THFA formation was also observed. As was mentioned in section 5.3, the C=O bond of CPO will get hydrogenated and generate CPL. Since CPL is a further hydrogenation product of CPO, further reactions were conducted for shorter reaction time (1.1 h). Highest 100% FOL conversion and 74% CPO yield were accomplished within 1.1 h. Further shortening the reaction period to 1.h, decrease in FOL conversion (96%) and CPO yield (70%) was observed.

Therefore, at 190°C and 13 bar H₂ pressure, 1.1 h is the optimal reaction time for converting FOL to CPO using commercial (5)Ru/Al catalyst.

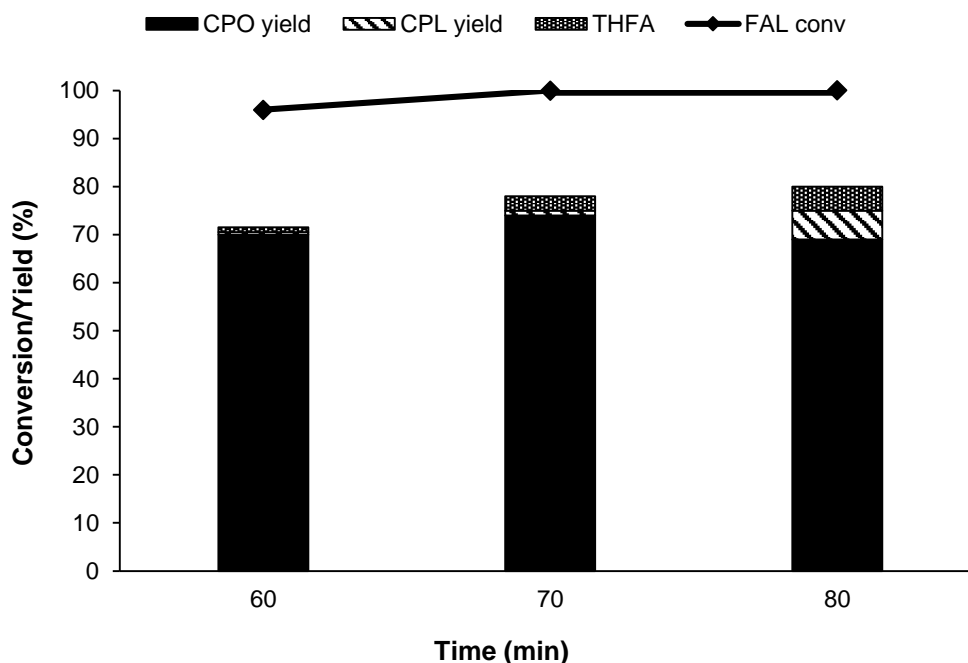


Figure 5.6. Effect of time for the conversion of FOL to CPO.

Reaction conditions: FOL, (5)Ru/Al catalyst, S/Ru (714 mol/mol), toluene/water 3:4 v/v (35mL), 13 bar H₂ at R.T., 190°C.

All the reactions are done at least three times and the obtained results are within the error of $\pm 1\%$ -2.5 % range.

5.5. Conclusion:

FOL can be efficiently hydrogenated to CPO under 190°C, 13 bar H₂ at R. T., 1.3 h reaction time using S/Ru-714 (mol/mol). Up to 74% CPO yield was achieved at 100% FOL conversion using (2)Ru(1.5)Co/Al-Basic catalyst. The experiments have also been conducted to study the effect of time, temperature, H₂ pressure, S/Ru ration etc. Under the reaction

conditions, it has been noted that the hydrogen pressure and catalyst concentration play a vital role for the selective synthesis of CPO from FOL. At lower catalyst concentration and H₂ pressure, CPO is produced exclusively with 74% yield and high catalyst concentration and H₂ pressure favours the CPL and THFA formation. Product stability study was conducted to determine the reaction pathways for the generation of side products and found that the FOL is a primary cause for the side product formation. Activity of commercial (5)Ru/Al catalyst was also tested for the transformation of FAL to CPO and attained maximum 74% yield of CPO with 100% FOL conversion under optimal reaction conditions (190°C, 13 bar H₂ at R. T., 1.1 h, S/Ru-714).

5.6. References:

1. R. Xing, W. Qi and G. W. Huber, *Energy and Environmental Science*, 2011, **4**, 2193.
2. P. Bhaumik and P. L. Dhepe, *RSC Advances*, 2014, **4**, 26215–26221.
3. Y. Nie, Q. Hou, W. Li, C. Bai, X. Bai and M. Ju, *Molecules*, 2019, **24**, 594.
4. A. Jaswal, P. P. Singh and T. Mondal, *Green Chemistry*, 2022, **24**, 510–551.
5. K. J. Yong, T. Y. Wu, C. B. T. L. Lee, Z. J. Lee, Q. Liu, J. M. Jahim, Q. Zhou, L. Zhang, *Biomass and Bioenergy*, 2022, **161**, 106458.
6. A. H. Motagamwala, W. Won, C. Sener, D. M. Alonso, C. T. Maravelias, J. A. Dumesic, *Science Advances*, 2018, **4**, eaap972.
7. Y. Tang, M. Qiu, J. Yang, F. Shen, X. Wanga and X. Qi, *Green Chemistry*, 2021, **23**, 1861–1870.
8. B. M. Reddy, G. K. Reddy, K. N. Rao, A. Khan, I. Ganesh, *Journal of Molecular Catalysis A: Chemical*, 2007, **265**, 276–282.
9. B.M. Nagaraja, A.H. Padmasri, B. David Raju, K.S. Rama Rao, *Journal of Molecular Catalysis A: Chemical*, 2007, **265**, 90–97.
10. J. Scognamiglio, L. Jones, C.S. Letizia, A.M. Api, *Food and Chemical Toxicology*, 2012, **50**, S608-S612.
11. M. Hronec, K. Fulajtárova, T. Liptaj, M. Štolcová, N. Prónayová, T. Soták, *Biomass and Bioenergy*, 2014, **63**, 291-299.
12. P. Karthikeyan, A. N. Uttaravalli, S. Dinda, *Materials Today: Proceedings*, 2018, **5**, 16313-16318.
13. A. Duereh, H. Guo, T. Honma, Y. Hiraga, Y. Sato, R. L. Smith, Jr. and H. Inomata, *Industrial and Engineering Chemistry Research*, 2018, **57**, 7331–7344.

14. T. Akashi, S. Sato, R. Takahashi, T. Sodesawa, K. Inui, *Catalysis Communications*, 2003, **4**, 411-416.
15. M. Renz, *European Journal of Organic Chemistry*, 2005, **2005**, 979–988.
16. A. Kishi, T. Higashino, S. Sakaguchi and Y. Ishii, *Tetrahedron Letters*, 2000, **41**, 99–102.
17. M. Hronec, K. Fulajtárova, T. Soták, *Applied Catalysis B: Environmental*, 2014, **154–155**, 294–300.
18. M. Choura, N. M. Belgacem, and A. Gandini, *Macromolecules*, 1996, **29**, 3839-3850
19. M. Hronec, K. Fulajtárová, I. Vávra, T. Soták, E. Dobrocka, M. Micusík, *Applied Catalysis B: Environmental*, 2016, **181**, 210–219.

Chapter 6.

Summary and conclusions

Summary and conclusions:

Chapter 1.

The general introduction, overview of biomass and biorefinary concept was discussed in this chapter. The detailed about lignocellulosic biomass, it's classification, sources and advantages of lignocellulosic biomass was also discussed in this chapter. Lignocellulosic biomass which is non-edible to human being is consist of cellulose, hemicellulose and lignin. cellulose and hemicellulose upon acid hydrolysis produces different C5 and C6 sugars. These sugars further converted to sugars alcohols and CPO. Sugar alcohol CPO has various applications in different fields including food, pharmaceuticals, cosmetics etc. Detailed literature reviews were discussed and found that many supported metal catalysts are reported for the synthesis of sugar alcohols and CPO. Moreover, these catalysts have limitations, which makes them commercially incompatible. Literature suggested that, bimetallic catalysts appeared to have high activity than monometallic catalysts. Hence, the aim of research work was set to synthesize different supported metal catalysts that can be cost effective and commercially viable for the conversion of sugars and furfural.

Chapter 2.

In this chapter synthesis of various supported metal catalysts (monometallic as well as bimetallic) and their characterization using different characterization method was discussed.

- ✓ A list of monometallic as well as bimetallic catalysts were prepared catalysts were prepared using wet impregnation method and co-impregnation method respectively. For the synthesis of catalysts, different commercially available materials including γ -Al₂O₃ (Al-Acidic, Al-Basic and Al-Neutral), SiO₂ (Si), SiO₂-Al₂O₃ (Si-Al), ZrO₂, activated carbon (C), SAPO were used as the supports
- ✓ Several physico-chemical techniques including XRD, XPS, TEM, 2 sorption, ICP-OES, etc. were used to characterize the prepared catalysts.

- ✓ XRD analysis of all the support and synthesized monometallic and bimetallic catalysts was done. XRD pattern of (1.5)Ru(3)Co/Al-Basic shows the diffraction peaks at 2θ of 19° , 37.6° , 39.4° , 42.5° , 45.8° , 67° and 85° (JCPDS 00-010-0425) which are correspond to basic alumina (Al-Basic). Besides this, no diffraction patterns for Ru and Co were observed in the XRD of catalysts which suggests that both Ru and Co are highly dispersed on the supports and also very low metal loading is another factor for the absence of the diffraction peaks for Ru and Co.
- ✓ XPS analysis of catalysts was performed to understand the oxidation states of metals present in catalysts. In both monometallic (1.5)Ru/Al-Basic, (3)Co/Al-Basic and bimetallic (1.5)Ru(3)Co/Al-Basic catalysts, Co present in higher (II) and (III) oxidation state and these oxidation states represented the formation of CoO and Co₃O₄ species while Ru present in (IV) and mainly in (0) (metallic state) oxidation state.
- ✓ Physicochemical properties of supports and synthesized materials were determined using N₂ sorption analysis. BET Analysis shows slight decrease in surface area and pore volume of catalysts compared to support, which is because after the metal has been impregnated on support, Ru and Co metal deposit on the surface of support and block the portion of its pores which causes decrease in surface area.
- ✓ Metal dispersion and metal practical size of synthesised catalysts was determined using TEM analysis. TEM analysis confirms particle size of monometallic (1.5)Ru/Al-Basic (2.2 nm), (3)Co/Al-Basic (4 nm) catalyst was found to be bigger than and bimetallic (1.5)Ru(3)Co/Al-Basic (1.6 nm) catalysts. Which concludes that in bimetallic (1.5)Ru(3)Co/Al-Basic catalysts, metal particles are well dispersion on support with the formation of smaller particle size which contributes to an increase the catalysts surface area and ultimately enhances the catalyst activity.
- ✓ ICP-OES analysis confirmed the metal loading on support. it showed that the metal content of all the synthesized catalysts is approximately near to the expected metal content

Chapter 3A.

In this chapter, the activity of various supported monometallic as well as bimetallic catalysts was investigated for the hydrogenation of glucose to sorbitol. Effects of different promoters, metals and supports as well as the effects of different reaction parameters including temperature, H₂ pressure, time, catalyst quantity etc. were also examined in order to maximize conversion and yield.

- ✓ Out of all the synthesized catalysts, (1.5)Ru(3)Co/Al-Basic catalyst exhibits excellent catalytic activity toward the conversion of glucose to sorbitol in aqueous medium. Under 15 bar H₂ reasure, 130°C and 6h synthesized catalyst showed 100% conversion of glucose with 91% yield of sorbitol at ideal reaction conditions.
- ✓ Promoter effect was studied and found that addition of Co increases the catalyst activity. Addition of Co minimizes the agglomeration and increases the dispersion of Ru particles which ultimately increases the active sites for the reaction and achieved better yields towards conversion of glucose to sorbitol.
- ✓ Additionally, as seen from XPS study, Co present in (II) and (III) oxidation state. Co present in higher oxidation states behaves as Lewis acid site, interaction with carbonyl oxygen and increase the electrophilicity of carbonyl carbon and promote the hydride attack on the same
- ✓ Basicity of Al-Basic support helps in opening ring structure of glucose, according to the Lobry de Bruyn–Alberda van Ekenstein mechanism.
- ✓ Influence of various reaction parameters was examined for the transformation of glucose to sorbitol and highest catalytic activity of (1.5)Ru(3)Co/Al-B catalyst was achieved at 130°C, 15 bar H₂ and 6 h time.
- ✓ Higher glucose concentration reactions (20 wt%) were carried out, and 82% sorbitol yield was attained.
- ✓ Catalyst shows good recyclability and hence can be opted as a stable catalyst system for scale up reactions.

- ✓ Reactions in continuous flow mode reactor at 150°C, 25 bar H₂ pressure with the flow rate of 10 mL·min⁻¹ as carried out and achieved 85% conversion with 76% sorbitol yield.
- ✓ Purification of the product is also performed and achieved 96% sorbitol purity.

Chapter 3B.

In this work, The hydrogenation of xylose to xylitol was examined using monometallic (3)Co/Al-Basic and (1.5)Ru/Al-Basic catalysts as well as bimetallic (1.5)Ru(3)Co/Al-Basic catalysts

- ✓ It has been shown that bimetallic (1.5)Ru(3)Co/Al-Basic catalysts possesses higher activity and selectivity towards xylitol production than monometallic catalysts. (1.5)Ru(3)Co/Al-Basic catalysts exhibit complete xylose conversion and 93% xylitol yield at optimum reaction condition.
- ✓ The study of effect of different reaction parameters investigated that, at 120°C, 15 bar H₂, and 6 h reaction time, (1.5)Ru(3)Co/Al-B catalyst exhibited the maximum catalytic activity.
- ✓ Achieved an 82% xylitol yield with higher xylose concentration (20 wt%).
- ✓ The catalyst exhibits high recyclability, making it a stable catalyst system suitable for larger scale reaction.
- ✓ When reaction was done in constant flow mode reactor reactions, an 86% conversion and 76% xylitol yield were obtained at 150°C, 25 bar H₂ pressure, and 10 mL·min⁻¹ of flow rate.
- ✓ Additionally, the product is purified, and 96% sorbitol purity is attained.

Chapter 4.

This chapter includes the transformation of FAL to CPO using (2)Ru(1.5)Co/Al-Basic catalyst in biphasic solvent system.

- ✓ For the conversion of FAL to CPO, the bimetallic (2)Ru(1.5)Co/Al-B catalyst exhibits better activity than monometallic (2)Ru/Al-B catalyst under ideal reaction conditions.
- ✓ (2)Ru(1.5)Co/Al-B catalyst exhibits highest 99% FAL conversion and 74% CPO yield at 160°C and 13 bar H₂ pressure.
- ✓ The selectivity of products mainly depends upon the catalysts concentration and the H₂ pressure. For the selective formation of CPO, lower catalyst concentration and H₂ pressure is needed and at higher catalyst concentration and H₂ pressure leads to the CPL and THFA formation.
- ✓ Commercial (5)Ru/Al catalyst demonstrated 100% FAL conversion and 62% CPO yield at ideal reaction condition. (180°C, 13 bar H₂, 4h).
- ✓ Additionally, the synthesis of FAL was also possible from hydrolysed hemicellulose in presence of acetic acid, yielded 82% FAL with 100% conversion at 180°C within 5 h reaction period.
- ✓ Further, with crude FAL, using (2)Ru(1.5)Co/Al-Basic catalyst, 63% CPO yield was achieved.

Chapter 5.

This chapter includes the precise reaction mechanism and pathways that lead to the formation side products during the transformation of FAL to CPO. To get the maximum CPO yield, optimization of reaction conditions for the conversion of FOL to CPO were also carried out.

- ✓ Using S/Ru-714 (mol/mol), FOL can be effectively hydrogenated to CPO at 190°C, 13 bar H₂ within 1.3 h reaction time. With (2)Ru(1.5)Co/Al-Basic catalyst, up to 74% CPO yield was obtained at 100% FOL conversion.

- ✓ It has been observed that the concentration of the catalyst and the hydrogen pressure plays essential role for the selective synthesis of CPO. Selective CPO formation was observed at lower catalyst concentration and lower H₂ pressure.
- ✓ High catalyst concentration and H₂ pressure favours the CPL and THFA formation
- ✓ A study on product stability was carried out in order to identify the reaction pathways that lead to the development of side products. The results indicated that the formation of side products is primarily caused by the FOL.
- ✓ Activity of commerce (5)Ru/Al catalyst was also investigated for converting FAL to CPO, and under ideal reaction conditions (190°C, 13 bar H₂ at R. T., 1.1 h, S/Ru-714), a maximum 74% yield of CPO with 100% FOL conversion was obtained

ABSTRACT

Name of the Student: Kadam Jyoti Ramesh

Registration No.: 10CC16A26003

Faculty of Study: Chemical Science

Year of Submission: 2023

AcSIR academic centre/CSIR Lab: CSIR-National Chemical Laboratory, Pune

Name of the Supervisor: Dr. Paresh L. Dhepe

Title of the thesis: “Cobalt promoted ruthenium catalysts for the hydrogenation of sugars, furfural and furfuryl alcohol”

Biomass is a biological material which is obtained from living or recently dead things like wood, grass, crops etc. and it can be processed into fuels, chemicals and energy. Lignocellulosic biomass originates from forest and agricultural residues is mainly consisting of cellulose (30-50%), hemicellulose (20-40%) and lignin (15-25%). These components can be converted into fuel, energy and other industrially important chemical intermediates. Cellulose on hydrolysis in presence of acid produces glucose and glucose on hydrogenation in presence of H₂ it gives Sorbitol. Similarly, hemicellulose on acid hydrolysis produces xylose which on hydrogenation it gives xylitol. Sorbitol and Xylitol have wide applications in food and pharmaceutical industries. Both are used as a low-calorie sweetener, refreshing agent and for the synthesis of Vitamin C. Xylose on dehydration produces furfural (FAL). Further furfural can be converted into furfuryl alcohol (FOL) and cyclopentanone (CPO). CPO have wide applications in various industries including fungicides, pharmaceuticals, rubber chemicals, flavour and fragrance chemicals, for the preparation of polyamides, jet fuels and polyolefin. Now a day, for the hydrogenation of glucose to sorbitol and xylose to xylitol, industries are using nickel based catalysts because of their low cost. But while using these catalysts leaching of nickel takes place so that activity of catalyst for the hydrogenation get decreased and also require extra purification cost and also these catalysts are active at very high temperature and pressure. So, to overcome these problems and to find out the alternatives to nickel based catalysts we have prepared a different class of supported metal catalysts as a most active hydrogenation catalyst and unlike nickel, catalyst does not leach into the reaction mixture. These catalysts are active at low temperature and low H₂ pressure. Catalysts are synthesized by wet impregnation method and characterization of catalyst was done by using TEM, TPR, XRD etc. (Chapter 2). After the synthesis, catalysts were applied for the conversion of glucose to sorbitol and xylose to xylitol (Chapter 3). A stable and recyclable supported metal catalyst for the hydrogenation of sugars to sugar alcohol was developed. Reactions at higher substrate concentration were also done to make the process industrially viable. Synthesized catalyst as also applied for the conversion of furfural to cyclopentanone (Chapter 4). Conversion of Furfuryl alcohol (FOL) to cyclopentanone (CPO) and detailed study on reaction mechanism and pathway for the conversion of FAL to CPO and FOL to CPO was covered in chapter 5.

List of publication(s) in SCI Journal(s) (published and accepted) emanating from the thesis work with bibliographic details

1. **J. R. Kadam**, T. S. Khan and P. L. Dhepe, Designing an industrially viable bimetallic catalyst for the polyol synthesis, *New Journal of Chemistry*, 2023, 47, 7548-7555.

Other publications (emanating from thesis work)

1. **J. R. Kadam** and Paresh L. Dhepe, Hydrogenative ring rearrangement of furfural to cyclopentanone (Manuscript under preparation).
2. **J. R. Kadam** and Paresh L. Dhepe, Hydrogenation of furfuryl alcohol to cyclopentanone (Manuscript under preparation)

List of Posters Presented with Details

1. Poster presented at “National Science Day” at CSIR-NCL, Pune (26th -28th February, **2019**).

2. Poster Presentation at “The 8th Asia Pacific Congress on Catalysis (APCAT-8)” held at Bangkok, Thailand (4th -7th August, **2019**).

Title: “Efficient method for the synthesis of sugar alcohols and an industrial approach”

Abstract: Lignocellulosic biomass originates from forest and agricultural residues. It is mainly consisting of three structural components, cellulose (30-50%), hemicellulose (20-40%) and lignin (15-25%). These components can be converted into fuel, energy and other industrially important chemical intermediates. The simple sugar glucose can be hydrogenated into the sugar alcohol sorbitol by using various catalysts. Sorbitol is an important intermediate for the synthesis of vitamin C, ascorbic acid, lower molecular weight polyols etc. Now a day, for the hydrogenation of glucose to sorbitol, industries are using nickel based catalysts because of their low cost. But while using these catalysts leaching of nickel takes place so that activity of catalyst for the hydrogenation get decreased and also require extra purification cost and also these catalysts are active at very high temperature and pressure. So, to overcome these problems and to find out the alternatives to nickel based catalysts we have prepared a different class of supported metal catalysts as a most active hydrogenation catalyst and unlike nickel, catalyst does not leach into the reaction mixture. These catalysts are active at low temperature and low H₂ pressure. Characterization of catalyst is done by using TEM, TPR, XRD etc. Also, we have done the reactions at higher substrate concentration to make the process industrially viable.

3. Poster presented at Symposium on “Catalysis & Multiphase Reactor Engineering (CATMUR)” at CSIR-NCL, Pune (23rd December, **2019**).

Title: “Efficient method for the synthesis of sugar alcohols and an industrial approach”

Abstract: Lignocellulosic biomass originates from forest and agricultural residues. It is mainly consisting of three structural components, cellulose (30-50%), hemicellulose (20-40%) and lignin (15-25%). These components can be converted into fuel, energy and other industrially important chemical intermediates. The simple sugar glucose can be hydrogenated into the sugar alcohol sorbitol by using various catalysts. Sorbitol is an important intermediate for the synthesis of vitamin C, ascorbic acid, lower molecular weight polyols etc. Now a day, for the hydrogenation of glucose to sorbitol, industries are using nickel based catalysts because of their low cost. But while using these catalysts leaching of nickel takes place so that activity of catalyst for the hydrogenation get decreased and also require extra purification cost and also these catalysts are active at very high temperature and pressure. So, to overcome these problems and to find out the alternatives to nickel based catalysts we have prepared a different class of supported metal catalysts as a most active hydrogenation catalyst and unlike nickel, catalyst does not leach into the reaction mixture. These catalysts are active at low temperature and low H₂ pressure. Characterization of catalyst is done by using TEM, TPR, XRD etc. Also, we have done the reactions at higher substrate concentration to make the process industrially viable.

4. Poster presented at Research Foundation Day at CSIR-NCL, Pune (29th -30th November, 2022).

Title: “Efficient method for the synthesis of sugar alcohols and an industrial approach”

Abstract: Lignocellulosic biomass originates from forest and agricultural residues. It is mainly consisting of three structural components, cellulose (30-50%), hemicellulose (20-40%) and lignin (15-25%). These components can be converted into fuel, energy and other industrially important chemical intermediates. The simple sugar glucose can be hydrogenated into the sugar alcohol sorbitol by using various catalysts. Sorbitol is an important intermediate for the synthesis of vitamin C, ascorbic acid, lower molecular weight polyols etc. Now a day, for the hydrogenation of glucose to sorbitol, industries are using nickel based catalysts because of their low cost. But while using these catalysts leaching of nickel takes place so that activity of catalyst for the hydrogenation get decreased and also require extra purification cost and also these catalysts are active at very high

temperature and pressure. So, to overcome these problems and to find out the alternatives to nickel based catalysts we have prepared a different class of supported metal catalysts as a most active hydrogenation catalyst and unlike nickel, catalyst does not leach into the reaction mixture. These catalysts are active at low temperature and low H₂ pressure. Characterization of catalyst is done by using TEM, TPR, XRD etc. Also, we have done the reactions at higher substrate concentration to make the process industrially viable

List of Conference Attended with Details

1. Poster presented at “National Science Day” at CSIR-NCL, Pune (26th -28th February, **2019**).
2. Poster Presentation at “The 8th Asia Pacific Congress on Catalysis (APCAT-8)” held at Bangkok, Thailand (4th -7th August, **2019**).
3. Poster presented at Symposium on “Catalysis & Multiphase Reactor Engineering (CATMUR)” at CSIR-NCL, Pune (23rd December, **2019**).
4. Poster presented at Research Foundation Day at CSIR-NCL, Pune (29th -30th November, **2022**).

Erratum

Erratum

Erratum